X-692-72-309
PREPRINT

NASA TM X- 66019

MODULATION OF LOW ENERGY COSMIC RAYS

JAMES W. SARI

AUGUST 1972

GODDARD SPACE FLIGHT CENTER
GREENBELT, MARYLAND

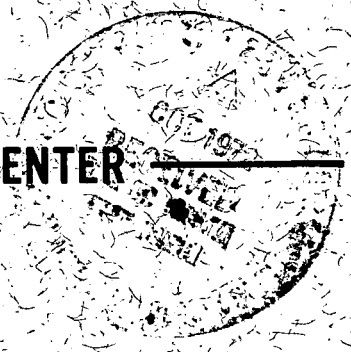

MODULATION OF LOW ENERGY COSMIC RAYS*

by

James W. Sari

Dissertation submitted to the Faculty of the Graduate School
of the University of Maryland in partial fulfillment
of the requirements for the degree of
Doctor of Philosophy
1972

*This work was supported in part by the National Aeronautics and Space Administration grant NGL 21-002-033.

ABSTRACT

Recent theories have related the propagation and diffusion of cosmic rays to the power spectrum of the interplanetary magnetic field. In this study, we directly test the power spectrum-diffusion coefficient relation at low energies (< 100 MeV) where the validity of the theories has been in doubt.

A first order perturbation solution of the Fokker-Planck equation governing the diffusion, convection and adiabatic deceleration of galactic cosmic rays in the solar medium is found to relate intensity fluctuations of low energy cosmic rays to local changes in the propagation parameters. Diffusion coefficients and their day to day variations are calculated from interplanetary magnetic field data obtained by Pioneer VI in 1965/1966. These are compared to simultaneous observations by IMP III of the proton flux in three energy channels (20-40, 40-60, 60-80 MeV).

Fluctuations in the higher energy proton flux (40-60, 60-80 MeV) are found to be related to changes in the modulation parameters as predicted by theory, if the contributions to the diffusion coefficients from directional discontinuities in the interplanetary magnetic field are subtracted. This is interpreted to imply that the discontinuities are basically tangential, and do not contribute significantly to the scattering of low energy cosmic rays. A lack of correlation between low energy (20-40 MeV) flux and parameter changes is interpreted as due to either a breakdown of the theory at low energies or to the presence of a continuous flux of high energy solar protons.

Observations of time profiles of solar flare events together with measurements of the low energy intensity spectrum of galactic cosmic ray

protons are found to imply a limit on the magnitude and average radial behavior of the diffusion coefficient near the orbit of earth. As Pioneer VI went from 1 to .8 AU in heliocentric radius calculations of the parallel diffusion coefficient indicate a magnitude and a negative radial gradient consistent with the implications of the particle measurements. A mechanism is found to explain the radial variation in terms of the diffusion coefficient's dependence on the magnetic field power spectrum.

Because of the correspondence in the relative changes of particle intensities and propagation parameters, and the correspondence in the predictions and observations of the magnitude and radial variation of the diffusion coefficients, it is concluded that the diffusion coefficient - power spectrum relation is valid to proton energies as low as 50 MeV.

TABLE OF CONTENTS

CHAPTER I

1.1 INTRODUCTION

Cosmic rays have been observed at earth for the last 40 years and, during that period, much of the efforts to understand the interplanetary medium have been to explain their origin and temporal fluctuations. It was Forbush (1938) who first noted that following large solar flares the cosmic ray intensity at earth would drop suddenly. It was also Forbush (1954) who noted an anti-correlation of cosmic ray intensity with the 11-year solar activity cycle. This led to the interpretation that there was a component of the cosmic rays of galactic origin which was being modulated by the interplanetary medium.

In 1956, Morrison (1956) pointed out that if the sun continuously emitted turbulent clouds of magnetized plasma, the charged cosmic rays traveling through the clouds might be scattered by the magnetic irregularities in a random fashion. The cosmic rays would then execute a random walk, and their transport might be described by a diffusion equation. Such an equation might than be used to explain a variety of temporal changes in the cosmic ray intensity.

Observations of comet tails by Biermann (1951, 1957) led to the suggestion of a continuous solar wind. This, in turn led to the explanation by Parker (1956, 1958a) of the 11-year solar cycle variation in terms of diffusion and convection. This model has been the basis for our understanding of the modulation of cosmic rays, and direct satellite observations of the solar wind and interplanetary magnetic field for the past ten years have confirmed its foundation.

With the observations of the interplanetary magnetic field have come attempts to derive the diffusion coefficients for the propagation of the cosmic rays. Work by Jokipii (1966) and Roelof (1966) and later by others has established a relationship between the spatial power spectrum of magnetic field fluctuations and the diffusion tensor. This has been tested by Gloeckler and Jokipii (1966) and Jokipii (1968a) by comparing the rigidity dependence of the diffusion coefficients as predicted from the power spectra to the rigidity dependence of the 11-year solar cycle modulation of cosmic ray protons and helium nuclei. These studies utilized magnetic field power spectra obtained over long periods, and applied them to the simple diffusion-convection theory. The results were consistent with theory at high energies (>500 MeV/nucleon) where the diffusion-convection model holds. However, this method has produced no conclusive results at low energies, where the appropriate power spectra have been shown to vary on a day to day basis (Coleman, 1966; Siscoe et al., 1968; Sari and Ness, 1969) and where the simple diffusion-convection model must be modified by the effects of adiabatic deceleration (Parker, 1965).

Recently, Klimas and Sandri (1971) have suggested that at low rigidities, (<1 GV), corresponding to proton energies less than 500 MeV, diffusion coefficients may not even be definable. This is due to a breakdown of the adiabatic approximation in computing the transport coefficients when the particles gyroradius approaches the magnetic field's autocorrelation length. More recently, Jokipii (1972) has rederived the diffusion coefficients showing that the adiabatic approximation is not strictly required. He finds that diffusion coefficients may be defined by the magnetic field power spectra for proton energies of 20-50 MeV and, perhaps, even lower. This controversy has not yet been resolved.

A further difficulty in the description of the diffusion of low energy cosmic rays was suggested in two studies by Sari and Ness (1969, 1970). There it was found that, at times, directional discontinuities in the interplanetary magnetic field may be the dominant contribution to the shape and level of the power spectra. If the directional discontinuities were basically tangential (parallel to the magnetic field lines) as suggested by Burlaga (1971), low rigidity particles ($\leq$300 MV), whose gyroradii are much less than the average distance between discontinuities, might rarely encounter discontinuities. These particles may then be scattered only by the fluctuations between discontinuities. Thus, the power spectra as measured by the spacecraft and applied to the determination of the diffusion tensor may not be the same spectrum of irregularities observed by the low rigidity cosmic rays.

It is the purpose of this work to provide a direct test of the effects of the predicted diffusion coefficients on the propagation of low energy cosmic rays. We will also test the relative contributions of the discontinuities and the turbulent fluctuations between discontinuities in the diffusion of the low energy cosmic rays. This will be done by comparing fluctuations in the intensity of low energy cosmic ray protons to changes in the propagation parameters calculated from the complete magnetic field, only the portion made up of the discontinuities, and the fluctuations between discontinuities.

The remainder of this chapter will cover the foundation of cosmic ray modulation theory and the relation of the diffusion tensor to the power spectrum of the interplanetary magnetic field. The successes and limitations of previous studies relating power spectra to high energy cosmic ray modulation will also be reviewed. Finally, we will explain the basis on which this present study is founded.

In the second chapter we will discuss the data and the techniques for data analysis employed. This will cover the methods of determining discontinuities and the calculation of the power spectra for the three data sets: the "real" data, the discontinuities, and the fluctuations between discontinuities. The relation of the results to magnetic field macrostructures such as "sectors" and to solar radio noise observations will also be discussed.

In the final chapter we will relate our calculations of the appropriate modulation parameters, as derived from Pioneer 6 satellite data, to simultaneous day to day measurements of low energy galactic cosmic ray proton fluxes as measured by the IMP III satellite. Fluctuations in the modulation parameters and corresponding fluctuations in the proton fluxes will be shown to be consistent with theoretical derivations presented in Chapter 1 and indicate that the scattering is primarily due to the magnetic irregularities between discontinuities. Temporal delays between changes in the modulation parameters and changes in the particle flux are observed and can be related to recent theoretical considerations of the macroscopic spatial trajectories of the average particle population.

The results indicate the possible existence of a local radial gradient in the parallel diffusion coefficients. The measurements of both the magnitude and gradient of the diffusion coefficient are found to give a consistent picture to observations of the galactic proton spectra and the behavior of energetic solar flare protons. Mechanisms which might lead to such a gradient are also discussed. Finally, we will suggest work for future studies.

1.2 Basic Elements of Cosmic Ray Modulation

Observations by Bridge et al. (1961) were the first to establish that the solar wind was an ionized, supersonic plasma with average velocity from 300 to 400 km/sec. Imbedded in this plasma is the interplanetary magnetic field. Since the plasma is highly conductive, the field is essentially "frozen" into the wind and convected radially outward from the sun eventually merging with the interstellar medium. It is within this "solar cavity" that the modulation effects on the galactic cosmic rays are expected. We will briefly sketch Parker's (1956, 1958a) explanation of the 11-year solar cycle modulation in terms of diffusion and convection.

We start with the assumption of an isotropic, constant galactic density of cosmic rays outside the solar cavity. In a spherically symmetric regime of magnetic scattering centers there would be an inward diffusive flux of galactic particles into the solar cavity given by

$$F_{diff} = - K \vec{\nabla} U \qquad (1.2.1)$$

where K is the diffusion coefficient and U is the particle density. Since the scattering centers are imbedded in the solar wind, which is moving radially outward with velocity V_w, there is a contribution to the flux due to convection:

$$F_{conv} = V_w U \qquad (1.2.2)$$

The equation of continuity then gives

$$\frac{\partial U}{\partial t} + \vec{\nabla} (V_w U - K \vec{\nabla} U) = 0 \qquad (1.2.3)$$

In the steady state, with no sources, and assuming spherical symmetry, we get:

$$K \frac{\partial U}{\partial r} = V_w U \qquad (1.2.4)$$

which can be integrated to give

$$U(r,T) = U_{\infty}(T) \exp[-\int_{r}^{r_c} V_w/K \, dr] \tag{1.2.5}$$

where r_c is the effective radius of the solar cavity.

Here, K is assumed to be isotropic but dependent on particle kinetic energy, T, and charge, Z. All the independent parameters, the radius of the solar wind boundary, r_c, the solar wind V_w, and K, are considered to vary in the solar cycle. Thus, the particle density can be expressed as

$$U(r,T) = U_{\infty}(T) \exp[-f(T,Z,t,r,r_c)] \tag{1.2.6}$$

This relatively simple diffusion-convection picture has, in large part, explained the general features of cosmic ray transport in the interplanetary medium and the 11-year solar cycle variation. Subsequent theoretical developments and experimental observations have, however, caused modifications of this model.

The prediction of the general spiral nature of the interplanetary magnetic field by Parker (1958b) and its subsequent observation by Ness et al. (1964) showed that the magnetic field had some average direction. This, in turn, implied that the diffusion was anisotropic. Thus, the diffusion coefficient in (1.2.1) is given by a tensor rather than a scalar.

Further, the fact that the solar wind is diverging radially leads to an adiabatic cooling of the cosmic rays in the steady state. Energy loss was first discussed by Singer et al. (1962) and fully developed by Parker (1965) who showed that the particle should lose momentun at a rate

$$\frac{1}{p}\frac{dp}{dt} = -\frac{1}{3}\vec{\nabla} \cdot V_w \tag{1.2.7}$$

or kinetic energy at a rate

$$\frac{1}{T}\frac{dT}{dt} = -\frac{\alpha(T)}{3}\vec{\nabla} \cdot V_w \tag{1.2.8}$$

where $\alpha(T) = (T + 2T_o)/(T + T_o)$, and T_o is the rest energy.

The steady energy loss requires the addition of a term $\partial/\partial T(U\ \partial T/\partial t)$ to the diffusion, or Fokker-Planck equation (1.2.3). In general, this is only valid in a frame of reference moving with the wind. However, Jokipii and Parker (1967) showed that to first order in V_w/v, with v the particle velocity, this was also valid in a fixed frame. The full Fokker-Planck equation describing the anisotropic transport of the cosmic rays is then

$$\frac{\partial U}{\partial t} = -\vec{\nabla}\cdot(\vec{V}_w U) + \frac{\partial}{\partial X_i}\left(K_{ij}\frac{\partial U}{\partial X_j}\right) + \frac{1}{3}(\vec{\nabla}\cdot\vec{V}_w)\frac{\partial}{\partial T}(\alpha T U) \tag{1.2.9}$$

(This equation was also derived by Gleeson and Axford (1967) starting with a Bolzmann equation including collisions.)

Although the full Fokker-Planck equation can be separated, for example, into equations for the number density and radial current density, a technique which facilitates the discussion of high energy approximations and anisotropies, equation (1.2.9) is the general equation governing the transport of cosmic rays in the solar cavity and is appropriate for cosmic rays of both galactic and solar origin. In the next section we will discuss the developments leading to the determination of the appropriate diffusion tensor, K_{ij}, for the Fokker-Planck equation.

1.3 Relation of the Diffusion Tensor to the Power Spectrum of the Interplanetary Magnetic Field

An early attempt to obtain transport coefficients in terms of magnetic field irregularities was made by Parker (1963). Here, the field was viewed as an array of isotropically distributed scattering centers, where each center had a scale size, ℓ, the distance over which the field was correlated with itself. A charged particle with gyroradius r_g should

suffer a deflection on the order of ℓ/r_g at each scattering center. After m random deflections, the angle through which the particle is scattered is roughly $m^{\frac{1}{2}}(\ell/r_g)$. If a mean free path is defined as the distance required for a scattering through an angle of one radian, then a particle traverses one mean free path after passing through n scatterers, where $n \approx (r_g/\ell)^2$. Thus, the mean free path should be proportional to the square of the particle's gyroradius, or the square of the particle's rigidity.

If, on the other hand, the gyroradius is such that $r_g < \ell$, then each deflection might cause a large scattering, and the mean free path, λ, is the correlation length. Thus, if the diffusion coefficient is given the classical definition of

$$K = \frac{1}{3} c\beta\lambda \qquad (1.3.1)$$

where $\beta = v/c$, the two limits imply different rigidity dependence of the diffusion. In the small gyroradius limit, the diffusion coefficient is proportional to velocity, while for large gyroradii the coefficient is proportional to velocity times the square of the rigidity. Although this approach is somewhat elementary, it is interesting to note that later, more rigorous, statistical analysis has produced similar results in these two limits.

Recently a number of authors have derived diffusion coefficients from a more general treatment of the effects of magnetic fluctuations on the orbits of fast charged particles. (Here "fast" is defined from Jokipii (1966) where the ratio of electric to magnetic forces on the particles in the interplanetary field is $F_e/F_B \sim V_{Alfven}/\beta c << 1$). These include Jokipii (1966, 1968b, 1971), Roelof (1966), Hasselmann and Wibberenz (1968), and Kulsrud and Pearce (1969). All procede from a Fokker-Planck

equation to describe the diffusion in pitch angle and position. (Roelof (1967) also showed that the Fokker-Planck formalism was derivable from the more generally applicable Liouville's equation). All obtain essentially similar, if not almost identical, results. Although the treatment of Hasselmann and Wibberenz (1968) is the most general of the four, and deals with the greatest number of models for the magnetic field, it is also the most intractable to apply observationally. Depending on the model, it requires knowledge of parameters such as wave polarization which are not unambiguously determinable by single spacecraft measurements in the solar wind. This treatment also uses the approximation for the probability density for the particle position and pitch angle of Jokipii (1966) to derive the diffusion coefficient for propagation along the average field, $K_{\parallel}$. In order to avoid difficulties when the particle pitch angle approaches 90°, Jokipii (1968b) revised his derivation to expand the probability density in terms of Legendre polynomials, which must be assumed to be small after the first order polynomial. For discussion of this point see Jokipii (1971).

In this study, we will employ the approach of Jokipii (1968b and 1971). Considering the similarity of results when identical magnetic field models are used, the fact that the models themselves are idealizations of rather disordered field configurations, and the inherent errors in measurements, we do not believe that our results can show a definitive bias toward a particular derivation. Since all the derivations depend relatively the same on the magnetic field power spectrum, solar wind velocity, particle rigidity, etc., changes in these parameters should affect the particle densities in approximately the same manner. For most observed magnetic field power spectra, differences among the

various derivations are within a factor of two in the magnitude of the diffusion coefficients. Likewise, the difference in the results obtained from the most physically reasonable models are also less than a factor of two, (c.f. Figure 6 of Hasselmann and Wibberenz (1968)). Future studies which we shall suggest may be able to differentiate between the various derivations. We shall only derive the diffusion coefficients from what we consider to be the most satisfactory statistical theory and probable magnetic field model.

We will briefly sketch the important points of Jokipii's (1971) derivations. This contains some of the more plausible assumptions and produces the most generally applicable results. Since the effects eventually depend on the magnetic field power spectra, we will first develop the formalism relating the spectra to the observations.

Consider a fluctuating magnetic field $\vec{B}$, which has an average value $\bar{B}$ which we choose to be in the Z direction of our cartesian coordinate system. The fluctuating part can then be defined as

$$\vec{B}_1(\bar{r},t) = \vec{B}(\bar{r},t) - \bar{B}_z \tag{1.3.2}$$

Since the Alfven velocity for propagation is approximately an order of magnitude smaller than the average solar wind velocity, V_w, we shall assume that inhomogeneities in the magnetic field as seen by a spacecraft represent principally convected spatial irregularities rather than explicit temporal variations. It should be noted that although the results will be discussed in terms of frequency spectrum, what is truly measured is a one-dimensional wave number spectrum along the solar wind velocity. The interchangeability with frequency spectrum is correct to first order in V_A/V_w.

We can then define the fluctuating part of the magnetic field in the frame of the solar wind to be

$$\vec{B}_1(\vec{r},t) \approx \vec{B}_1(\vec{r} - \vec{V}_w(t-t_o),\ t_o) \tag{1.3.3}$$

The three dimensional autocorrelation tensor of the field fluctuations is then

$$R_{ij}(\vec{\xi}=0,\tau) = < B_{1i}(\vec{r}_o,t),\ B_{1j}(\vec{r}_o,t+\tau) > \tag{1.3.4}$$

where

$$R_{ij}(\vec{\xi}=0,\tau) = R_{ij}(\vec{\xi}= -\vec{V}_w\tau,0) \tag{1.3.5}$$

We also define the observed power spectrum of field fluctuations as is conventional:

$$P_{ij}(f) = \int_{\infty}^{\infty} < B_{1i}(\vec{r}_o,t)\ B_{1j}(\vec{r}_o,t+\tau) > \ell^{-2\pi i f\tau}\ d\tau \tag{1.3.6}$$

or

$$P_{ij}(f) = \int_{-\infty}^{\infty} R_{ij}(0,\tau)\ \ell^{-2\pi i f\tau}\ \ d\tau \tag{1.3.7}$$

Then if ξ_3 is radial along the wind direction, the simple transformation of $\xi_3 = V_w\tau$ gives

$$P_{ij}(f) = \frac{1}{V_w}\int_{-\infty}^{\infty} R_{ij}\ (0,0,\xi_3,0)\ \ell^{2\pi i f\xi_3/V_w}\ \ d\xi_3 \tag{1.3.8}$$

Thus, the observed power spectra is related to the correlation tensor as measured along the solar wind velocity.

It should be pointed out that these considerations have assumed that the wavelengths of fluctuations inferred from spacecraft measurements are the same as seen in the frame of the wind. This is generally true only if

the wave number of the fluctuations, $\vec{k}$, is along the solar wind direction, $(\vec{k} \cdot \vec{V}_w) = |\vec{k}||\vec{V}_w|$. Since we are reviewing Jokipii's derivation, we will not make the necessary modifications to either the power spectra or diffusion coefficients until later. The interested reader is referred to section 2.5 for further discussion.

Now, let there be a charged particle of gyrofrequency ω_o in the average field, $\omega_o = Ze\ B/\gamma mc$, where Ze, γm, c are the standard notations for charge, relativistic mass and speed of light. Let $\mu = v_z/v$ be the particle's pitch angle, and $R = \gamma m\beta c^2/Ze$ be the particle's rigidity, where $\beta = v/c$. If the orbit changes of the particle caused by the fluctuating magnetic field are small in a correlation length of the fluctuations, the evolution of the particle's distribution in position and pitch angle can be governed by a Fokker-Planck equation.

In order to facilitate computation, it is assumed that the fluctuations are axially symmetric about the Z axis. This is probably a good approximation. Sari and Ness (1970) found that in a coordinate system aligned with the field, the power in the fluctuations in two coordinates normal to the average field tended to be equal and approximately two times the power in the fluctuations along the field. Somewhat similar results were obtained by Belcher and Davis (1971) who observed power anisotropies of 5:4:1 for two coordinates normal and one along the field.

Finally, Jokipii (1971) considers two magnetic field models: one where the fluctuations depend only on the Z direction, and one in which the fluctuations are isotropic. The first implies that the correlation tensor is diagonal in a field aligned frame or that cross-correlations between components are zero. This leads to the simplest results with no conditions on the magnetic field power spectrum slope. However, this is

a limiting case and has never been observed. The second model, the isotropic field, is also idealistic. The results of Sari and Ness (1969) indicated that the field was not isotropic, although this was only for limited times and only within the confidence limits of the observed power spectra. The true case is probably intermediate, and, as mentioned above, the results should be similar within a factor of two.

For the diagonal correlation tensor the Fokker-Planck coefficients for scattering in pitch angle and position are derived to be

$$\frac{\langle \Delta\mu^2 \rangle}{\Delta t} = \frac{1-\mu^2}{|\mu| v} \frac{Z^2 e^2}{\gamma^2 m^2 c^2} \int_{-\infty}^{\infty} R_{xx}(\xi)\, \ell^{i\omega_o \xi/\mu v}\, d\xi \tag{1.3.9}$$

$$\frac{\langle \Delta x^2 \rangle}{\Delta t} = \frac{\langle \Delta y^2 \rangle}{\Delta t} = \frac{1}{2\omega_o{}^2 |\mu| v} \int_{-\infty}^{\infty} \left[2\mu^2 v^2 \frac{Z^2 e^2}{\gamma^2 m^2 c^2} R_{xx}(\xi) + (1-\mu^2) v^2 R_{zz}(\xi)\, \ell^{-i\omega_o \xi/\mu v} \right] d\xi \tag{1.3.10}$$

From (1.3.7) we see that the scattering in pitch angle occurs at a resonant wave number, $k = \omega_o/\mu v = 1/\mu r_g$. which corresponds to the gyroradius of the particle in the fluctuating field. The scattering across the field line depends both on resonant scattering and on the power at zero wave number, $P_{xx}(k=0)$, corresponding to the random walk of field lines across the Z axis.

These can be related to the diffusion coefficients for propagation parallel and perpendicular to the mean field according to the formulation of Jokipii (1968b):

$$K_{\parallel} = \frac{2}{9} v^2 \left[\int_0^1 \frac{\langle (\Delta\mu)^2 \rangle}{\Delta t} d\mu \right]^{-1} \tag{1.3.11}$$

$$K_{\perp} = \frac{1}{2} \int_0^1 \frac{\langle (\Delta x)^2 \rangle}{\Delta t} d\mu \tag{1.3.12}$$

We would like to compare these results to the power spectra of the magnetic field as viewed by a spacecraft stationary in the solar wind. From (1.3.8) we note that the correlation tensors in the expressions for the scattering coefficients can be identified with $V_w P_{xx}(f)$ when $f = V_w \omega_o/2\pi\mu v$, or, in terms of the particle rigidity, $f = V_w \bar{B}/2\pi\mu R$. If the power spectrum is also smoothly varying with frequency, $P_{xx}(f) = Af^{-\alpha}$, simple integration gives the following results for the diffusion coefficients in terms of rigidity and the observed power spectra,

$$K_{\parallel}(R) = 2\alpha(\alpha+2)\, c\beta R^2/9V_w P_{xx}\ (f = V_w \bar{B}/2\pi R) \tag{1.3.13}$$

$$K_{\perp}(R) = \frac{1}{8}\,\frac{v}{\bar{B}^2}\, V_w\, P_{xx}\ (f=0) + \frac{1}{4}\,\frac{vV_w}{\alpha(2+\alpha)\,\bar{B}^2}\, P_{zz}(f = V_w\bar{B}/2\pi R) \tag{1.3.14}$$

Since the spectra is usually calculated for only positive frequencies, with the normalization that the variance or total power, $R_{xx}(0) = \int_0^\infty P_{xx}(f)\, df$, we have replaced the power spectra in the above formulae by $P_{xx}(f) \Rightarrow P_{xx}(f)/2$.

With Pioneer 6 measurements in 1966, spectra given by Sari and Ness (1970) indicate that the parallel diffusion coefficient for a 70 MeV proton, ($R = .37$ BV, $\beta = .36$, $\bar{B} = 6\gamma$, $V_w = 4 \times 10^7$ cm/sec), has an average value of $K_{\parallel}$ (70 MeV) $\approx 2 \times 10^{21}$ cm^2/sec. For perpendicular diffusion, and a power spectra that falls off at high frequencies, the first term in (1.3.14) dominates, and from Figure 3 of Sari and Ness (1970) we find a typical value for perpendicular diffusion to be, $K_{\perp}(70\ \text{MeV}) \approx 1.5 \times 10^{20}$ cm^2/sec.

It is interesting to note the dominance of the field line random walk in (1.3.14). If that term were not present, then within a factor of two, (assuming $P_{zz}(f) = P_{xx}(f)$), the expression for the diffusion across

field lines would be the same as given by Axford (1965), $K_\perp = K_\parallel/(1 + \omega_o^2 \tau^2)$, where $\tau_\parallel$ is the collision time for scattering, $\tau_\parallel = 3K_\parallel/v^2$. If there were no field line "random walk", the coefficient for perpendicular diffusion would be smaller by more than an order of magnitude.

It should also be noted that if the 70 MeV protons are not scattered by the tangential discontinuities, the power spectrum used in (1.3.13) is perhaps too high and $K_\parallel$ should be larger. Likewise if the particles do not "see" the discontinuities, their contributions to the low frequency power spectrum, (which may be considerable), may cause $K_\perp$ to be overestimated. This should be remembered when we employ "order of magnitude" calculations in the following sections.

Finally, Jokipii (1971) also calculates the scattering coefficients for the isotropic field model. In the limit that the particle gyroradius is much less than the field autocorrelation length, $r_g \ll \ell$, and if the magnetic field power spectrum does not fall off steeper than f^{-2}, the results are approximately equivalent to (1.3.9) and (1.3.10). Power spectra which we obtain do not generally fall off faster than f^{-2}. Therefore, in this study we will employ (1.3.13) and (1.3.14) as reasonable approximations to the diffusion coefficients as predicted from statistical theory.

1.4 Past Tests of Theory

In the previous two sections we have traced the developments of equations describing the behavior of cosmic rays in the interplanetary medium and the relation of their propagation parameters to a statistical description of the interplanetary magnetic field. Because of the difficulty in obtaining analytic solutions to the full Fokker-Planck equation (1.2.9) in all except the most idealized cases, approximations appropriate

for limited energy ranges have been utilized to test the relation between power spectra and modulation.

The simplest approximation is that of diffusion-convection. This ignores the energy loss process on the cosmic ray spectrum and, therefore, is applicable only at high energies, $T \gtrsim 500$ MeV/nucleon, where the effects of adiabatic deceleration are negligible, (Goldstein, et al. (1970)). The steady state solution for the cosmic ray density at some time, t, is given by (1.2.5), or

$$U(r,T,t) = U_{\infty}(T) \exp\left[-\int_{r}^{r_c} V_w(r',t)/K_{\parallel}\ (r',T,t)dr'\right] \qquad (1.4.1)$$

If the diffusion coefficent is separable in energy, (rigidity), and radius,

$$K_{\parallel}\ (r,T,t) = \beta K_1(r,t)\ K_2(R,t) \qquad (1.4.2)$$

we can express the particle density as

$$U(r,T,t) = U_{\infty}(T) \exp[-\eta(t)/\beta K_2(P,t)] \qquad (1.4.3)$$

where the spatial dependence of the modulation, solar wind velocity, and cavity boundary are included in the parameter $\eta(t)$.

From equation (1.3.13) it is clear that if the transverse power spectrum of the interplanetary field has the variation, $P(f) = Af^{-\alpha(t)}$, the rigidity dependent diffusion coefficient has the form,

$$K_2(R,t) \propto R^{2-\alpha(t)} \qquad (1.4.4)$$

If the cosmic ray intensity is then measured at two widely separated times, the fractional modulation, or the logarithm of the ratio of densities observed at times t_2 and t_1, will be given by

$$\ell n\ U(r,T,t_2)/U(r,T,t_1) = -\eta(t_2)/\beta R^{2-\alpha(t_2)} + \eta(t_1)/\beta R^{2-\alpha(t_1)} \quad (1.4.5)$$

If, fortuitously, the power spectral slope is the same at t_1 and t_2, then

$$\ell n\ U(r,T,t_2)/U(r,T,t_1) = [\eta(t_1) - \eta(t_2)]/\beta R^{2-\alpha} \quad (1.4.6)$$

Thus, we should be able to compare the rigidity dependence of the fractional modulation with the observed magnetic field power spectrum.

Calculations by Gloeckler and Jokipii (1966) and Jokipii (1968a) on observations of proton and helium nuclei between 1962 and 1965 indicate that the fractional modulation at high rigidities, R > 2 BV, varies as $1/\beta R$, in agreement with measurements of the magnetic field power spectra at those times (Coleman, 1966). However, at lower rigidities the fractional modulation indicated rigidity independent diffusion or modulation proportional to $1/\beta$, in disagreement with power spectra observations.

Power spectra obtained for interplanetary conditions in 1965 by Siscoe et al. (1968) and in 1966 by Sari and Ness (1969, 1970) indicated a frequency dependence of close to f^{-2} at high frequencies, ($f > 2.8 \times 10^{-4}$Hz), corresponding to rigidities $R \lesssim .5$ BV, and a dependence of $f^{-3/2}$ to $f^{-5/3}$ at lower frequencies, corresponding to higher rigidities. These results were in agreement with the fractional modulation between 1965/1966 as measured by Ormes and Webber (1968). They found a fractional modulation proportional to $1/\beta$ below .5 BV and proportional to $1/\beta R^{\frac{1}{2}}$ at greater rigidities. Assuming that the shape of the power spectrum is invariant in the intervals over which the cosmic ray data were obtained, these results are in agreement with the observed power spectra.

However, some caution must be used in interpreting the results at low rigidities. First, rigidities below .5 BV, or approximately 150 MeV/nulceon are well below the range in which diffusion-convection is applicable. Secondly, observations of Webber (1967) and Lezniak and Webber (1971) have shown a splitting in the fractional modulation between protons and helium nuclei at low rigidities, with a greater modulation for protons than helium. This cannot be accounted for by simple diffusion-convection, since in this picture the predictions are purely rigidity dependent. Thus, the results of Siscoe et al. (1968) and Sari and Ness (1969, 1970), although attractive, cannot be considered as testing the validity of the diffusion coefficient-power spectrum relation at low energies.

One may instead use the quasi-static form of the full Fokker-Planck equation (1.2.9) and various diffusion coefficients in order to numerically fit the observed cosmic ray spectrum. However, with this, one is required to specify not only the rigidity dependence of the diffusion coefficient, but its radial dependence as well, and the unmodulated cosmic ray spectrum. A numerical solution has been made by Fisk (1971) to fit the proton and helium intensities observed near solar minimum in 1965. The unmodulated spectrum was assumed to be $U_\infty(T) \alpha T^{-2.65}$ and the diffusion coefficient to have the separable form $K_{\parallel} = K_e \beta R \exp(r/r_e)$, where $r_e = 1$ AU and $K_e = 7.5 \times 10^{20}$ cm^2 sec^{-1} BV^{-1}. The results for protons are shown in Figure 1. The numerical solution is obviously a good fit to the cosmic ray intensity spectrum, and the rigidity dependence of the diffusion coefficient is in reasonable agreement with the shape of magnetic field power spectra (at frequencies below 10^{-4} Hz). However, the magnitude of the diffusion coefficient at the orbit of earth in this model is generally smaller than that derived from Jokipii's formula and related to observed magnetic field power

spectra. For example, for protons of T = 70 MeV, the given diffusion coefficient has the value of $K_e \sim 10^{20}$ cm^2/sec. This is more than an order of magnitude smaller than the value we derived in Section 1.3 from Pioneer 6 data in 1965/1966. Moreover, as will be discussed below, such small values are clearly inconsistent with the fast rise times to maximum of energetic solar flare particles.

It should be noted that the magnitude of the diffusion coefficient necessary to fit the cosmic ray spectrum, particularly the positive slope at low energies, is closely wedded to the choice of radial dependence and boundary conditions. (This will also be discussed below.) Thus, although Fisk's results are in disagreement with the observed magnitude of the diffusion coefficients, they do not rule out other values of $K_{\parallel}$ with different radial variation, and a rigidity dependence still corresponding to magnetic field observations.

Numerical solutions of the full Fokker-Planck equation have also been shown by Lezniak and Webber (1971) to account for the splitting in the modulation of protons and helium nuclei for the years 1965 and 1968. They employed a diffusion coefficient increasing exponentially with radius and a magnitude approximately equal that of Fisk (1971). However, they assumed an unmodulated spectrum varying as total energy to the -2.5 rather than kinetic, and a rigidity dependence in diffusion as predicted by the results of Sari and Ness (1969). Their results, likewise, depended on the various parameters and boundary conditions which were specified.

Although the above results indicate that the observations at low energies can be accounted for with the full Fokker-Planck equation, they do not conclusively test the validity of the power spectrum-diffusion coefficient relation. It should be noted that any test at low energies must include the process

of energy loss. It should also be noted that direct fits to the cosmic ray spectrum cannot test the relation unless one knows both the unmodulated spectrum and the variation of diffusion coefficient with radius. In order to test the relation we would like to develop a method which contains the adiabatic deceleration process yet depends on only local observations.

1.5 Perturbation Solutions to the Transport Equation

We wish to develop a formalism to relate changes in the observed modulation parameters, V_w/K, to variations of the particle densities at low energies. From the considerations of the past section, we would prefer a dependence solely on local, or single spacecraft observations. We should also bear in mind the result of Sari and Ness (1970) that the effects of the magnetic discontinuities on the power spectra vary over a twelve hour to one day period, and if we wish to determine their contribution to the scattering we should apply our observations over as short a time period as possible (i.e., daily). Thus power spectra which are obtained over long periods and usually applied to diffusion-convection solutions are inappropriate.

We propose a model which depends on day to day fluctuations or perturbations in the galactic cosmic ray intensity, rather than on the magnitude of that intensity. Clearly, a measurement of the interplanetary magnetic field power spectrum and solar wind velocity for a short period can only be considered as representative of local conditions. The average particle intensity, on the other hand, depends on conditions averaged over the entire solar cavity, conditions which change macroscopically on a time scale of the solar cycle, 11 years. However, if we measure changes in the appropriate modulation parameters over short periods, we might expect corresponding perturbations in the particle density superimposed on some average value.

Unlike fits to the particle spectrum, we will then be concerned with changes in the modulation parameters and particle intensity, rather than their particular magnitudes.

If we assume that a single spacecraft can, in some period, measure representative interplanetary conditions over some volume, we should expect that changes in those conditions would most clearly affect those cosmic rays which, within the same period, sample approximately the same volume. This implies that the subsequent analysis will only be valid for low energy particles. High energy particles will simply traverse too large a distance in our measuring period. Whatever perturbations they suffer will represent conditions over a much larger volume.

Let us expand these ideas quantitatively. We will show later that power spectra taken over one day provide good statistics. Likewise, we will relate these measurements to daily averaged proton fluxes of a characteristic energy of 70 MeV. Therefore, the following calculations will be considered to be over one day periods appropriate to approximately 70 MeV protons.

Assume that the average magnetic field at 1 AU is along the spiral direction predicted by Parker (1963). Cosmic ray protons arriving at a spacecraft located at 1 AU during a one day period will have traversed, on the average, an ellipsoid in space (Figure 2) whose major axis is centered at the earth along the spiral direction and whose minor axis, $d_\perp$, is determined by the perpendicular diffusion coefficient, $K_\perp$, and the time interval, t,

$$d_\perp \approx (K_\perp t)^{\frac{1}{2}} \qquad (1.5.1)$$

For a 70 MeV proton, a typical value for the perpendicular diffusion coefficient as derived in Section 1.3 is $K_\perp \approx 10^{20}$ cm^2/sec. During a one day period, $t \sim 8.6 \times 10^4$ sec, the protons we observe have typically sampled conditions normal to the average field of width, $d_\perp \sim 3 \times 10^{12}$ cm.

Let us assume that the point measurements of the magnetic field by the spacecraft are representative of conditions along the field lines in the ecliptic plane, and at least somewhat representative of conditions normal to the ecliptic. During that same period of one day, the solar wind transports the "frozen-in" field past the spacecraft. We should measure conditions perpendicular to the average field of length

$$\ell_\perp \sim V_w t \sin\psi$$

For $\psi \sim 45°$, and an average solar wind speed of 4×10^7 cm/sec, this implies $\ell_\perp \sim 2.5 \times 10^{12}$ cm. Thus, $\ell_\perp \sim d_\perp$, and with the assumption that interplanetary conditions are somewhat isotropic, the field sampled by a single spacecraft in one day should be representative of the same field seen by protons arriving at the spacecraft with energies equal to or less than 70 MeV. Then, if the theory relating the parameters to magnetic field and solar wind conditions is correct, day to day changes in the particle intensities should be related to the appropriate changes in the calculated modulation parameters.

It should be noted that the above consideration ignored the adiabatic energy loss of the particles during the measurement period. However, a calculation of the energy loss using equation (1.2.8) with $\alpha(T) = 2$, appropriate for non-relativisitc particles, indicates that the particles we observe at 70 MeV during one day have lost no more than 25 MeV. Any revision due to energy loss is minor and will not affect these conclusions.

We would now like to estimate how the low energy cosmic rays will respond to local perturbations in interplanetary conditions. If we ignore energy loss in the Fokker-Planck equation, (diffusion-convection picture), we note from equation 1.4.1 that changes in the modulation parameter, $V_w/K_{\parallel}$, should be anti-correlated with changes in the particle intensity. This should be a general characteristic of the results, regardless of formalism.

Both Jokipii (1969) and Gleeson and Axford (1968) have obtained perturbation solutions for the cosmic ray density from the quasi-static, spherically symmetric Fokker-Planck equation. Although proceeding in slightly different fashions, they achieve the same results, and both require that $V_w\tilde{R}/K_{\parallel} << 1$, where $\tilde{R}$ is a characteristic heliocentric distance, typically 1 AU. If $\Delta U(r,T,t)$ is the change in the particle density resulting from the perturbation in $V_w/K_{\parallel}$, they find that

$$\frac{\Delta U(r,T,t)}{U(r,T,t)} = - \left[1 - \frac{1}{3U}\frac{\partial}{\partial T}(\alpha TU)\right] \Delta \int_r^{r_c} V_w(r',t)/K_{\parallel}(r',T,t)\, dr' \qquad (1.5.2)$$

where $1 - 1/3U\ \partial/\partial T(\alpha TU)$ can be considered to be the Compton-Getting factor of the locally observed spectrum. If the differential intensity, $j = vU/4\pi$, has a variation in kinetic energy, $j(T) = AT^{\gamma}$, we can express the Compton-Getting factor to be $(2-\alpha\gamma)/3$. Thus,

$$\frac{\Delta U(r,T,t)}{U(r,T,t)} = - \left(\frac{2-\alpha\gamma}{3}\right) \Delta \int_r^{r_c} V_w(r',t)/K_{\parallel}(r',T,t)dr' \qquad (1.5.3)$$

For general interplanetary conditions $V_w\tilde{R}/K_{\parallel} << 1$ only for protons whose energies are greater than 400 MeV, and these results may not be applicable to our considerations. These also require knowledge of $V_w/K_{\parallel}$ from the point of observation to boundary of the solar cavity, or measurements of interplanetary conditions over long times, which is of no aid to us.

Finally, Rygg and Earl's (1971) conclusion that over a solar cycle the proton intensity spectrum from 50-200 MeV has the shape $j = AT$, or $\gamma = 1$, implies that at low energies ($\alpha(T) = 2$) the Compton-Getting factor is zero. Thus, $\Delta U/U$ would be zero regardless of the change in the modulation parameter, $V_w/K_{\parallel}$. This is in conflict to what we observe.

Therefore, we would like to develop a perturbation solution to the transport equation to determine the response of the particle density as a function of changes in V_w/K appropriate for low energies where $V_w \tilde{R}/K \sim 1$ and the Compton-Getting factor is zero.

Let us start with the full Fokker-Planck equation (1.2.9) for which we assume conditions to be spherically symmetric,

$$\frac{\partial U}{\partial t} = -\frac{1}{r^2}(r^2 V_w U) + \frac{1}{r^2}\frac{\partial}{\partial r}(r^2 K_{rr}\frac{\partial U}{\partial r}) + \frac{1}{3}\frac{1}{r^2}\frac{\partial}{\partial r}(r^2 V_w)\frac{\partial}{\partial T}(\alpha T U) \qquad (1.5.4)$$

where $K_{rr} = K_{\parallel}\cos^2\psi + K_{\perp}\sin^2\psi \approx K_{\parallel}\cos^2\psi$, (Jokipii, 1971), and K_{rr} is defined along the radius vector, while $K_{\parallel}$ is measured in a system aligned along the average magnetic field. Since we shall be dealing with low energies we let $\alpha \approx 2$, a constant; and for visual convenience we let $V_w \Rightarrow V$, $K_{rr} \Rightarrow K$.

The considerations of Parker (1963) indicate that following coronal expansion the solar wind velocity is approximately constant. Thus, we let $\partial V/\partial r \approx 0$. This is equivalent to saying $2V/r >> \partial V/\partial r$ in the Fokker-Planck equation. Our measurements of changes in the solar wind velocity over one day are, on the average, less than 40 km/sec. Thus, $\partial V/\partial r \sim \Delta V/V\Delta t \sim 10^{-6}$ sec^{-1}, while at r = 1 AU, $2V/r \sim 5 \times 10^{-6}$ sec^{-1}. Then $2V/r/\partial V/\partial r \gtrsim 5$, and our assumption cannot be very bad.

The Fokker-Planck equation can then be written as,

$$\frac{\partial U}{\partial t} = K \frac{\partial^2 U}{\partial r^2} + \left(\frac{\partial K}{\partial r} + \frac{2K}{r} - V \right) \frac{\partial U}{\partial r} - \frac{2V}{r} \left(U - \frac{2}{3} \frac{\partial}{\partial T} (TU) \right) \tag{1.5.5}$$

We would like to determine under what conditions the time derivative in (1.5.5) can be ignored. Let us assume that we perturb the medium by varying V/K. Let us also assume that in response the particle density changes as

$$U(r,T,t) = U_o(r,T) \; [1 + \mu \; (r,T,t)] \tag{1.5.6}$$

where $U_o(r,T)$ is the unperturbed value and $\mu(r,T,t)$ is the perturbation. By multiplying (1.5.5) by r^2/KU we see that the density, U, will be responding to parameters, Vr/K, which are of order unity. We expect that we can ignore explicit time dependence when $r^2/KU \; \partial U/\partial t << 1$. By (1.5.6), $1/U \; \partial U/\partial t \approx \Delta U/U\Delta t \approx \mu/\Delta t$, and we will satisfy the requirement if we sample over times $\Delta t >> (r^2/K)\Delta\mu$. From observations, U changes on the average less than 30% per day. If at the same time we assume that we perturb a volume whose characterisitic radius is somewhat less than 1 AU, we find that

$$\Delta t >> \frac{2\times10^{26}}{2\times10^{21}} (.3) \text{ sec} \sim .3 \text{ day} .$$

This implies that if we instantaneously perturb the interplanetary medium over 1 AU, the low energy particle densities, (with $K \sim 2 \times 10^{21}$ cm^2/sec), will not have relaxed to equilibrium values until after times greater than .3 days. Thus, by averaging our results over 3 days we should satisfy this requirement by an order of magnitude, and we can ignore explicit time dependence. We then write the Fokker-Planck equation in the convenient form:

$$\frac{\partial^2 U}{\partial r^2} + \left(\frac{1}{K}\frac{\partial K}{\partial r} + \frac{2}{r} - \frac{V}{K}\right)\frac{\partial U}{\partial r} = \frac{2}{r}\frac{V}{K}\left(U - \frac{2}{3}\frac{\partial}{\partial T}(TU)\right) \qquad (1.5.7)$$

O'Gallagher and Simpson (1967) first pointed out that their results relating the cosmic ray radial gradient to the variation of the diffusion coefficients as given by Gloeckler and Jokipii (1966) implied that K is separable into functions of R and β and a function of space and time. Since this greatly simplifies the computation, we make the same assumption here:[1]

$$K(r,T,t) = \beta K_1(r,t)\ K_2(T,t) \qquad (1.5.8)$$

which implies that

$$\frac{1}{K}\frac{K}{r} + \frac{2}{r} = f(r) \quad \text{in (1.5.7).}$$

We wish to perturb the modulation parameter, V/K, and obtain a solution to first order in the perturbation. For simplicity, let us assume that only the energy dependence of the modulation parameter is perturbed; or let

$$\frac{V}{K}(r,T,t) = \frac{V_o}{K_o}(r,T)\ (1+p(T,t)) \qquad (1.5.9)$$

---

[1] A number of authors, Burger and Tanaka (1970), and Burger (1971), have questioned the validity of this assumption. However, they base their objections to results predicted from the simple diffusion-convection model. Gleeson and Urch (1971) find that separability is not incompatible with observations in the framework of the full transport equation. We will assume that (1.5.8) is at least approximately valid.

where $p(T,t)$ is the relative perturbation and V_o/K_o is the unperturbed modulation parameter. This implies that $f(r)$ is unperturbed. This also implies that we are, in essence, perturbing the whole solar medium. However, since the low energy particles we observe in one day are responding to only local conditions, what occurs over the rest of the solar cavity is of little consequence.

We define the response to the perturbation to be $\mu(r,T,t)$ as in (1.5.6), and we shall attempt to find an explicit solution for μ in terms of p. We start by assuming that the unperturbed solution, $U_o(r,T)$ depends only on $V_o/K_o(r,T)$, and satisfies the quasi-static Fokker-Planck equation:

$$F_o\left(\frac{V_o}{K_o},\ U_o\right) \equiv \frac{\partial^2 U_o}{\partial r^2} + \left(f(r) - \frac{V_o}{K_o}\right)\frac{\partial U}{\partial r} - \frac{2}{r}\frac{V_o}{K_o}\left(U_o - \frac{2}{3}\frac{\partial}{\partial T}(TU_o)\right) = 0 \quad (1.5.10)$$

We put (1.5.9) and (1.5.6) into (1.5.7) and obtain

$$\frac{\partial^2 U_o}{\partial r^2} + \frac{\partial^2}{\partial r^2}(U_o\mu) + \left(f(r) - \frac{V_o}{K_o} - p\frac{V_o}{K_o}\right)\frac{\partial}{\partial r}(U_o+U_o\mu) = \frac{2}{r}\frac{V_o}{K_o}(1+p)\left[U_o+U_o\mu - \frac{2}{3}\frac{\partial}{\partial T}(T(U_o+U_o\mu))\right] \quad (1.5.11)$$

By subtracting $F_o(V_o/K_o,\ U_o)$ from (1.5.11) we are left with,

$$\frac{\partial^2}{\partial r^2}(U_o\mu) + \left(f(r) - \frac{V_o}{K_o}\right)\frac{\partial}{\partial r}(U_o\mu) - p\frac{V_o}{K_o}\frac{\partial}{\partial r}(U_o+U_o\mu) = \frac{2}{r}\frac{V_o}{K_o}p\left(U_o - \frac{2}{3}\frac{\partial}{\partial T}(T\,U_o)\right) + \frac{2}{r}\frac{V_o}{K_o}(1+p)\left(U_o\mu - \frac{2}{3}\frac{\partial}{\partial T}(TU_o\mu)\right) \quad (1.5.12)$$

which can be rewritten as

$$\mu \; F_o\left(\frac{V_o}{K_o}, U_o\right) + 2\,\frac{\partial U_o}{\partial r}\,\frac{\partial \mu}{\partial r} + U_o\,\frac{\partial^2 \mu}{\partial r^2} + U_o\left(f(r) - \frac{V_o}{K_o}\right)\frac{\partial \mu}{\partial r}$$

$$- p\,\frac{V_o}{K_o}\,\frac{\partial}{\partial r}\,(U_o + U_o\mu) = \frac{2}{r}\,\frac{V_o}{K_o}\,p[U_o\mu - \frac{2}{3}\,\frac{\partial}{\partial T}\,(TU_o\mu)]$$

$$+ \frac{2}{r}\,\frac{V_o}{K_o}\,p\,[U_o - \frac{2}{3}\,\frac{\partial}{\partial T}\,(T\,U_o)] - \frac{4}{3}\,\frac{V_o}{K_o r}\,T\,U_o\,\frac{\partial \mu}{\partial T} \qquad (1.5.13)$$

By (1.5.10) $\mu F_o\,(V_o/K_o, U_o) = 0$, and since this calculation is to first order, we set second order terms in $p\mu$, i.e.,

$$p\,\frac{V_o}{K_o}\,\frac{\partial}{\partial r}\,(U_o\mu) \quad \text{and} \quad p\left(U_o\mu - \frac{2}{3}\,\frac{\partial}{\partial T}\,(T\,U_o\mu)\right),$$

to zero also. Finally, the observations of Rygg and Earl (1971) that the Compton-Getting factor is zero, implies that

$$\frac{2}{r}\,\frac{V_o}{K_o}\,p[U_o - \frac{2}{3}\,\frac{\partial}{\partial T}\,(TU_o)]$$

is certainly of second order, and approximately zero.

We then have,

$$2\,\frac{\partial U_o}{\partial r}\,\frac{\partial \mu}{\partial r} + U_o\,\frac{\partial^2 \mu}{\partial r^2} + U_o\left(f(r) - \frac{V_o}{K_o}\right)\frac{\partial \mu}{\partial r}$$

$$- p\,\frac{V_o}{K_o}\,\frac{\partial U_o}{\partial r} = -\frac{4}{3}\,T\,\frac{U_o}{r}\,\frac{V_o}{K_o}\,\frac{\partial \mu}{\partial T} \qquad (1.5.14)$$

or,

$$\frac{rK_o}{V_o}\,\frac{\partial^2 \mu}{\partial r^2} + \frac{K_o}{V_o}\left(\frac{r}{U_o}\,\frac{\partial U_o}{\partial r}\right)\frac{\partial \mu}{\partial r} + \frac{K_o}{V_o}\left(f(r) - \frac{V_o}{K_o}\right)\frac{\partial \mu}{\partial r} \qquad (1.5.15)$$

$$= p\left(\frac{r}{U_o}\,\frac{\partial U_o}{\partial r}\right) - \frac{4}{3}\,T\,\frac{\partial \mu}{\partial T}$$

We are left with an equation only slightly less formidable than the one we started with. However, if we make some simplifying and plausible assumptions, we can find an explicit solution for μ in terms of p.

Note, if the unperturbed radial gradient of the cosmic ray density, $r/U_o \; \partial U_o/\partial r$, is only a weak function of radius, or if we can assume that the cosmic ray density's radial dependence is a power law in r, then the "driving" term of (1.5.15), $p(T,t)\ (r/U_o \; \partial U_o/\partial r)$, is only a function of energy and time, $p(T,t)\ (r/U_o \; \partial U_o/\partial r) = g(T,t)$. In this case we can get a simple solution to (1.5.15).

First we need not be concerned with a solution of the homogeneous equation, i.e., when $g = 0$, for this gives the physically unreasonable result of a change in the cosmic ray intensity μ, when there is no change in the modulation parameter. We desire only a solution to the particular equation, $g \neq 0$. Since by assumption, g is only a function of energy and time, a perfectly valid, albeit simple solution to (1.5.15) is given when $\mu(r,T,t) = \mu(T,t)$. In this case

$$\frac{4}{3} \; T \; \frac{\partial}{\partial T} \; \mu(T,t) = g(T,t) = p(T,t) \; \frac{r}{U_o} \; \frac{\partial U_o}{\partial r} \qquad (1.5.16)$$

or

$$\mu(T,t) \; = \; \frac{3}{4} \int p(T',t) \; \frac{r}{U_o} \; \frac{\partial U_o}{\partial r} \; dT'/T' \qquad (1.5.17)$$

To see what a solution of (1.5.17) may be like, let $r/U_o \; \partial U_o/\partial r \; (T) = n_o (T/T_o)^{\sigma}$, where n_o is the radial gradient when $T = T_o$, and σ is the slope of the energy dependence. Let the energy variation in p(T,t) be determined by the average dependence of $K_{\parallel}$ on energy, $p(T,t) = p_o(t) \; (T/T_o)^{-\gamma}$, (with γ to be related later in terms of the power spectrum of the magnetic field).

Then (1.5.17) becomes,

$$\mu(T,t) = \frac{3}{4} n_o p_o(t) \int^T (T'/T_o)^{\sigma-\gamma-1} \, d(T'/T_o) \tag{1.5.18}$$

or

$$\mu(T,t) = \frac{3}{4} \frac{n_o p_o(t)}{\sigma-\gamma} (T/T_o)^{\sigma-\gamma} \tag{1.5.19}$$

where we have set the constant of integration to zero to satisfy the requirement that $\mu = 0$ when $p = 0$. Evaluating at $T = T_o$ we get that

$$\mu(T_o,t) = \frac{3}{4} n_o p_o/(\sigma-\gamma) \tag{1.5.20}$$

In terms of the definition of μ and p, and our observations, we can write (1.5.20) as

$$\frac{\Delta U}{\langle U \rangle} = \frac{3}{4} \frac{n_o}{(\sigma-\gamma)} \Delta V_w/K_{\parallel} \, / \langle V_w/K_{\parallel} \rangle \tag{1.5.21}$$

where we could also replace U with particle intensity or flux.

Thus, we have developed a formalism relating changes in particle densities at low energies, (where the spectral slope is +1), directly to changes in the locally observed modulation parameters. Unlike previous theories, this should be applicable on short time scales and does not require knowledge of the radial variation of the diffusion coefficients or the distance to the solar cavity "boundary". However, it does couple the observations to the cosmic ray radial gradient. Because our physical expectation, as well as observation, is that μ is anti-correlated with p we hope that $(\sigma-\gamma) < 0$. We note that (1.5.20) is, at least, a physically reasonable result, with the response of μ to p being proportional to the density gradient established by the ambient

modulating region. That is, the more effective the medium is in establishing a gradient, the more responsive it will be to changes. Or, conversely, if no gradient is established, or the intensity is isotropic, then a local perturbation in the modulation parameter will, to first order, leave the intensity isotropic.

We will apply these results directly to our observations in later chapters. We should point out that if, indeed, the cosmic ray gradient has the form we assumed, measurements of μ/p at various energies would provide an indirect determination of the gradient and its energy dependence. Thus, we may indirectly test the theory to see if our results are in reasonable agreement with gradient observations.

1.6 Contribution of Discontinuities

The relationship between magnetic field fluctuations and particle propagation has implicitly assumed that the spectrum of magnetic irregularities as viewed by a spacecraft magnetometer is approximately equivalent to the spectrum sampled by the cosmic ray. This may not be a correct assumption if tangential discontinuities are significant in determining the shape and level of the magnetic field power spectrum. We shall examine this point.

Classes of hydromagnetic discontinuities have been described in a review article by Colburn and Sonett (1966), and discontinuous structures in the solar wind have been observed by a number of authors. The classes of discontinuities we shall be concerned with are either "rotational" or "tangential"; other discontinuous structures, such as fast or slow shocks, occur too infrequently to be of interest to this study.

A rotational discontinuity can be thought of as a sharp change in the magnetic field direction where the change occurs along the magnetic field line. Hudson (1970) has derived relations between the various plasma parameters for a rotational discontinuity from shock conditions. Since this discontinuity propagates at the Alfven velocity, it has been thought of as a sharply crested Alfven wave. A tangential discontinuity also involves a change in the magnetic field, but the change occurs normal to the magnetic field direction. This structure is non-propagating and can be thought of as separating two adjacent plasma regions in equilibrium.

Directional discontinuities in the magnetic field have been observed by Siscoe (1968) and Burlaga (1969). Their conclusions, with, respectively, Mariner 4 and Pioneer 6 data, are that discontinuities with changes greater than 30° generally occur on the order of one per hour, and are completed within 30 seconds. If these structures are basically tangential discontinuities, then the interplanetary medium might be considered as relatively disordered filamentary tubes of plasma, lying on top of each other, and transported radially outward by the solar wind.

Single spacecraft magnetometer measurements cannot distinquish between rotational and tangential discontinuities when the discontinuity takes place between successive averages. However, with simultaneous plasma data, one can determine if the discontinuity does or does not satisfy the rotational or "Alfvenic" shock conditions. Burlaga (1971) has done this for part of the Pioneer 6 data we will be utilizing in this study. He finds that during the early Pioneer 6 mission, (December 18 - December 25, 1965), less than 25% of the discontinuities can satisfy the "Alfvenic" criteria, and, therefore, the majority must be tangential.

For this study, therefore, we will assume that the majority of discontinuities will be tangential.

One would expect that, insofar as the low energy cosmic rays are concerned, rotational and tangential discontinuities should have different effects. A low energy cosmic ray, generally following the average magnetic field between rotational discontinuities should be strongly scattered when it encounters a discontinuity along the field line. However, if the discontinuities are tangential, the cosmic ray whose gyroradius is less than the average discontinuity separation may follow the field in the filamentary flux tubes and rarely encounter, or be scattered by the discontinuities. Let us examine this in more detail.

Assume that the field structure is basically turbulent or Alfvenic fluctuations separated by tangential discontinuities occuring on the order of one per hour, or of a typical cross section of $\ell_d \sim V_w \tau_d \sim 1.5 \times 10^{11}$ cm. A 70 MeV proton, whose rigidity is $\approx .36$ BV, has a gyroradius in the average interplanetary magnetic of 6×10^{-5} gauss of $\approx 2 \times 10^{10}$ cm or approximately an order of magnitude less than the average discontinuity separation. Clearly, it will rarely encounter a discontinuity except by drift or perpendicular diffusion processes. A relevant parameter we might consider would be the typical time for the cosmic ray to suffer a large angle scattering in the normal course of parallel diffusion. If the cosmic ray experiences numerous "scatterings" by the fluctuations between discontinuities before it encounters a discontinuity boundary, the discontinuities will have little effect, on the average, on the process of diffusion parallel to the magnetic field.

The time for a cosmic ray to suffer a large angle scattering in parallel diffusion is typically given by $\tau_s \sim K_{\parallel} / v_{\parallel}^{\ 2}$. For a 70 MeV

proton with $v_{\parallel} \sim .36c$, $K_{\parallel} \sim 2 \times 10^{21}$ cm^2/sec, (where $K_{\parallel}$ is an upper bound since it has contained the contributions of directional discontinuities, tangential or rotational), τ_s is approximately 15 seconds.

Drifts in the magnetic field will be represented approximately by the curvature drift velocity. This is given by $\vec{v}_c = v_{\parallel}{}^2/\omega_B r_c \, (\vec{r}_c \times \vec{B}/r_c B)$, where r_c is the radius of curvature and ω_B is the gyrofrequency. In terms of the particle gyroradius, this is approximately $v_c \sim v_{\parallel} \, R/Br_c$. For a 70 MeV (.36 BV) proton in a field of curvature radius 1 AU, $v_c \sim 1.5 \times 10^7$ cm/sec, and the time required to drift 10^{11} cm is approximately 2 hours, certainly over an order of magnitude greater than the 15 second scattering time.

Perpendicular diffusion, however, may be more effective. A particle will diffuse perpendicular to the average field a distance d in time $\tau_\perp \sim d^2/K_\perp$. For $K_\perp \sim 10^{20}$ cm^2/sec, and $d \sim 10^{11}$ cm, this implies $\tau_\perp \sim 100$ sec. With $\tau_s \sim 15$ sec, the particle should still suffer numerous scatterings before it "sees" a tangential discontinuity.

If we can estimate the contributions of the discontinuities and fluctuations between discontinuities to the power spectrum, we should be able to detect differences in modulation from these separate effects, assuming the discontinuities are basically tangential. Thus, by utilizing the considerations of the previous section, (1.5), as applied to the theoretical determination of diffusion parameters, we may for the first time, be able to directly test the relation of magnetic field power spectra to low energy cosmic ray propagation. We should also be able to test relative effectiveness of the discontinuities and the fluctuations between them in the scattering process.

CHAPTER II

2.1 Data

The magnetic field data used in this study were obtained by a flux-gate magnetometer aboard the Pioneer 6 satellite in 1965-1966. This experiment has been described in Ness et al. (1966), Scearce et al. (1968), and Ness (1970). Three orthogonal components of the magnetic field were sampled at an average interval of 1.5 sec with a quantization error of $\pm$ .25γ, (1 γ = 10^{-5} gauss). These measurements were then averaged over 30 sec intervals with a resultant precision of approximately $\pm$ .05γ. Typical interplanetary field values were 6γ. The 30 sec averages were utilized to compute the power spectra over twenty-four hour periods for approximately five solar rotations, December 17, 1965 - April 23, 1966.

The solar wind velocity measurements we employ were also obtained on Pioneer 6. This experiment has been described by Lazarus et al. (1966). We use only daily averages of the velocity in order to compute the diffusion coefficients. The precision of the daily averages is approximately given by their standard deviation. This was usually less than 7% of the average speed of 4×10^7 cm/sec.

The daily modulation parameters we computed from the Pioneer 6 data have been compared to particle measurements obtained simultaneously by the scintillator telescope on the IMP III satellite. This data has been kindly provided by Dr. Frank McDonald, and the experiment has been described by Kinsey (1969). For this study we have utilized measurements of the proton flux in three energy channels: 20-40, 40-60, and 60-80 MeV. These will hereafter be referred to by their average energies, 30, 50, and 70 MeV. The typical uncertainty on a daily averaged 70 MeV flux measurement was on the order of 25%.

During this study, IMP III was in orbit about earth, while Pioneer 6 was injected into a heliocentric orbit. From December 17, 1965 to April 23, 1966, Pioneer 6 fell from 1 AU to a heliocentric radius of .82 AU. As shown in Figure 3, the Earth-Sun-Pioneer angle is always less than 15 degrees. Considering both angular and spatial effects, a field line transported by the solar wind along the classic Archimedes spiral will intersect earth always less than .5 days after intersecting the Pioneer 6 satellite. Thus, we can essentially neglect the separation of the two spacecraft in comparing daily averaged IMP III proton fluxes and modulation parameters computed from Pioneer 6 data.

2.2 Measurement of Power Spectra

Unless otherwise specified, the power spectra we obtain were computed from finite Fourier Transforms of time series' correlation functions according to procedures given in Blackman and Tukey (1958). A computationally more efficient technique, the "fast Fourier Transform", would be more desirable if there were the absence of numerous data gaps. This method requires continuous data. Only isolated missing 30 second averages in the magnetic field data would permit extrapolation without seriously affecting the results. However, there are frequently large gaps in the data, and extrapolation in order to use the fast Fourier Transform is inappropriate. Therefore, we must employ the finite Fourier Tansform.

Our procedure is as follows: assume we have N data points, sampled at equispaced intervals Δt over the time interval $N\Delta t$. Since the data is digitized, we can only estimate the power spectrum in the frequency range of $0 - f_c$, where f_c is the cut-off or Nyquist frequency, $f_c = 1/2\Delta t$. We compute M autocorrelation lags on each field component's time series,

where the 1'th lag is given by:

$$R(\ell) = \left(\frac{1}{N-\ell}\right) \sum_{i=\ell+1}^{N} x_{i-\ell} x_i - \left(\frac{1}{N-\ell}\right)^2 \sum_{i=\ell+1}^{N} x_{i-\ell} \sum_{i=\ell+1}^{N} x_i \qquad (2.2.1)$$

If either x_i or $x_{i-\ell}$ is a missing data point, it is ignored in the summations, and the quantity $1/(N-1)$ is correspondingly reduced. Thus N in (2.2.1) is the number of actual measurements.

The autocorrelation function is used in computing M "smoothed" spectral estimates:

$$P(k) = \frac{2}{f_c} \left[\sum_{\ell=0}^{M=1} \frac{1}{2} \left(1+\cos \frac{\ell\pi}{M}\right) \cos \frac{k\ell\pi}{M} R(\ell) \right] \qquad (2.2.2)$$

Our smoothing function is $1/2\ (1+\cos\ \ell\pi/M)$, the "hanning" function. If $P'(k)$ is the k'th raw estimate, smoothing by the hanning function gives

$$P(k) = \frac{1}{2} P'(k) + \frac{1}{4} (P'(k-1) + P'(k+1)).$$

Each spectral estimate we compute is a measure of the power in the frequency range $(k - 1/2)\ f_c/M - (k + 1/2)\ f_c/M$, centered at $k\ f_c/M$, (except for the first and last estimates which sample the power from $0 - 1/2\ f_c/M$, and $(M - 1/2) f_c/M - f_c$, respectively). Since we have computed only for positive frequencies, we have the factor of 2 times the summation. This gives the normalization that the sum of each spectral estimate times its bandwidth is equal to the total power or variance in the time series.

Since we are dealing with a non-infinite, digitized data set, we do not have the one-to-one correspondence in the time and frequency domain which is obtained with continuous data of infinite extent. Instead, each power spectral computation is aptly called an "estimate" over some frequency range. Each estimate has an associated degree of freedom, $\nu = 2N/M$. From a multiple of a chi-square variate at the equivalent degree of freedom one can compute the degree of statistical confidence in each spectral estimate. Because the greater our degrees of freedom, the greater our "confidence", we try to compute the spectrum with as high a ν as possible, without sacrificing resolution in the frequency domain. Clearly one of the effects of missing data is to decrease the degrees of freedom at constant M and to increase the errors in the spectral estimates.

Digitizing may also present problems in spectral analysis from noise and aliasing. The quantization noise of the magnetometer aboard Pioneer 6 is 0.13 γ^2/Hz. This is quite low relative to the spectral levels we shall be considering and manifests itself in a flattening of the power spectrum when the Nyquist frequency, f_c, is approached.

Aliasing, however, may be more serious. This occurs when the bandpass of the instrument is greater than the Nyquist frequency. For Pioneer 6 the bandpass is from 0-5 Hz while the Nyquist frequency for the 30 second averages is $f_c = 1.67 \times 10^{-2}$ Hz. Signals for frequencies greater than the Nyquist frequency, but lower than the instrument bandpass, are "aliased" to lower frequencies. It is easily shown that power at frequency f will have contributions from frequencies $(2n\ f_c - f)$ and $(2n\ f_c + f)$ where n is an integer greater than one. The possibility that aliasing can cause error in our spectral estimates cannot be eliminated.

If the spectrum falls off rapidly with frequency, the effects of aliasing can be assumed to be fairly small. Typically, spectra we observe at high frequencies, (up to 1.6×10^{-2} Hz), fall off close to f^{-2}. Aliasing, therefore, should not be too significant. Russell (1971) has shown that with a high instrument bandpass to Nyquist frequency ratio, aliasing of even an f^{-2} spectrum might be significant down to frequencies as low as $f_c/2$, as a worst case. When we make power law fits to the spectra necessary in computing the diffusion coefficients, we only use estimates up to frequencies $f_c/2 \sim 8 \times 10^{-3}$ Hz. For a 70 MeV proton we are concerned with frequencies of $f \sim V_w \bar{B}/2\pi R \sim 3 \times 10^{-4}$ Hz, which are much smaller than $f_c/2$. By utilizing estimates only for frequencies lower than $f_c/2$ in computing diffusion coefficients, we should then be negating any effects due to quantization noise and aliasing.

In limited cases we have used the method of nested variances to obtain spectral estimates over broad frequency bands. This provides ease and speed of computation but introduces a large loss in frequency resolution. The conception is rather simple. The variance of the time series represents the observable power between 0 and f_c, the cutoff frequency. If the time series is ergodic, i.e. stationary, then the variance of that series averaged in twos should be representative of the power in the range $0 - f_c/2$. Likewise for the range $0 - f_c/4$ for averages in consecutive groups of 4. We can use these to compute the power spectrum. If we take L averages of 2^L length, the l'th spectral estimate, representing the power in the range $f_c/2^{L-(\ell-1)} - f_c/2^{L-\ell}$ will be

$$P_\ell = \frac{1}{Nf_c}\left[2\sum_{i=1}^{N/2^{L-\ell}}\left(\sum_{j=2^{L-\ell}(i-1)+1}^{2^{L-\ell}i} X_j\right)^2 - \sum_{i=1}^{N/2^{L-(\ell-1)}}\left(\sum_{j=2^{L-(\ell-1)}(i-1)+1}^{2^{L-(\ell-1)}i} X_j\right)^2\right] \qquad (2.2.3)$$

except for the first estimate which will be

$$P_1 = \frac{2^{2L-2}}{Nf_c}\sum_{i=1}^{N/2^{L-1}}\left(\sum_{j=2^{L-1}(i-1)+1}^{2^{L-1}i} X_j/2^{L-1}\right)^2 \qquad (2.2.4)$$

where each average in (2.2.3) and (2.2.4) is weighted corresponding to the number of missing data points. This is equivalent to the method of Jokipii and Coleman (1968).

These will give rough, broad band spectral estimates over large frequency ranges. Here the ranges go in inverse powers of two of the Nyquist frequency, whereas the finite Fourier Transform method provides equi-spaced spectral estimates. We only employed the nested variance analysis to determine the power at low frequency and estimate the perpendicular diffusion coefficients. In that case we used 13 estimates (L = 13) with a frequency range 2×10^{-6} to 1.6×10^{-2} Hz (Figure 4).

2.3 Selection of Discontinuities

Since this study covers approximately five solar rotations, selection of the microscale directional discontinuities in the interplanetary magnetic field had to be accomplished with computer assistance. We used various

techniques for identifying the discontinuities by computer and found that these would identify essentially the same set of discontinuities that were obtained by previously established techniques relying on both computer and visual determination. After we were satisfied that the subjective visual criteria did not significantly alter our results, all discontinuity selection was accomplished automatically via the computer, removing personal bias.

For both historical and physical reasons we select discontinuities with the criteria established by Burlaga (1969). There, discontinuities were defined by a change in the field occurring within the 30 second averaging period in the Pioneer 6 data and resulting in a greater than 30° change in the magnetic field direction. The field both before and after the discontinuity was required to be relatively undisturbed, and thus the discontinuity would appear to be a "step-function".

Siscoe et al. (1968) showed from higher resolution Mariner 4 data that directional discontinuities have a "thickness" on the order of 4×10^8 cm, or are completed within 10 seconds. We therefore use Burlaga's 30 second criteria to avoid selecting longer period phenomena, which would most likely be wave structures which would be "seen" by the 70 MeV protons.

We also set the 30° change as a minimum. We do this first because smaller changes are difficult to distinguish from the ambient fluctuations in the field. Secondly, Burlaga (1969) found that a small discontinuity tends to occur more frequently than a large angle discontinuity, with an occurrence frequency proportional to $\exp[-\omega^2]$, where ω is the angle between the magnetic field vector before and after the discontinuity. Small discontinuities occur on the average of one per hour, or at a separation of 10^{11}cm. If we selected those discontinuities smaller than

30°, these would, supposedly, occur at even smaller separations, on the order of the 70 MeV protons' gyroradii. These discontinuities would then contribute to the protons' scattering, regardless of whether they were tangential or not.

Before the discontinuities were identified, noise points had to be filtered out of the data. Such points, which would be seen as delta functions in the data, were generally obvious and infrequent. They were eliminated since such delta functions would give a large, white noise contribution to the power spectra. Only three 24 hour periods during the five solar rotations were considered so noisy that their spectra were ignored in our results.

The fifty largest successive differences in the coordinate and magnitude data for each day were examined for "noise". The maximum allowable difference for each coordinate was set when noise data was visually indistinguishable from fluctuations. The data was then re-processed removing data points whose difference between the point previous was greater than the permitted maximum. A data point removed in one coordinate was also eliminated in the others. On quiet days there was no problem in distinguishing noise. For disturbed days, if there was doubt, we allowed the data.

After bad data was eliminated, each day's discontinuities were identified in the 30 second average Pioneer 6 data. The data was originally in solar ecliptic format with X_{SE} the vector from the spacecraft to the sun, Z_{SE} out of the ecliptic, and Y_{SE} completing a right-handed system. We used the following procedure:

(1) Each magnetic field average was rotated into the vector system (F,θ, ϕ), where F was the magnitude, and θ and ϕ the direction out of, and in the ecliptic plane, respectively. The angular change, ω, between each successive 30 second average was computed from,

$$\cos \omega = \cos\theta_1 \cos\theta_2 \cos(\phi_1-\phi_2) + \sin\theta_1 \sin\theta_2 \qquad (2.3.1)$$

The time gap between successive vectors had to be 30 seconds and $\omega \geq 30°$ for a discontinuity to be chosen and to be subjected to further tests.

(2) Only discontinuities occurring in relatively continuous data were kept. Thus, those points which had a change $\geq 30°$, but had data missing within 2 points (one minute) before and 2 points after the change were rejected. This was done since those points were required for further tests.

(3) We tested to see if the discontinuity was imbedded in large changes. Thus, discontinuities for which the vector change between either two points before and two after were greater than 45° were also rejected.

(4) We required that change be relatively constant or linear. That is, the change in the vector field calculated from the average of two points before the discontinuity and two points after must also satisfy the $\geq 30°$ change criterion.

(5) Since the change could be occurring between the 30 sec. averaging period, two successive discontinuities, (double discontinuities), which satisfied the preceeding criteria, would be permitted. Any other discontinuities occurring within a two minute period caused the rejection of

both. This eliminated step-step or box-like structures which would more likely be waves than tangential discontinuities. The times of the discontinuities which passed all these tests were then saved for later referral.

We compared the discontinuities we chose via this program to those selected by Burlaga (1969) using both computer and visual criteria with a limited period of the Pioneer 6 data. For the comparable 24 hour periods, the two sets of discontinuities were almost identical, with only an average of one to two different choices. Thus, our computer criteria was judged to be essentially identical to Burlaga's.

Burlaga (1971), using three separate data periods from Pioneer 6, found that the number and characteristics of the discontinuities do not change significantly from 1 to .8 AU. We have calculated the discontinuities over the same periods continuously and arrive at similar conclusions. Table 1 gives a representation of the number of discontinuities $\geq 30°$ as a function of heliocentric radius. Given are the six 27 day averages and standard deviations of the number of discontinuities per day for those days where at least half the 30 second data is present. This is presented with the corresponding Earth-Sun-Pioneer angle and heliocentric radii over that period. In agreement with Burlaga (1971) we see that the frequency of occurrence of discontinuities does not change appreciably. The average is 28 discontinuities per day or 1.1 discontinuities per hour.

2.4 Calculation of Power Spectra

Since the theory relating diffusion parallel to the average field depends on the power spectra of fluctuations perpendicular to the field, we rotate the solar ecliptic magnetic field data into a coordinate system

aligned with the field. For each 24 hour period, we define the Z axis to be along the average magnetic field direction. Our other two axes are arbitrary. We choose the X axis to be in the ecliptic plane. Since this axis will be perpendicular to both the Z axis and the Z_{SE} (solar ecliptic), it will be either in the $\vec{Z} \times \vec{Z}_{SE}$ or $\vec{Z}_{SE} \times \vec{Z}$ direction. We arbitrarily choose the direction $\vec{Z} \times \vec{Z}_{SE}$. The Y axis completes a right handed system. The power spectra P_{xx} and P_{yy} will then represent fluctuations perpendicular to the average field direction.

We would like to derive not only the power spectra from the real field, but also the contributions of the discontinuities and the fluctuations between discontinuities. Sari and Ness (1969) showed that a time series based on step functions generated by discontinuities could, at times, duplicate the spectra of the real field. They used discontinuities greater than 15° and found a one to one correspondence in the step function spectra and real spectra during quiet field conditions. We employ the same technique here.

After the field has been rotated from solar ecliptic to field aligned coordinates, the discontinuities previously identified from the methods of section 2.3 are used to calculate a simulated time series for each coordinate, X, Y, Z, and field magnitude F. Each simulated 30 sec average is given a constant, (initially zero), value until an identified discontinuity in the real data is reached. When one is, the difference between the average value of the true field two points before, (1 minute), and two points after is added to the constant value. This value remains constant until the next discontinuity is reached. The resultant time series then resembles a set of step functions. These series are used to calculate the "discontinuity" power spectra.

Two different methods were employed to determine the spectra of the fluctuations between discontinuities. We first tried the method used in Sari and Ness (1970) of spectra from nested variances for the periods between discontinuities. Although this gave adequate results, it gave poor frequency resolution, and comparison with discontinuity spectra proved difficult. One could simply compute the difference between the real and "discontinuity" spectra for the "between" spectra, but this gives no comparison of the adequacy of either "discontinuity" or "between" spectra. It was felt that the best results occurred when one computed the spectra of the real time series with the discontinuities subtracted.

This "between" series was computed in the following manner. The rotated data was used as measured until the minute before the first discontinuity occurred. The difference between the average value of the field coordinate two points before and two points after the discontinuity was subtracted from all the data points following the discontinuity, until the next discontinuity was reached, and the same method applied.

Since subtracting the value of the discontinuity from the points immediately preceeding or following might give rise to either sinusoidal fluctuations or delta functions at a discontinuity, a special technique was employed for calculating the data at a discontinuity. After the discontinuity had been subtracted a linear fit between two data points (1 minute) before and two after the discontinuity was computed. The values of the fit at 30 second intervals were computed and substituted for the component values at the discontinuity. It was found that this substantially improved the results, such that the ratio of the power from discontinuities to real power at some frequency, plus the similar ratio of between power to real power was usually close to 1.

Power spectra were then computed for the real, between and discontinuity time series for each component, (X, Y, Z), and field magnitude F in the field aligned system. Each spectra covered 24 hours of data for the period of December 17, 1965 to April 30, 1966, approximately 5 solar rotations. One hundred twenty spectral estimates were calculated for each time series. This gave a high equivalent degree of freedom, while retaining good frequency resolution. If all the data in one day were present, N=2880, the equivalent degree of freedom per estimate, $\nu = 2N/M \approx 48$. This implies that we have 95% confidence that each estimate's true value lies between 1.5 and .75 times its calculated value. Days where enough data was missing such that $\nu < 15$, were rejected as giving unreliable spectra.

The spectra then represented 120 equi-spaced estimates of the magnetic field energy in the frequency range $0 - f_c$, or $0 - 1.67 \times 10^{-2}$ Hz. Each estimate covered the bandwidth of 1.38×10^{-4} Hz and was centered at frequencies $k(1.38 \times 10^{-4})$Hz, $k = 0,\cdots 120$.

As had been observed in previous studies, the power spectra could generally be represented by a power law dependence on frequency, $A f^{-\alpha}$, where α typically varied in the range $1.5 < \alpha < 2.0$. Spectra calculated from the discontinuity series and the series representing fluctuations between discontinuities tended to have separate and relatively characteristic frequency dependence. As discussed in Siscoe et al. (1968) the power spectra of an ensemble of discontinuities will vary as f^{-2} at frequencies greater than the frequency corresponding to the average separation between discontinuites. This was observed by Sari and Ness (1969, 1970) for a limited sample of Pioneer 6 data, and our results

over this larger sample were the same. The average slope of the discontinuity spectra was $\alpha = 1.95$.

The power spectra from the fluctuations between discontinuities, however, had an average slope of $\alpha = 1.65$. This was also noted in Sari and Ness (1970) using the cruder technique of nested variances to compute the spectra. This is interesting since this is almost precisely the slope (-5/3) corresponding to Kolmagoroff's analysis of homogeneous turbulence in the regime of high Reynolds numbers, (Batchelor, 1960).

Power spectral slopes for the real data generally varied between the flatter slopes characteristic of the fluctuations between discontinuities and the steeper slopes associated with the discontinuties. The average value of the slopes of the coordinate (X, Y, Z) spectra of the real data was $\alpha = 1.71$. During days of quiet field conditions, characterized by low values of the geomagnetic activity index K_p, and clearly observable discontinuities separating regions of relatively constant ambient field, the real spectra tended to have the steep slopes similar to discontinuity spectra. During disturbed periods, the real spectra had flatter slopes similar to the "between" spectra. Although disturbed periods were characterized by more frequent discontinuities, at these times the activity in the field between discontinuities is also much greater. This should account for the greater influence on the real spectra apparently exercised by the between spectra during disturbed times.

Since disturbed periods have power levels nearly an order of magnitude greater than quiet times, they tend to dominate spectra obtained over long periods. This is shown in Figure 4 for power spectra taken over

10 days in 1965-1966 using the method of nested variances. At frequencies greater than 10^{-4} Hz the spectral slopes are -5/3, typical of the fluctuations between discontinuities.

We should like to determine how accurately the power spectra of the time series we generated from the discontinuities and fluctuations between discontinuities represent their contributions to the real spectra. Figure 5 shows a representative period with the real, discontinuity and between spectra for the components and field magnitude. The average value of K_p was 1- , and the number of discontinuities that day was 20. The real spectra is seen to have a slope intermediate to the between and discontinuity spectra. The discontinuity spectra, having a steeper slope, is seen to have a relatively larger contribution at low frequencies, (appropriate for a 70 MeV proton), while the between spectra shows better correspondence at higher frequencies.

Both discontinuity and between spectra show inordinately large power in the first two estimates. We can attribute this to the random nature of discontinuous changes in each separate component. The addition or subtraction of these changes to the component values of the discontinuity or between series causes an artificial random walk away from the average field value in each component which does not occur in the real field (which is constrained to an average value). This random walk causes an addition of power in the simulated series at frequencies below the average occurrence frequency of the discontinuities, $f_d \sim (3.6 \times 10^3 \text{ sec})^{-1} \sim 2.8 \times 10^{-4}$ Hz. If we take the ratio of the total power in each component's spectra from the simulated series to the real spectra for frequencies higher than f_d, we should get an estimate of how good our representation is. For the spectra in Figure 5 the ratio between the total power in

each component for the discontinuity to real, P_D/P_R, and between to real P_B/P_R, for frequencies greater than f_d is given in Table 2. The ratio of $P_D/P_R + P_B/P_R$ for each component is close to one. We have calculated this ratio for each component for each day in our five solar rotations. We find that the average value of $P_D/P_R + P_B/P_R$ summed over all three components for each day is 1.16 ± .03. Thus, we feel that our representation of discontinuity and "between" contributions gives an apt description of the true physical processes.

On the average, the value of $1/3 \sum_{X,Y,Z} P_D/P_R$ was .25. However, the spectra of discontinuities is generally steeper than the real. Hence, at low frequencies, corresponding to the frequencies sampled by 70 MeV protons, the contribution of discontinuities was greater than 25%, usually on the order of 40%. Figure 6 shows the value of $1/3 \sum_{X,Y,Z} P_D/P_R$ as a function of the number of discontinuities ($\geq$ 30°) per hour for each day's data. There appears to be a definite tendency for a greater contribution from discontinuities when more are observed. However, as mentioned before, more frequent discontinuities are often observed at more disturbed periods when the relative contributions of fluctuations between discontinuities may also be greater. Thus, a good deal of scatter is seen in Figure 6.

As had been noted in previous studies, spectral levels of the real data for fluctuations in the field magnitude were usually an order of magnitude smaller than corresponding levels in the real component spectra. Likewise, the levels of the X and Y spectra, representing fluctuations normal to the average field, were generally greater than levels of the Z component spectra. These results imply that the fluctuations are basically transverse.

As the Pioneer 6 spacecraft went from 1 to .8 AU no significant change was noted in the average slopes of the real, discontinuity and between

spectra. Table 3 shows 27 day averages of the slopes of the X (ecliptic) component spectra for the real, discontinuity and between data and the standard deviations. On the other hand, the change in the power levels of all spectra from day to day was often an order of magnitude. Figures 7 through 11 show contour plots of the real spectra over the five solar rotations. Here the spectra are over 12 hour periods, with 60 estimates per spectra, (leaving $\nu \approx 48$). Time is plotted on the horizontal and frequency (Hz) on the vertical. The spectral densities are plotted in shadings of 6 powers of 10 with solid representing 10^5-10^6 γ^2/Hz. Also plotted is the average solar wind velocity for each 12 hour period, δV_w, the number of discontinuities and K_p. Dashed vertical lines represent sector boundaries between regions where the interplanetary field is generally outward, +, and inward, -. On a 27 day basis we see that the average power levels do not seem to change, implying that the fluctuations are essentially constant from .8 to 1 AU.

On a day to day basis much variation is observed in the spectral levels. Periods of high power are generally located at or near sector boundaries. One excepts somewhat higher power at a sector boundary since it entails a large angular change in the field. However, the increase is over longer periods, with some indication that there is more power before than after a boundary passage. The increase of fluctuations over a large area near a sector boundary is consistent with the association of sectors near active regions on the sun. This is seen during the Pioneer 6 data when one transposes the sector boundary to the central meridian passage of magnetic active regions. The possible asymmetry in the power about the sector is consistent with a recent

observation by Sakurai and Stone (1971) where they note that type I radio noise is generally associated west of where one would expect the solar origin of the sector boundary. Their interpretation was that the field structure above the active region where the sector boundary originates is inclined to the east. Our results are not definitive enough to draw the same conclusion. However, they do show that the fluctuations in the magnetic field can be related to photospheric disturbances.

2.5 Calculation of the Diffusion Coefficients

In order to calculate the parallel diffusion coefficients by Jokipii's formulation (1968b, 1971) the slope of the spectra as well as their magnitude are needed. We therefore fit all the spectra, real, discontinuity and between to a least square power law in frequency, $P(f) = Af^{-\alpha}$. Since at frequencies below the average separation of discontinuities, f_d, there occurs anomolous power in the simulated time series as discussed above, we use only estimates greater than k = 3 or $f = 4 \times 10^{-4}$ Hz in calculating fits to the between and discontinuity spectra. Since aliasing may be a factor, only the first 60 estimates, $f \leq f_c/2$, are used in the fit. Using the average magnetic field value and solar wind velocity for each day the diffusion coefficients $K_{\parallel}$ are then calculated from (1.3.13) for 30, 50, and 70 MeV protons from the real, between and discontinuity spectra.

The parallel diffusion coefficients depend on the fluctuations perpendicular to the average field. Since the spectra $P_{xx}(f)$ and $P_{yy}(f)$ may not be equal, we compute K_{xx} and K_{yy} individually. We then use the average of the two for the parallel diffusion coefficients for the three data sets, $K_{\parallel} = 1/2(K_{xx} + K_{yy})$. Table 4 gives diffusion

coefficients computed at 50 and 70 MeV for the real, discontinuity and between data for five solar rotations.

Jokipii (1971) notes that when applying the diffusion coefficients to the modulation equations one should properly use the transformation:

$$K_{rr} = K_{\parallel} \cos^2\psi + K_{\perp} \sin^2\psi \qquad (2.5.1)$$

where ψ is the angle between the solar wind velocity and the spiral direction of the field. This results from the rotation from a system along the field to one along the radius vector. From section 1.3 and Jokipii (1971), $K_{\perp} << K_{\parallel}$ which implies

$$K_{rr} \approx K_{\parallel} \cos^2\psi \qquad (2.5.2)$$

However, this assumes that the fluctuations as observed by the spacecraft and applied to $K_{\parallel}$ are the same seen by the particle. A simple consideration shows this is not so. Assume that all the fluctuations in the field are transverse to the average field and are polarized in the ecliptic plane, (the same argument will hold if the polarization is out of the ecliptic); then $P_{ij}(f) = P_{xx}(f)$. Let us also assume momentarily that the actual fluctuations are monochromatic, with a single wavelength λ, (this will hold for all wavelengths). If the wavelengths are frozen into the wind and convected past the spacecraft, where the angle between the field and the solar wind is ψ, the observed wavelength seen by the spacecraft is not equal to the real. Instead the observed wavelength is

$$\lambda_{obs} = \lambda/\cos\psi \qquad (2.5.3)$$

and the observed frequency

$$f_{obs} = (\cos\psi) \cdot f \tag{2.5.4}$$

Since the diffusion coefficient is proportional to f^{α}, the observed K will be related to the real in the frame of the field as

$$K_{obs} = (\cos\psi)^{\alpha} \; K_{\parallel} \tag{2.5.5}$$

This holds for all frequencies and polarizations in and out of the ecliptic, thus, the diffusion coefficient we should be using in (2.5.2) is

$$K_{rr} \approx K_{\parallel} \; \cos^2\psi = K_{obs} \; (\cos\psi)^{2-\alpha} \tag{2.5.6}$$

For this study α typically is between 1.6 and 2.0 and ψ is close to 45°. Thus, $K_{rr} \hat{\approx} K_{obs}$ and we shall assume that the values of K we have computed are a good approximation to what should be applied to the modulation equations.

CHAPTER III

3.1 Relation of Changes in the Modulation Parameter to Changes in the Particle Flux

Having obtained the diffusion coefficients for the Pioneer 6 data, we are now prepared to compare changes in the relevant parameters, V_w, K, and V_w/K to changes in the proton fluxes at average energies of 30, 50, and 70 MeV (20-40, 40-60, 60-80 MeV) as observed concurrently on the IMP III satellite. According to the considerations of section 1.5, we expect changes in the particle flux to be negatively proportional to changes in V_w/K. Since these results also indicate that the particle flux does not relax to equilibrium following a change in V_w/K until approximately 0.3 day has passed, we shall average all data by 3 days in order to be confident that the time derivative in the Fokker-Planck equation can be ignored. Unless otherwise stated, all following results represent 3 day running means of both propagation parameters and particle fluxes.

Since we are concerned with modulation of galactic particles, days which indicate the presence of solar flare or plage effects are not included in the flux averages. For instances where the effects of a large flare are not immediately obvious we use as an indicator of a "non-quiet" day the criteria of large increases in all energy channels with a greater intensity at 50 MeV for protons than at 70 MeV, (in general under quiet conditions $j(50\ \text{MeV}) < j(70\ \text{MeV})$). The excluded days for the three channels and additional days for the 30 MeV data are given in Table 5. The remaining data are used in the averages if at least two of the three days in each averaging period are present.

C-2

In Figure 12 we plot our results for the three day running means of the 70 MeV proton flux, (top line), and the means of V_w/K, where K is calculated for 70 MeV protons from the real, between and discontinuity magnetic field times series, (second, third and fourth lines). The values of V_w/K are multiplied by a characteristic heliocentric radius, $\tilde{R}$ = 1 AU. Since we expect that changes in $V_w\tilde{R}/K$ to be anticorrelated with changes in j(70 MeV), we plot the negative of $V_w\tilde{R}/K$. The heavily dashed lines are to indicate trends, and the lightly dashed lines are the standard deviations. The vertical dashed lines are included for ease of following simultaneous changes in j(70 MeV) and the various $V_w\tilde{R}/K$'s. On the bottom line the daily contribution of the discontinuities to the total power in the magnetic field components are plotted.

Inspection shows that in the first part, Dec. 17 - Jan. 25, and, interestingly enough the last half, Feb. 22 - April 23, when the spacecraft are most separated, changes in the particle flux are correlated with changes in $-V_w\tilde{R}/K$, as predicted. It is obvious that the correlation extends to changes greater than statistical error, and that the best correlation exists between changes in j(70 MeV) and $-V_w\tilde{R}/K$ where K is calculated from the power spectra of the fluctuations between discontinuities. It is not surprising that if changes in j(70 MeV) are correlated with one of the series of $V_w\tilde{R}/K$ it should be correlated with the others as well, since all include parameters in common, such as V_w and $\bar{B}$.

The times when the correlation breaks down, notably for the ten days centered at Feb. 11, are characterized by generally quiet field conditions where the real power spectra are often dominated by the discontinuities.

Here the particle flux is decreasing to a minimum on Feb. 10, increasing to maximum on Feb. 13, and decreasing to a minimum on Feb. 16. During these times $-V_w \tilde{R}/K$ computed from the real and discontinuity power spectra vary in the opposite manner. Only the relevant modulation parameters calculated from the fluctations between discontinuities vary in the same manner as the proton data.

At other times, Jan. 26 - Feb. 5, and Feb. 17 - Feb. 22, the changes are neither clearly correlated or anticorrelated, within experimental error.

In Figure 13 we plot significant changes in the flux during periods greater than our three day smoothing time as a function of corresponding changes in the modulation parameters. Nineteen such periods are identified and plotted. Changes in the 70 MeV flux are plotted on the horizontal and simultaneous changes in $V_w \tilde{R}/K$ for the real, between, and discontinuity data are plotted on the vertical. For visual convenience, only the minimum and maximum error bars are included. We see that for all three series the points tend to fall in the second and fourth quadrants, implying an anti-correlation between changes in $V_w \tilde{R}/K$ and changes in the proton flux. However, only variations calculated from fluctuations between discontinuities are, within errors, consistently anticorrelated with changes in the flux. The dashed line in the "between" graph in Figure 13 is within all the errors, and the indication of a linear relation is consistent with the results of section 1.5, particularly equation 1.5.20.

If both the fluctuations between discontinuities and the discontinuities themselves contributed to the scattering process, we would expect that the best anticorrelation in changes of the particle flux would be with changes in the "real" parameters, with poorer anticorrelation with the between and

discontinuity parameters. However, we clearly see that the poorest relation is with the discontinuity parameters and the best, (and only consistent one), with the between. Thus, we conclude that it is basically the fluctuations between discontinuities which are scattering the 70 MeV protons, a result to be expected if the discontinuities are tangential rather than rotational.

In Figure 14 we plot the 70 MeV flux, but now with the diffusion coefficients and the solar wind velocity. Since we expect changes in the flux to be correlated to changes in K, and anticorrelated to changes in V_w we plot +K, (real, between and discontinuity), and $-V_w$. As before, we see that changes in the particle flux are best correlated with changes in K calculated from the fluctuations between discontinuities, especially after Feb. 1, when the correspondence is almost one to one. What is more interesting is that after Feb. 1 there is essentially no correspondence between changes in the particle flux and $-V_w$. This does not invalidate our previous conclusions, since theory predicts a relation between flux and V_w/K, not V_w or K separately. It does, however, indicate the relation between power spectra and diffusion coefficient holds at least down to 70 MeV, since the particles are clearly responding to changes in the diffusion coefficient, rather than solely to changes in the wind velocity.

Further evidence of our conclusions that it is the fluctuations between discontinuities causing the scattering is shown in Figure 15 where we plot the flux of the 30 and 50 MeV protons against $-V_w\hat{R}/K$ for the real, between and discontinuity series calculated for 50 MeV. From Dec. 17, 1965 to March 3, 1966, the correlation between changes in j(50 MeV), (second line) and $-V_w\hat{R}/K$ (Bet), (fourth line), is, within errors, consistent with an anticorrelation between $\Delta V_w\hat{R}/K$ (Bet) and Δj.

A poorer correlation between $V_w\tilde{R}/K$ (Real), and V_wR/K (Discontinuity), (third and fifth lines), is also evident.

After March 3, any correlation breaks down, and the large changes in $V_w\tilde{R}/K$ in April are not reflected in the 50 MeV proton flux. However, this may be the result of statistical fluctuations in the flux measurements. The 40-60 MeV differential intensity is the minimum of the low energy cosmic ray proton spectrum, and probable errors in the particle measurements are large. Therefore, it is difficult to make definite conclusions in this energy range.

For the 30 MeV channel, (20-40 MeV), statistics are better since the spectrum has turned up. Here, the lack of correlation between any of the $-V_w\tilde{R}/K$'s and j(30 MeV) is evident. Although our analytical perturbation solution of the Fokker-Planck equation in section 1.5 does not hold at the low energies, where the proton intensity spectrum no longer has the slope of +1, we still expect changes in flux to be anticorrelated to changes in $V_w\tilde{R}/K$. Instead, while the modulation parameters exhibit large changes, the quiet time 30 MeV flux is comparatively constant. This result is subject to two interpretations. First, the relationship between the magnetic field power spectrum and particle propagation parameters might be breaking down below 40 MeV, as suggested by Jokipii (1972). Or secondly, as suggested by Kinsey (1969) in analysis of IMP III and IMP IV data, such low energy protons are basically of solar origin. If so, the processes which produced a continuous component of high energy solar protons might be unrelated to the processes which cause fluctuations in V_w/K, thus causing the lack of correlation. Future studies might resolve this by accurately measuring the radial gradient of the proton flux below 30 MeV to determine whether or not the particles are solar.

We summarize our results for all three energy channels in Figures 16 through 18. Here we plot the normalized cross-correlations between the day to day changes in the three day averaged particle fluxes and the $V_w \partial R/K$'s and K's. Changes in the particle flux $\Delta j(t)$ are correlated between $\Delta V_w \partial R/K(t+\tau)$ and $\Delta K(t+\tau)$ where $\tau = 1, 2 \cdots$ days.

In Figure 16 we seen the results for the 70 MeV channel. As expected, there is an anticorrelation between flux changes and $\Delta V_w \partial R/K$, and a positive correlation between flux and K, with the best correlation with the "between" parameters. However, we note that the main peaks all occur when $\tau = 2$ days. Although the fact of our 3 day averaging causes an uncertainty of ± 1 day, the time delay in the changes in flux followed later by the appropriate changes in the modulation parameters is observable in the unaveraged data as well. This implies that the particles are responding to modulation changes between the earth and the sun, since changes in the modulation parameters are expected to be convected outward at the solar wind velocity. The fact that the Pioneer 6 satellite, from which we determine the modulation parameters, is slightly closer to the sun than IMP III reinforces this conclusion. Since we assume that the 70 MeV protons are of galactic origin, this seems at first an unexpected result.

A possible explanation may be provided by Fisk et al. (1972). They find that because the low energy proton intensity spectrum has a slope of +1 in a regime where the effects of adiabatic deceleration are important, it implies that the low energy protons we observe at 1 AU have, on the average, come into the solar system at higher energies, traveled to heliocentric radii less than 1 AU, and been scattered and convected back outward. Although their model for the radial variation of K is different

than we observe, their results do imply that the low energy galactic particles should respond to changes in the modulation parameters between 1 AU and the sun, changes we should observe after the corresponding changes in the particle flux.

As seen before in Figure 13, the results of Figure 16 show that the strongest anticorrelation with Δj (70 MeV) is from $\Delta V_w \tilde{R}/K$ (Bet), and the strongest correlation with ΔK (Bet); the poorest correlations are with the discontinuity parameters. The approximate seven day periodicity in the cross-correlations resulting in positive peaks at +5 and -2 days essentially reflects the quasi-sinusoidal periodicity in both the changes in flux and modulation parameters.

In Figures 17 and 18 we see the decreasing correlations in the 50 MeV and 30 MeV fluxes. The results for 50 MeV tend to show best correlations when $\tau = -1$. However, as mentioned before, there is an uncertainty of $\pm$ 1 day. The lower correlations may be the result of some combination of either poorer statistics, solar contamination or diffusion coefficient breakdown. On the other hand, the results for the 30 MeV protons in Figure 18 show zero correlations. Since statistics are better, this is the result of either solar contamination or breakdown in the fomulation of diffusion coefficients.

In Figure 19 we plot the values of $\Delta V_w \tilde{R}/K$ (Bet) (t+2) and Δj(70 MeV) (t). As suggested by the error bars in Figure 12 there is a good deal of scatter in the day to day changes, as opposed to the trends of 3 days or more. This is due to statistical fluctuations. The correlation coefficient is -0.25 and the mean regression coefficient is -0.35. The least square fit is indicated by dashed lines. The standard "t" test implies 90% confidence that a trend exists.

We have shown that changes in the 70 MeV proton intensity are anti-correlated to changes in the modulation parameters. These results will now be related to the theoretical considerations of section 1.5. Recall from (1.5.20) that if the cosmic ray gradient near 1 AU was independent of radius, $(r/U_o)\partial U_o/\partial r = n_o(T/T_o)^{\sigma}$, and the relative change in the modulation parameter depended only on energy, and had the form $p = p_o(T/T_o)^{-\gamma}$, the relative change of particle density, (or flux), was related to relative change in modulation parameter by

$$\mu(T) = \frac{3}{4}\frac{n_o p_o}{\sigma-\gamma}(T/T_o)^{\sigma-\gamma} \tag{3.1.1}$$

or, in terms of the definition of μ and p, at $T = T_o$,

$$\frac{\Delta U}{\langle U\rangle} = \frac{3}{4}\frac{n_o}{(\sigma-\gamma)}\frac{\Delta V_w \tilde{R}/K}{\langle V_w \tilde{R}/K\rangle} \tag{3.1.2}$$

We have measured ΔU versus $\Delta V_w \tilde{R}/K$, and since we know $\langle U\rangle$ and $\langle V_w \tilde{R}/K\rangle$ we can see if our results are consistent with measurements of the cosmic ray radial gradient at 70 MeV, n_o, and its energy dependence, σ.

First, we must be able to make a reasonable estimate as to the values of γ. From the definition of p we have

$$\frac{V}{K} = \left\langle \frac{V}{K}\right\rangle (1+p), \quad \text{or}$$

$$p = \frac{V}{K}\left\langle \frac{K}{V}\right\rangle - 1 \tag{3.1.3}$$

The theoretical relation of power spectrum to diffusion coefficient given in (1.3.13) states that if the power spectrum varies as $f^{-\alpha}$, the diffusion coefficient will vary as $\beta R^{2-\alpha}$. Thus, the rigidity dependence of p will be $R^{\langle\alpha\rangle-\alpha}$. Since $\langle\alpha\rangle = 1.7$, and α is observed to vary between 1.4 and 2,

p will have a rigidity dependence $R^{-\cdot 3} < p < R^{\cdot 3}$. At 70 MeV, a proton's rigidity and energy dependence is related by $R \alpha T^{\cdot 52}$. This implies that γ will typically have a value of $-.15 < \gamma < .15$.

From Figure 13 we should be able to estimate the value of μ/p (70 MeV). We expect that only lines through the origin are possible, ($\mu = 0$ when $p = 0$). We shall also only use the changes of flux with changes in the between parameters. With $\langle j(70\ \text{MeV})\rangle = 1.5 \times 10^{-3}$ #/sec cm^2 str, $\langle V_w \tilde{R}/K\ (\text{Bet})\rangle = .18$, and the slopes of the lines of $\Delta j(70\ \text{MeV})$ vs. $\Delta V_w \tilde{R}/K$ (Bet) through the origin and consistent with all the error bars, we find that μ/p (70 MeV) $= -1.1 \pm .2$. That is, a 100% increase in $V_w \tilde{R}/K$ (Bet) leads to a 100% decrease in j(70 MeV).

Figure 20 shows the family of curves for the radial gradient, n, and its energy dependence for (3.1.1) when $\gamma = .15$, (as long as $|\gamma| \lesssim .15$ our choice is not too important), and μ/p (70 MeV) = -1.1. It is a general feature of the set of curves that the lower the magnitude of the gradient at 70 MeV the more positive is its energy dependence, while the greater the gradient the more negative σ must be. The upper three points are measurements of the differential proton gradient in 1965 by O'Gallagher and Simpson (1967), and the two lower points are measurements in 1968 by Lezniak and Webber (1970). (Not plotted are other measurements of the integral gradient for energies > 30 MeV which are generally small and on the order of Lezniak and Webber [1970]).

It is encouraging that our results are consistent with these two measurements in terms of magnitude and energy dependence. Clearly, a determination of μ/p at 50 MeV would indicate the curve appropriate for the time of our observation, (early 1966). Unfortunately,

the errors on the 50 MeV measurements are large. Using a graph similar to Figure 13 for $\Delta V_w \tilde{R}/K$ (Bet) and Δj(50 MeV), (not shown), and neglecting two points inconsistent with the expected anticorrelation, we can get only the crudest estimate of μ/p (50 MeV) and thus a measure of n and σ. It is interesting, but not too instructive that these results, together with the values for the 70 MeV protons and standard error analysis gives a gradient at 70 MeV of $n = 1.60 \pm 1.45$, and an energy dependence, $\sigma = -1.05 \pm .95$, or an average value which is the same magnitude and energy dependence as observed by O'Gallagher and Simpson. However, the errors are so large as to give results consistent as well with the measurements of Lezniak and Webber. Thus, better particle measurements at low energies are required before we could estimate the gradient from these data.

The result that our entirely indirect measurements are consistent with both the magnitude and energy dependence of the observed cosmic ray gradient indicate the validity of our theoretical considerations of section 1.5. It also indicates that with finer measurements we can use observations of modulation parameter and flux changes to either compute or check direct measurements of the low energy gradient on future spacecraft missions.

3.2 The Radial Variation of the Parallel Diffusion Coefficient

So far we have discussed day to day fluctuations in the diffusion coefficient and modulation parameter, $V_w \tilde{R}/K$, as related to changes in the cosmic ray intensity. As such, we have been interested only in relative changes rather than absolute magnitudes or radial variation.

We have shown that at least 70 MeV protons seem to be responding to changes in the modulation parameter and diffusion coefficient as predicted from Jokipii's formulation. We would like to see if the magnitude and possible radial variation of the computed diffusion coefficients can be related to observations.

Since Pioneer 6 went from 1 to approximately .8 AU during our observations, we might determine if there was any secular change in the diffusion coefficient, indicating a radial gradient. Unfortunately, the large sinusoidal changes in $K_{\parallel}$, especially toward the end of our computations, which gave the good correspondence with changes in the proton flux, make an accurate determination of a radial gradient difficult. However, over the past ten years of interplanetary satellite observations, numerous observations of phenomenon such as magnetic sectors, recurrent solar wind and solar particle events, which exhibit periodicities characteristic of the solar rotation, indicate the existence of quasi-static structures on the sun affecting the interplanetary medium. Thus, by averaging our results over the solar rotation period ($\approx$ 27 days) we may be able to lessen those temporal effects in the interplanetary medium due to relatively static effects on the solar surface.

In Figure 21 we plot 27 day averages of $K_{\parallel}$ (Real) and V_w versus the heliocentric radius of the Pioneer 6 satellite during those times. Although the standard deviations are understandably large, the results indicate that the diffusion coefficient may be increasing (less scattering of the 70 MeV protons) or at least stays constant as we approach the sun. If we assume $K_{\parallel} = K_e(r/r_e)^{\beta}$, we see that K_e (70 MeV) $\approx 1.9 \pm .4$ cm^2/sec and $-3.5 < \beta \lesssim 0$. This is somewhat surprising in view of the fact that since the discovery of the spiral nature of the interplanetary magnetic

field by Ness et al. (1964), whose magnitude, $\bar{B}$, should increase as r decreases, most models have assumed $K_{||}$ proportional to some positive power of r.[2]

Although we have hopefully eliminated temporal effects by averaging over approximately the solar rotation period, the possibility of temporal variation exists. If so, it would be expected to appear as a change in one of the parameters from which $K_{||}$ is computed. Assuming that the averaged values of $K_{||}$ are correct, we would have to explain a 50% increase in the diffusion coefficient. Let us examine V_w first.

From (1.3.13):

$$K_{||} = 2\alpha(\alpha+2)\ c\beta\ R^2/9V_w\ P_{xx}(f = V_w\bar{B}/2\pi R)$$

we see that $K_{||}$ depends explicitly on $1/V_w$. However, if P_{xx} varies as $Af^{-\alpha}$, then $K\alpha V_w^{\alpha-1}$. From Figure 21 we see that V_w is either constant or slightly decreasing, on the average, as the spacecraft approaches the sun. Since the power spectral slopes, α , are always steeper than 1, a temporal decrease in V_w would tend to decrease $K_{||}$ rather than increase it.

Other variables which might effect a temporal change in K are the power spectrum slope and levels, and the magnetic field strength. The results of Table 3 indicate that the average slopes of the power spectra are quite constant and could not account for a 50% increase in $K_{||}$. The contour plots in Figures 7 through 11 also indicate that although day to day changes in the power levels are significant, there does not seem to be any average decrease which might account for an

---

[2]There have been recent indications that $K_{||}$ increases toward the sun, notably the interpretations of Jokipii and Parker (1968) to explain the low radial anisotropy of 10 MeV protons observed by Rao et al. (1967).

increase in K(r) in time. This is borne out by measurements of the average power at a single wavelength, 10^{11} cm, shown in Figure 23, which will be discussed later. Likewise, changes in $\bar{B}$ shown in Figure 23 are consistent with the theoretically predicted average increase in the interplanetary magnetic field as r decreases. Thus, we are unable to account for the apparent negative radial gradient in $K_{||}$ as a function of time.

It is interesting that Jokipii and Coleman (1968) obtained similar results for 1965 data taken between 1 and 1.5 AU by Mariner 4. Although their uncertainties were also large, they noted a slight decrease in $K_{||}$ as r increased. Therefore, the indications are that near 1 AU the parallel diffusion coefficient has a negative instead of a positive radial gradient. In the following sections we will examine the implications of the gradient and magnitude of $K_{||}$ on observations of both solar and galactic protons and discuss a possible mechanism to explain our observations of $K_{||}$ as a function of r.

3.3 Implications of observations of Solar and Galactic Protons

Since the same Fokker-Planck equation (1.2.9) should govern both solar flare propagation and galactic modulation, we should expect that our results be consistent with both phenomena. Most studies have treated the two separately. Because of the freedom in the choice of relevant parameters, estimates of the magnitude and radial variation of the parallel diffusion coefficient from the behavior of solar and galactic cosmic rays have generally not been incompatible. However, with recent observations and some plausible assumptions we can use the solar and galactic phenomena to find limits on the magnitude and local

gradient of the diffusion coefficient and compare these limits to our calculations of $K_{\parallel}(r)$. We begin with the observations of flare associated cosmic rays.

One of the first successes of diffusion theory in explaining cosmic ray processes was the work of Meyer et al. (1956) on the intensity time profile of the February 23, 1956 solar flare event. Meyer et al. concluded that the results could indicate a relatively scatter-free inner solar system and a thick diffusive shell past 1 AU extending to 5 AU, which would then be the boundary of the solar cavity. This would account for the rapid rise of the diffusive pulse of particles at earth, followed by their decline and loss to the interstellar medium depending inversely on time to some power. Although, as mentioned above, the idea of a scatter-free inner solar system has fallen out of vogue, it is consistent with our observations of a parallel diffusion coefficient which increases toward the sun.

Flare events are usually complex. There are, however, characteristics in common. For those flares, especially on the west limb of the sun where the interplanetary magnetic field lines near earth are predicted to be rooted and little perpendicular diffusion of observed particles at either the sun or in interplanetary space is expected, the general features of flare events have been similar: a fast rise time to maximum on the order of a few hours or less following the visual flare, followed by a decline in intensity either varying exponentially or as 1/t to some power. These have generally been fitted quite well by the diffusion approximation to the Fokker-Planck equation:

$$\frac{\partial U}{\partial t} = \vec{\nabla} \cdot (\overleftrightarrow{K} \cdot \vec{\nabla} U) \qquad (3.3.1)$$

The solution of (3.3.1) for diffusion from a point source into isotropic three-dimensional space has been a good approximation to the results. If $\overleftrightarrow{K}$ is identified with the parallel diffusion coefficient, $K(r) = K_e(r/r_e)^{\beta}$, where K_e is the value at 1 AU, Parker (1963) finds the time and radial behavior of the injected particles to be:

$$U(r,t) = N_o r_e^{2\beta/2-\beta}/(2-\beta)^{(\beta+4)/(2-\beta)} \Gamma(3/2-\beta) * \frac{1}{t^{3/2-\beta}} \exp\left[-\frac{r_e^{\beta} r^{2-\beta}}{(2-\beta)^2 t}\right] \quad (3.3.2)$$

At early times, the pulse decays as $1/t^{(3/2-\beta)}$, later exponentially, while the rise time to maximum at $r = r_e$ is given by

$$t_{max} = r_e^2/3(2-\beta)K_e \quad (3.3.3)$$

The decay phase of flare events has been fitted to this model by a number of authors, notably Krimigis (1965). He finds that values of β of $0 < \beta < 1$, with β generally 1 are good fits to most high energy (>40 MeV) observations. Burlaga (1967) using a different (anisotropic diffusion) model and $K_{\parallel}(r) = \text{const.}$ also finds good correspondence with the time profiles.

At first, this might seem to be in contradiction to our results. However, since one eventually expects the interplanetary medium to merge (by shock transition or otherwise) with the interstellar medium, where there should be little scattering, one eventually expects $K_{\parallel}$ to increase as a function of r. Moreover, the decay phase of the event represents the loss of the particles into the interstellar medium after the diffusive wave has passed the earth. As such, it is mainly responsive to conditions of the interplanetary medium past 1 AU, not in toward the sun.

On the other hand, the rise time to maximum is essentially responsive only to conditions between the sun and 1 AU, conditions for which we have measured the diffusion coefficient gradient. Thus, we should be able to use the rise times and (3.2.3) to check our results.

Although ignoring convection and adiabatic deceleration is not strictly valid for protons of energies <100 MeV (Jokipii 1971), the rise time to maximum is usually over too short a time scale for convection or deceleration to be significant. Recent work by Webb and Quenby (1972), numerically solving the full Fokker-Planck equation including the effects of convection and adiabatic deceleration indicates that even at low energies ($\approx$ 1 MeV) the rise times are generally only a factor of two less than the predictions of (3.3.3). For rise times less than 10 hours, the results are essentially the same. (They also conclude that β should be less than zero). Thus, (3.3.3) should be a close approximation.

Burlaga (1967) has shown that the rise times to maximum are associated with the solar longitude of the flare, with the fastest times corresponding to flares west of solar central meridian. Since these longitudes should be associated with magnetic field lines at earth, the particles whose average arrivals are the fastest will have directly sampled conditions along the magnetic field from the sun to the earth. These should be the most representative tracers of the parallel diffusion coefficient. In accord with other observations through the solar cycle, McCracken et al. (1967) finds that the fastest rise times for protons of energies 45-90 MeV in 1966 are on the order of 1-3 hours. It will be for these values of t_{max} that we will compare our observations.

We note the general feature of (3.3.3) is that for a chosen value of t_{max} the more positive β, the larger K_e is required to be. In particular, if $\beta = 1$ all the way to the sun, Krimigis finds that for conditions in 1961 with $t_{max} \approx 3$ hours, $K_e(70\ \text{MeV}) \approx 8 \times 10^{21}\ \text{cm}^2/\text{sec}$. Since r_e is a minimum path length for the particle to travel (due to the spiral field), the $K_e(70\ \text{MeV})$ that Krimigis predicts is a minimum and almost 4 times larger than even our largest measurement of $K_{\|}$ at 1 AU. Measurements of power spectra in 1962 by Coleman (1966) indicate it is unlikely K increases at all at solar maximum. If we assume the worst value of β in our measurements, $\beta \sim 0$, our measured value of $K_e \approx 2 \times 10^{21}\ \text{cm}^2/\text{sec}$. gives a minimum rise time of only 5 hours. However, if $\beta \sim -2$ and $K_e \approx 2 \times 10^{21}$, we easily get a 3 hour rise time. Thus, solar flare observations indicate that if the magnitude of the diffusion coefficients we calculate at earth is correct, its observed negative gradient between .8 and 1 AU is also real.

We can also use the observations of the galactic proton spectrum to get some limit on β and K_e near 1 AU. The observation of Rygg and Earl (1971) that the Compton-Getting factor is zero in the range 50-200 MeV, as mentioned in Chapter 1, implies that the quasi-static, spherically symmetric Fokker-Planck equation (1.5.7) has the value near 1 AU of

$$\frac{\partial^2 U}{\partial r^2} + \left(\frac{1}{K}\frac{\partial K}{\partial r} + \frac{2}{r} - \frac{V_w}{K}\right)\frac{\partial U}{\partial r} = 0 \qquad (3.3.4)$$

or

$$\frac{r}{U}\frac{\partial^2 U}{\partial r^2} + \left(\frac{r}{K}\frac{\partial K}{\partial r} + 2 - \frac{V_w r}{K}\right)\frac{1}{U}\frac{\partial U}{\partial r} = 0 \qquad (3.3.5)$$

Although this does not limit K(r), observations of the cosmic ray radial gradient, $1/U\ \partial U/\partial r$, and estimates of the unmodulated spectrum and solar cavity boundary can give us some idea of the behavior of the second derivative $\partial^2 U/\partial r^2$, and, therefore, a possible limit on the variables.

Most observations of the radial gradient in the 70 MeV range tend to be small (20% per AU) and positive (O'Gallagher, 1972). The observations of Rygg and Earl (1971) indicate that between solar minimum and maximum, the intensity of 70 MeV protons varies by a factor of 6. If one also assumes that the unmodulated cosmic ray spectrum varies as some function of energy, $T^{-\gamma}$, normalized to the high energy observations where the modulation is relatively ineffective, the difference between the minimum intensity at 1 AU and the assumed unmodulated value is between a factor of 10 (Figure 1) and a factor of 60 (Goldstein et al., 1970).

Most deductions from solar flares, (Parker, 1963; Burlaga, 1967; Lanzerotti, 1969) indicate the solar cavity boundary is within 6 AU. Since fast rise times of flare particles indicate little scattering between the sun and 1 AU, the gradient cannot be too large in toward the sun. Thus, to account for a factor of 6 change in intensity over the solar cycle (not to mention a possible factor of 60) with a 6 AU modulating region, requires an average gradient much greater than 20% per AU. For at least some distance beyond the orbit of earth, the radial gradient must increase. This, in turn, implies that the derivative of the gradient, $\partial^2 U/\partial r^2$, is positive. In order that both $\partial^2 U/\partial r^2$ and $\partial U/\partial r > 0$, the result of (3.3.5) demands that

$$\left(\frac{r}{K}\ \frac{\partial K}{\partial r} + 2 - \frac{V_w r}{K}\right) \leq 0 \qquad (3.3.6)$$

in the vicinity of 1 AU. If at 1 AU, $K = K_e(r/r_e)^{\beta}$, (3.3.6) gives

$$\left(\beta + 2 - \frac{V_w r_e}{K_e}\right) \leq 0 \qquad (3.3.7)$$

O'Gallagher and Simpson's (1967) measurements which gave a gradient on the order of 200% per AU at 70 MeV might conflict with our conclusion of $\partial^2 U/\partial r^2 \geq 0$. However, even this is less than required for the difference in the presumed unmodulated spectrum. Moreover, those measurements were on board Mariner 4, and were between 1 and 1.5 AU. If K is decreasing radially, as both we and Jokipii and Coleman (1968) suggest, the modulation should be more effective and the gradient should be increasing. O'Gallagher may have then measured the average gradient between 1 and 1.5 AU, greater than the gradient at 1 AU. This might explain the discrepancy with measurements near 1 AU where the gradient was always small. In that case $\partial^2 U/\partial r^2$ is still greater than zero at 1 AU and (3.3.7) still holds.

Note, that (3.3.7) is an important result. Given r = 1 AU and the average solar wind velocity, V_w, it puts a limit on β as a function of K_e. With $V_w = 4 \times 10^7$ cm/sec, a value of $\beta = 1$ implies that $V_w r_e/K_e \sim 3$, a value 6 times greater than we measure, or a value of K_e 6 times less than computed. On the other hand, a value of $\beta < -1.5$, is consistent with our calculations of $V_w r_e/K_e \sim .5$.

While the rise times of solar flares, (3.3.3), implied the more positive β, the greater K_e must be, the observations of the galactic spectrum at 1 AU imply the opposite: the more positive β, the smaller K_e to satisfy (3.3.7). We can use this fact to get a limit on the values of β and K_e which mutually satisfy the solar and galactic observations.

In Figure 22 we plot the results of (3.3.3) and (3.3.7) for r_e = 1 AU, $V_w = 4 \times 10^7$cm/sec, and various values of t_{max} as a function of β and K_e. Our measurement of the average value of K_e and its possible gradient is shown as the shaded area. The dotted line, $\beta \leq \beta$ critical is the solution of (3.3.7) for $(\beta + 2 - V_w r_e/K_e) = 0$. Only values of β and K_e to the right and below $\beta \leq \beta$ critical will satisfy the galactic observations. If we wish then to be consistent as well with the solar observations, they must also intersect the curves for t_{max}. We note that in order to get a Compton-Getting factor of zero[3] and a rise time of 2 hours for 70 MeV protons, as is commonly observed, β between the sun and earth must be less than -1 and K_e must be greater than 2×10^{21} cm^2/sec.

We see that our calculations do satisfy this for 3 hours but not quite for 2 hours. For such small rise times, the results of Webb and Quenby (1972) imply that any correction due to deceleration and convection will be small but will cause the curves for t_{max} to be lowered. More significantly, the indications of section 3.1 are that the proper K should be computed from fluctuations between discontinuties. Our results give K (Bet) > K (Real) with an increase in K_e of approximately 30%. We then get a good correspondence with solar and galactic observations.

Note that the limits in β and K_e from Figure 22 are based on only two assumptions: that for r < 1 AU, the effective diffusion coefficient

---

[3]The recent theoretical work of Fisk et al. (1972) also demonstrates that fits to the Fokker-Planck equation give a Compton-Getting factor most constantly zero when there is no scattering between 0 and .7 AU. However, their model of an exponentially increasing diffusion coefficient at 1 AU is inconsistent with our observations.

is given by $K_{\parallel}(r) \alpha (r/r_e)^{\beta}$; and that $\partial^2 U/\partial r^2 \geq 0$ for galactic protons at 1 AU. Since rise times are so fast, any large decrease in $K_{\parallel}$ within a few solar radii of the sun is either not occurring, or is over too small a distance to significantly slow the propagation of solar flare cosmic rays to earth. $K \alpha (r/r_e)^{\beta}$ should then be a good approximation. Likewise a small solar cavity and a small cosmic ray radial gradient at 1 AU implies $\partial^2 U/\partial r^2 \geq 0$. Thus, previous assumptions of a diffusion coefficient increasing monotonically with heliocentric radius were probably in error. With both direct observations and theoretical considerations this study indicates that from near the sun to some distance past 1 AU the parallel diffusion coefficient is decreasing with increasing radius.

3.4 A Mechanism for the Radial Variation of the Diffusion Coefficient

Just as the correspondence between changes in $V_w \tilde{R}/K$ (Bet) and the particle flux with the measurements of the cosmic ray radial gradient was encouraging, so is the correspondence between the magnitude and gradient of the diffusion coefficient with solar and galactic observations. These also imply that the coefficients, as predicted in Jokipii's theory, are correct. For a final consideration it would be interesting if we could explain the increase of the diffusion coefficient toward the sun.

One such mechanism might be Belcher's (1971) theoretical considerations of Alfven waves in the solar wind. He suggests that as the magnetic field spirals, the ratio of $\Delta B/B$ for outward propagating Alfven waves increases until they become magneto-acoustic waves and are damped. Thus, for a while, fluctuations in the field should grow as a function of radius,

implying more scattering and a decrease in $K_{\parallel}$. A recent private communication with Jokipii indicates that for small heliocentric radii both propagating (Alfvenic) and stationary (tangential discontinuities) phenomena can give a decrease in K as a function of r. However, we shall consider only our observations here.

In the earlier discussion of the lack of temporal dependence in the parameters which determine $K_{\parallel}$, we noted that both V_w and the average spectral slopes remained constant. Likewise, the contour plots indicated the average power levels did not change. This is verified in Figure 23 where we plot the average power at $f = V_w/10^{11}$ cm, or at the wavelength of 10^{11} cm. We do not include the correction of section 2.5 for the angle of the average field, $\cos\psi$, not along V_w. However, this is relatively constant, and, in view of the uncertainty does not affect the results.

In Figure 23 we see that the average value of $P(\lambda=10^{11}$ cm) remains constant as a function of r, and cannot account for the increase in the average value of $K_{\parallel}$. The only parameter which shows significant change is the magnitude of field $\bar{B}$, which is also plotted in Figure 23. We do not expect that this is temporal since it closely corresponds to the theoretical increase in $\bar{B}$ in the ecliptic plane as r decreases (Parker, 1963):

$$B_r(r,\theta=\tfrac{\pi}{2},\phi) = B_r(r_e)\,(r_e/r)^2$$

$$B_\theta(r,\theta,\phi) = 0$$

$$B_\phi(r,\theta=\tfrac{\pi}{2},\phi) = B_r(r_e)\,\frac{r_e\,\Omega}{V_w}\,\frac{r_e}{r} \qquad (3.4.1)$$

where Ω is the solar angular velocity. Between .8 and 1 AU this gives a variation in $\bar{B}$ approximately as

$$\bar{B}(r) \approx \bar{B}(r_e)\ (r/r_e)^{-3/2} \tag{3.4.2}$$

We, therefore, can see the cause of the increase in $K_{||}$ as r decreases. As the particle goes toward the sun its gyrofrequency increases due to the increase in $\bar{B}$. Therefore, the frequency of those fluctuations which reasonantly scatter it, $f = V_w\bar{B}/2\pi R$, is increasing. If both the power spectral slope and power levels remain constant, as indicated, the particle is responding to fluctuations of higher frequency, and, since the spectral slope is negative, fluctuations of smaller magnitude. Let us see if we can account for $-3 < \beta < -1.5$ in this manner. Assuming all other parameters in (1.3.13) remain constant, the variation in K(r) will be due to the variation $\bar{B}(r)$. Since $K \alpha f^{\alpha}$ and $f = V_w\bar{B}/2\pi R$, $K(r) \alpha \bar{B}(r)^{\alpha}$. From (3.4.2) B(r) varies as $r^{-3/2}$. Thus, with $\alpha = 1.7$, $K(r) \alpha r^{-2.5}$, or $\beta \sim -2.5$. This is in agreement, within our errors, and is essentially the best value of β we measure from Figure 21. Thus, we have a mechanism which can explain the radial variation of K.

Although our results do not indicate that $\Delta B/B$ increases with r, they do imply that the ratio $\Delta B/B$ is relatively constant. As long as the spectral slope does not change, this indicates a regime where K(r) decreases as r increases. From (3.4.1) we see that B varies as r^{-2} near the sun, and r^{-1} for large r. Thus, a regime of constant power levels gives a more negative β nearer the sun. We expect that other processes will cause $K_{||}$ to increase toward the solar cavity boundary, but there is no reason why the power levels should not remain relatively constant

for much of the distance between the sun and the earth, causing a negative gradient in K.

We have then seen that both our calculations and order of magnitude considerations of solar and galactic effects predict a local negative gradient in the parallel diffusion coefficient. We have arrived at a simple but physically reasonable explanation for this.

3.3 Summary

In this study, we have set out to directly test the magnetic field power spectrum-diffusion coefficient relation for low energy cosmic rays, at energies where the theory has been in doubt. We have attempted to determine if the particles are being scattered by the magnetic field discontinuities or by the fluctuations between discontinuities. Finally, we have compared the magnitude and possible radial variation of the predicted diffusion coefficients to observations of solar and galactic cosmic rays. Now, we would like to briefly summarize our more important results and suggest the possibility for future studies.

1. We feel that we have been able to describe the relative contribution of the discontinuities and fluctuations between discontinuities to the power spectra of the interplanetary magnetic field and, hence, to the predicted diffusion coefficients.

2. At energies between 60-80 MeV, galactic cosmic ray protons are responding to changes in the predicted diffusion coefficients, implying that the power spectrum-diffusion coefficient relation holds to these low energies.

3. The relation between changes in the proton flux and modulation parameters is best when the contribution of discontinuities is subtracted, indicating that the fluctuations between discontinuties are causing the scattering.

4. Since the correspondence between flux and parameter changes is poorest in the coefficients calculated from the contribution of discontinuities, this suggests that a large percentage of the discontinuities are tangential rather than rotational.

5. The response of the 60-80 MeV proton flux to changes in the modulation parameters is in agreement with a perturbation solution of the Fokker-Planck equation appropriate for low energies where the Compton-Getting factor is zero. Our computations indicate a general class of of results compatible with measurements of the magnitude and energy dependence of the cosmic ray radial gradient for T < 100 MeV. Since direct gradient measurements are difficult, this technique might lead to either checks or determinations of the gradient on future deep space probes.

6. There is little relation to changes in the modulation parameters and changes in the intensity of 20-40 MeV protons. This may be due to either a break down of the power spectrum-diffusion coefficient relation at lower energies or the predominance of a large "quiet time" flux of solar origin. Accurate determinations of the low energy differential cosmic ray radial gradient might clarify this.

7. The computations of the magnitude and radial variation of the parallel diffusion coefficient indicate an average value at the orbit of earth of $K_{\parallel}$ (70 MeV) $\approx 2 \times 10^{21}$ cm^2/sec, and a local radial gradient between .8 and 1 AU on the order of -200% per AU. This is found to be consistent with the predictions of diffusion fits to solar event rise times

and the observation that the Compton-Getting factor is zero for galactic cosmic ray protons between 50-200 MeV.

8. A mechanism is found to explain the gradient in the diffusion coefficient in terms of its relation to the magnetic field power spectra.

Hopefully, future satellite studies which monitor the interplanetary field will make measurements of the diffusion coefficient over larger radii. Future numerical fits of the Fokker-Planck equation to the galactic spectrum using diffusion coefficients with negative gradients from the sun to 1 AU, and positive gradient perhaps after 1.5 AU may resolve the discrepancy between various cosmic ray gradient measurements.

Recently, Earl (private communication) has rederived the expression for the diffusion coefficients suggesting that Jokipii's original (1966) formulation, which does not utilize the Legendre expansion, may be more correct than the 1968 formulation. As we mentioned in section 1.3, the differences between the two are not large unless the power spectrum slope approaches $\alpha = 2$, and the diffusion coefficient (1966) approaches infinity. This is interpreted as insufficient power at high frequencies to scatter the low pitch angle particles, $\mu \approx 0$, which sample wave numbers $k = 1/\mu r_g$. These particles can never be scattered and cause the diffusion coefficient to diverge.

By rederiving the diffusion coefficients via the Jokipii (1966) formulation we would probably see even poorer correspondence between intensity changes and $V_w \tilde{R}/K$ (Discontinuity), since the power spectrum from the discontinuities generally varies as $\alpha = 2$. It is doubtful, however, that a rederivation would demonstrate a better relation with the flux and the "between" parameters, since within errors this correspondence is as good as it probably can be.

Our results may also imply that the mechanism suggested by Noerdlinger (1968) is correct. Here the low pitch angle particles may be scattered by mirroring when $\Delta B/B$ is large. This keeps the diffusion coefficient (1966) from diverging when $\alpha = 2$. Such a possibility is physical and is not covered in the statistical theories of Jokipii. We propose a future study comparing the results of Jokipii's (1966) and (1968b) calculations to changes in the cosmic ray intensity. If such a study showed that Jokipii's earlier (1966) formulation gave poorer rather than better results, this may imply that Noerdlinger's mechanism is operative in the interplanetary medium.

ACKNOWLEDGEMENTS

The author would like to express his appreciation to those who have been of assistance to this study. To my advisor, Dr. Norman F. Ness, I extend the greatest thanks. He has been a constant source of inspiration, and without his patient guidance this study would not have been possible.

I have shared many fruitful discussions with Drs. G. Gloeckler, L. F. Burlaga, A. M. Lenchek and J. J. O'Gallagher for which I am most grateful.

I give special thanks to Dr. L. A. Fisk for his careful analysis of my ideas and his suggestion of the approximation which made possible the perturbation solution of the transport equation.

I thank Drs. F. B. McDonald and J. H. Kinsey for providing the IMP III data.

Frank Ottens, Gayle Richardson, and Maureen Brown have my appreciation for their helpful assistance.

I am grateful to Rose Pryor for her fine typing job.

No matter how inopportune the moment, David Howell was always willing to share his expertise with computers, and he has my sincere gratitude.

Finally, for her assistance in preparing this manuscript and her companionship I cannot thank my wife, Sharon, enough.

LIST OF TABLES

FIGURE CAPTIONS

Figure 1. A comparison between a numerical solution of the Fokker-Planck equation and the observed proton spectrum at solar minimum from Fisk (1971).

Figure 2. Idealization of the interplanetary magnetic field and the volume of space sampled by the average particle population in time t.

Figure 3. Relation of Pioneer 6 to earth from December 17, 1965 to April 23, 1966.

Figure 4. Power spectra of the interplanetary magnetic field for a 10 day interval computed via the method of nested variances. Ninety-five percent confidence limits are indicated on the field magnitude spectra.

Figure 5. Power spectra of the interplanetary magnetic field for an interval of intermediate field conditions. The number of directional discontinuities ($\geq 30°$) was 20. Dotted lines indicate f^{-2} and $f^{-5/3}$ frequency dependence. Ninety-five percent confidence limits shown at bottom.

Figure 6. The relative contribution of discontinuities ($\geq 30°$) to the total power in all three components as a function of frequency of discontinuities for each day.

Figure 7 - Figure 11. Contour plots of power spectra for 12 hour periods, December 17, 1965 - April 30, 1966. Spectral densities are plotted in descending powers of 10 with solid representing 10^5 - 10^6 γ^2/Hz and white representing 10^{-1} - 10^0 γ^2/Hz. Also plotted for each 12 hour period are V_w, δV_w, $\bar{K}_p$, and the number of discontinuities ($\geq 30°$).

Figure 12. Three day running means of the 60-80 MeV proton flux observed on IMP III against the modulation parameters calculated from Pioneer 6 data. Relative contribution of discontinuities ($\geq 30°$) to the total component power shown on bottom line.

Figure 13. Changes in the proton flux over periods $\geq$ 3 days versus corresponding changes in the modulation parameters. Minimum and maximum errors are indicated.

Figure 14. 60-80 MeV proton flux versus the diffusion coefficients and solar wind velocity.

Figure 15. 20-40 MeV and 40-60 MeV proton fluxes versus the modulation parameters calculated at 50 MeV.

Figure 16 - Figure 18. Cross correlations (normalized to 1.0) between changes in the flux and changes in the modulation parameters and diffusion coefficients.

Figure 19. Daily changes in $\Delta V_w \tilde{R}/K$ (Bet) (t + 2 days) and Δj(70 MeV) (t). Correlation coefficient is -.25. Dotted line indicates least square fit.

Figure 20. Family of curves for the cosmic ray radial gradient as predicted from $\Delta V_w \tilde{R}/K$ (Bet) and Δj(70 MeV). Solid circles are measurements of the proton gradient in 1965 (O'Gallagher and Simpson, 1967), and lower points are measurements in 1968 (Lezniak and Webber, 1970).

Figure 21. Parallel diffusion coefficient at 70 MeV and solar wind velocity as a function of Pioneer 6 heliocentric radius.

Figure 22. Magnitude of the parallel diffusion coefficient at 1 AU versus its radial gradient between 1 AU and the sun. Solid lines give values consistent with rise times to maximum of solar flare associated events. Values to right of dotted line $\beta \leq \beta_{critical}$ are consistent with a zero Compton-Getting factor. Pioneer 6 observations between .8 and 1 AU are shown as the shaded area.

Figure 23. Average power at wavelength of 10^{11} cm and magnetic field magnitude as a function of Pioneer 6 heliocentric radius. Theoretical value of $|\bar{B}|$ from Parker (1963).

REFERENCES

Axford, W. I., The modulation of galactic cosmic rays in the interplanetary medium, *Planet Space Sci., 13,* 115, 1965.

Batchelor, G. K., The theory of homogeneous turbulence, Cambridge University Press, Cambridge, 1960.

Belcher, J. W., Alfvenic wave pressures and the solar wind, *Astrophys. J., 168,* 509, 1971.

Belcher, J. W. and L. Davis, Large-amplitude Alfven waves in the interplanetary medium, 2, *J. Geophys. Res., 76,* 3534, 1971.

Biermann, L., Comet tails and solar corpuscular radiation, *Z. Astrophys., 29,* 274, 1951.

Biermann, L., Solar corpuscular radiation and the interplanetary gas, *Observatory, 107,* 109, 1957.

Blackman, R. B., and J. W. Tukey, *The Measurement of Power Spectra,* Dover Publications, Inc., New York, 1958.

Bridge, H., C. Dilworth, A. J. Lazarus, E. F. Lyon, B. Rossi, and F. Scherb, Paper presented to intern. conf. on cosmic rays, Kyoto, Japan, *J. Phys. Soc. Japan, 17,* Suppl. A-11, 1961.

Burger, J. J., A phenomenological approach to the solar modulation of cosmic rays, *Astrophys. J., 166,* 651, 1971.

Burger, J. J., and Y. Tanaka, Implications of the observed solar modulation of cosmic ray electrons, *Astrophys. J., 162,* 305, 1970.

Burlaga, L. F., Anisotropic diffusion of solar cosmic rays, *J. Geophys. Res., 72,* 4449, 1967.

Burlaga, L. F., Directional discontinuities in the interplanetary magnetic field, *Solar Physics, 7,* 54, 1969.

Burlaga, L. F., Nature and origin of directional discontinuities in the solar wind, *J. Geophys. Res., 76,*4360, 1971.

Colburn, D. S. and C. P. Sonett, Discontinuities in the solar wind, *Space Science Reviews, 5,* 439, 1966.

Coleman, P. J., Jr., Variations in the interplanetary magnetic field: Mariner 2, 1, Observed properties, *J. Geophys. Res., 71,* 5509, 1966.

Fisk, L. A., Solar modulation of galactic cosmic rays, 2, *J. Geophys. Res., 76,* 221, 1971.

Fisk, L. A., M. A. Forman, and W. I. Axford, Solar modulation of galactic cosmic rays, III: Implications of the Compton-Getting coefficient, GSFC preprint, X-661-72-124, 1972.

Forbush, S. E., On world-wide changes in cosmic-ray intensity, *Phys. Rev.*, *54*, 975, 1938.

Forbush, S. E., World-wide cosmic-ray variations, 1937-1952, *J. Geophys. Res.*, 59, 1954.

Gleeson, L. J. and W. I. Axford, Cosmic rays in the interplanetary medium, *Astrophys. J.*, *149*, L115, 1967.

Gleeson, L. J. and W. I. Axford, Modulation of galactic cosmic rays, *Astrophys. J.*, *154*, 1011, 1968.

Gleeson, L. J. and I. A. Urch, On the cosmic ray diffusion coefficient in interplanetary space, preprint, Monash University, Australia, 1971.

Gloeckler, G. and J. R. Jokipii, Low energy cosmic ray modulation related to observed interplanetary magnetic field irregularities, *Phys. Rev. Letters*, *17*, 203, 1966.

Goldstein, M. L., L. A. Fisk, and R. Ramaty, Energy loss of cosmic rays in the interplanetary medium, *Phys. Rev. Letters*, *25*, 832, 1970.

Hasselmann, K. and G. Wibberenz, Scattering of charged particles by random electromagnetic fields, *Z eits. fur Geophysik*, *34*, 353, 1968.

Hudson. P. J., Discontinuities in an anisotropic plasma and their identification in the solar wind, *Planet, Space Sci.*, *18*, 161, 1970.

Jokipii, J. R., Cosmic-ray propagation, 1, Charged particles in a random magnetic field, *Astrophys. J.*, *146*, 480, 1966.

Jokipii, J. R., Modulation of low rigidity cosmic rays and the power spectrum of the interplanetary magnetic field in 1962 and 1965, *Canadian J. of Phys.*, *46*, S950, 1968a.

Jokipii, J. R. , Addendum and erratum to "Cosmic ray propagation, I", *Astrophys. J.*, *152*, 671, 1968b.

Jokipii, J. R., Stochastic variations of cosmic rays in the solar system, *Astrophys. J.*, *156*, 1107, 1969.

Jokipii, J. R., Cosmic ray propagation in the solar wind, *Reviews of Geophys. and Space Phys.*, *9*, 27, 1971.

Jokipii, J. R., Fokker-Planck equations for charged particle transport in random fields, *Astrophys. J.*, *172*, 319, 1972.

Jokipii, J. R. and P. J. Coleman, Jr., Cosmic-ray diffusion tensor and its variation observed with Mariner 4, *J. Geophys. Res.*, *73*, 5495, 1968.

Jokipii, J. R. and E. N. Parker, Energy changes of cosmic rays in the solar system, *Plant. Space Sci.*, *15*, 1375, 1967.

Jokipii, J.R. and E.N. Parker, Implications of the small observed anisotropy of 7.5 to 45 MeV cosmic rays, *J. Geophys. Res.*, *73*, 3367, 1968.

Kinsey, J.H., A study of low energy cosmic rays at 1 AU, Ph. D. Thesis, University of Maryland, 1969.

Klimas, A.J. and G. Sandri, Foundation of the theory of cosmic ray transport in random magnetic fields, *Astrophys. J.*, *169*, 41, 1971 .

Krimigis, S.M., Interplanetary diffusion model for the time behavior of intensity in a solar cosmic ray event, *J. Geophys. Res.*, *70*, 2943, 1965.

Kulsrud, R. and W.P. Pearce, The effect of wave particle interactions on the propagation of cosmic rays, *Astrophys. J.*, *156*, 445, 1969.

Lanzerotti, L.J., Low energy solar protons and alphas as probes of the interplanetary medium: the May 28, 1967, solar event, *J. Geophys. Res.*, *74*, 2851, 1969.

Lazarus, A.J., H.S. Bridge and J. Davis, Preliminary results of the Pioneer 6 MIT plasma experiment, *J. Geophys. Res.*, *71*, 3787, 1966.

Lezniak, J.A. and W.R. Webber, Measurements of gradients and anisotropies of cosmic ray in interplanetary space: Pioneer 8, *Proc. 11th Int. Conf. on Cosmic Rays*, Budapest, III, 1970.

Lezniak, J.A. and W.R. Webber, Solar modulation of cosmic ray protons, helium nuclei, and electrons, *J. Geophys. Res.*, *76*,1605, 1971.

McCracken, K.G., U.R. Rao and R.P. Bukata, Cosmic ray propagation processes, 1, A study of the cosmic ray flare effect, *J. Geophys. Res.*, *72*, 4293, 1967.

Meyer, P.E., E.N. Parker and J.A. Simpson, Solar cosmic rays of February 1956 and their propagation through interplanetary space, *Phys. Rev.*, *104*, 768, 1956.

Morrison, P., Solar origin of cosmic ray time variations, *Phys. Rev.*, *101*, 1397, 1956

Ness, N.F., Magnetometers for space research, NASA-GSFC preprint X-690-70-78, 1970.

Ness, N.F., C.S. Scearce and S. Cantarano. Preliminary results from the Pioneer 6 magnetic field experience, *J. Geophys. Res.*, *71*, 3305, 1966.

Ness, N.F., C.S. Scearce and J.B. Seek, Initial results of the IMP I magnetic field experiment, *J. Geophys. Res.*, *69*, 3531, 1964.

Noerdlinger, P.D., An improved model for cosmic ray propagation, *Phys. Rev. Lett.*, *20*, 1513, 1968.

O'Gallagher, J.J., Observations of the radial gradient of galactic cosmic radiation over a solar cycle, University of Maryland Technical Report No. 72-068, 1972.

O'Gallagher, J.J. and J.A. Simpson, The heliocentric intensity gradients of cosmic ray protons and helium during minimum solar modulation. *Astrophys. J.*, *147*, 819. 1967.

Ormes, J.F. and W.R. Webber, Proton and helium nulcei cosmic ray spectra and modulations between 100 and 2000 MeV/nulceon, *J. Geophys, Res.*, *73*, 4231, 1968.

Parker, E.N., Modulation of primary cosmic ray intensity, *Phys. Rev.*, *103*, 1518, 1956.

Parker, E.N., Cosmic ray modulation by solar wind, *Phys. Rev.*, *110*, 1445, 1958a.

Parker, E.N., Dynamics of the interplanetary gas and magnetic fields, *Astrophys. J.*, *128*, 664, 1958b.

Parker, E.N., *Interplanetary Dynamical Processes*, Interscience Publ., New York, 1963.

Parker, E.N., The passage of energetic charged particles through interplanetary space, *Plant. Space Sci.*, *13*, 9, 1965.

Rao, U.R., K.G. McCracken and W.C. Bartley, Cosmic ray propagation processes, 3, The diurnal anisotropy in the vicinity of 10 MeV/nulceon, *J. Geophys. Res.*, *72*, 4343, 1967.

Roelof, E.C., Statistical theory of charged particle transport in disordered magnetic fields, Ph. D. thesis, University of California, Berkeley, 1966.

Russell, C.T., Comments on the measurement of power spectra of the interplanetary magnetic field, Paper presented at the Asilomar Solar Wind Conference, 1971.

Rygg, T.A. and J.A. Earl, Balloon measurements of cosmic ray protons and helium over half a solar cycle 1965-1969, *J. Geophys. Res.*, *76*, 7445, 1971.

Sakurai, K. and R.G. Stone, Active solar radio regions at metric frequencies and the interplanetary sector structure, *Solar Physics*, *19*, 247, 1971.

Sari, J.W. and N.F. Ness, Power spectra of the interplanetary magnetic field, *Solar Physics*, *8*, 155, 1969.

Sari, J.W. and N.F. Ness, Power spectral studies of the interplanetary magnetic field, *Proc. 11th Int. Conf. on Cosmic Rays*, Budapest, II, 373, 1970.

Scearce, C.S., C.H. Ehrmann, S.E. Cantarano and N.F. Ness, Magnetic field experiment: Pioneers 6, 7 and 8, NASA-GSFC preprint X-616-68-370, 1968.

Singer, S.F., H. Laster and A.M. Lenchek, Forbush decreases produced by diffusive decleration mechanism in interplanetary space, *J. Phys. Soc. Japan, 17*, Suppl. A-11, 583, 1962.

Siscoe, G.L., L. Davis Jr, P.J. Coleman Jr. E.J. Smith and D.E. Jones, Power spectra and discontinuities of the interplanetary magnetic field: Mariner 4, *J. Geophys. Res.*, *73*, 61, 1968.

Webb, S. and J.J. Quenby, Numerical studies of the transport of solar protons in interplanetary space, Imperical College, London, preprint, 1972.

Webber, W.R, The modulation of galactic cosmic rays by interplanetary magnetic fields, Invited paper at 10th IUPAP Int. Conf. on Cosmic Rays, Calgary, Canada, 1967.

TABLE 1

Period	Earth-Sun-Pioneer Angle	Heliocentric Radius	No. of Discontinuities/ Day > 30°
65/351 - 66/12	0° - 1.4°E	1.0 - .99 AU	30.4 ± 10.6
66/13 - 66/39	1.4°E - 1.7°E	.99 - .96 AU	25.3 ± 12.2
66/40 - 66/66	1.7°E - 0.6°W	.96 - .91 AU	36.6 ± 17.1
66/67 - 66/93	0.6°W - 6.5°W	.91 - .85 AU	24.4 ± 13.6
66/94 - 66/120	6.5°W - 16.1°W	.95 - .81 AU	24.7 ± 10.6
66/121 - 66/147	16.1°W - 27.4°W	.81 - .81 AU	26.5 ± 13.9

TABLE 2

Day 66/32

	$< P_D/P_R >$	$< P_B/P_R >$	$<P_D/P_R+P_B/P_R>$
X	0.45	0.62	1.07
Y	0.51	0.58	1.09
Z	0.24	0.90	1.14
F	0.14	0.79	0.93

TABLE 3

Period	Heliocentric Radius	α_x(real)	α_x(bet)	α_x(dis)
65/351 - 66/12	1.0 - .99 AU	1.72 $\pm$ .36	1.70 $\pm$ .18	1.95 $\pm$ .04
66/13 - 66/39	.99 - .96 AU	1.75 $\pm$ .17	1.71 $\pm$ .19	1.94 $\pm$ .06
66/40 - 66/66	.96 - .91 AU	1.70 $\pm$ .13	1.61 $\pm$ .23	1.93 $\pm$ .07
66/67 - 66/93	.91 - .85 AU	1.70 $\pm$ .11	1.64 $\pm$ .22	1.94 $\pm$ .09
66/94 - 66/120	.95 - .81 AU	1.70 $\pm$ .11	1.57 $\pm$ .28	1.95 $\pm$ .07

Table 4

YEAR	DAY	K(50)*(10**21) CM2/SEC			K(70)*(10**21) CM 2/SEC		
		REAL	DISCONTINUITY	BETWEEN	REAL	DISCONTINUITY	BETWEEN
65	351	2.90	11.19	4.12	3.53	13.27	5.08
65	352	1.16	3.46	1.72	1.39	4.08	2.09
65	353	1.93	6.91	2.90	2.37	8.32	3.62
65	354	0.96	2.61	1.66	1.18	3.14	2.10
65	355	1.38	2.16	5.07	1.70	2.60	6.62
65	356	1.19	3.33	2.13	1.47	4.02	2.69
65	357	1.62	3.59	3.17	1.94	4.25	3.89
65	358	0.71	2.48	1.23	0.88	3.03	1.52
65	359	1.13	3.74	1.75	1.40	4.48	2.21
65	360	1.09	3.31	1.77	1.35	4.01	2.22
65	361	1.58	3.61	3.83	1.99	4.42	4.98
65	362	1.41	2.95	4.35	1.79	3.69	5.82
65	363	1.37	2.34	4.11	1.68	2.81	5.31
65	364	2.09	4.92	4.08	2.56	5.93	5.13
65	365	1.98	5.38	3.94	2.46	6.55	5.04
66	1	1.82	5.30	3.00	2.23	6.34	3.73
66	2	1.21	2.81	2.08	1.46	3.30	2.54
66	4	1.11	4.29	1.71	1.35	5.14	2.10
66	5	1.91	5.27	3.30	2.33	6.26	4.14
66	6	2.28	6.27	3.08	2.72	7.24	3.73
66	7	1.20	4.33	1.97	1.49	5.24	2.49
66	8	1.72	6.23	2.70	2.12	7.55	3.38
66	9	1.31	3.89	2.90	1.66	4.84	3.72
66	10	1.84	4.96	3.95	2.32	6.02	5.20
66	11	1.41	3.77	2.61	1.73	4.56	3.29
66	12	2.51	7.59	4.15	3.12	9.14	5.30
66	17	2.13	6.13	3.15	2.57	7.25	3.84
66	18	2.10	16.12	2.14	2.44	18.46	2.50
66	20	2.25	12.76	2.94	2.70	15.28	3.52
66	21	1.92	5.84	3.23	2.42	7.05	4.24
66	22	2.15	7.48	3.55	2.72	9.07	4.65
66	23	1.49	6.14	2.78	1.93	7.67	3.71
66	24	1.00	2.95	2.14	1.27	3.62	2.83
66	25	1.21	3.73	2.51	1.54	4.62	3.25
66	26	1.95	7.66	3.47	2.46	9.51	4.42
66	27	3.46	15.04	5.39	4.39	18.14	6.97
66	29	2.12	9.19	2.12	2.50	10.38	2.52
66	31	1.44	10.04	3.63	1.72	14.35	4.26
66	32	1.27	2.87	2.19	1.52	3.41	2.65
66	33	1.77	5.78	2.24	2.11	6.67	2.72
66	34	1.41	3.83	2.69	1.77	4.62	3.47
66	35	1.70	5.34	3.31	2.14	6.59	4.25
66	36	2.64	15.88	3.35	3.30	18.96	4.25
66	37	1.50	2.57	5.48	1.85	3.11	7.51
66	38	2.35	10.55	3.21	2.89	12.51	3.99
66	39	1.74	6.70	2.43	2.10	7.89	2.98
66	40	1.79	9.01	1.86	2.18	11.05	2.27
66	41	2.15	10.44	3.17	2.66	12.68	3.98
66	42	1.07	3.60	1.64	1.34	4.27	2.14
66	43	0.85	1.90	2.91	1.06	2.34	3.67
66	44	1.34	2.04	2.99	1.60	2.39	3.83
66	45	2.86	20.85	3.59	3.55	24.94	4.48
66	46	1.25	2.92	2.42	1.53	3.51	3.02
66	47	1.80	8.83	2.64	2.23	10.63	3.30
66	49	1.30	3.76	4.01	1.59	4.57	5.04
66	50	0.57	2.14	1.80	1.09	2.61	2.37
66	51	0.66	5.31	1.32	0.84	7.01	1.69

Table 4 con.

YEAR	DAY	K(30)*(10**21) CM2/SEC			K(70)*(10**21) CM 2/SEC		
		REAL	DISCONTINUITY	BETWEEN	REAL	DISCONTINUITY	BETWEEN
66	52	2.27	7.03	3.98	2.81	8.48	5.01
66	53	1.45	4.20	2.65	1.81	5.11	3.40
66	54	0.79	2.82	1.83	1.02	3.59	2.38
66	55	1.63	8.69	2.93	2.11	10.99	3.82
66	56	1.72	5.91	3.30	2.22	7.31	4.40
66	57	3.15	19.88	5.49	3.93	25.94	6.90
66	58	1.53	5.34	3.88	1.98	6.85	5.16
66	59	1.44	3.28	2.94	1.79	3.98	3.85
66	60	1.29	2.80	4.39	1.64	3.49	5.93
66	61	1.65	10.42	2.42	2.07	12.50	3.07
66	62	0.95	2.49	1.84	1.16	2.95	2.37
66	63	1.10	2.01	3.40	1.42	2.53	5.22
66	64	2.81	9.58	4.18	3.61	11.51	5.66
66	65	1.48	5.96	2.39	1.85	7.26	3.05
66	66	2.46	7.94	4.68	3.09	9.45	6.10
66	67	1.83	5.83	3.24	2.35	7.14	4.41
66	68	1.05	3.42	2.20	1.31	4.16	2.85
66	69	1.20	2.63	2.99	1.45	3.17	3.58
66	70	1.30	2.99	2.57	1.62	3.60	3.49
66	71	2.43	9.52	3.38	2.89	11.14	4.17
66	73	1.75	4.60	3.51	2.18	5.55	4.53
66	74	1.63	8.62	1.82	1.99	9.96	2.25
66	75	1.61	6.06	2.95	2.05	7.43	3.85
66	76	1.30	3.49	2.94	1.62	4.20	3.84
66	79	2.40	44.31	2.81	3.04	53.41	3.61
66	80	1.62	13.43	1.93	2.08	15.70	2.54
66	81	1.55	7.80	1.99	1.95	9.15	2.60
66	82	2.83	6.13	7.17	3.41	7.21	8.30
66	85	1.96	12.77	2.86	2.37	15.45	3.47
66	86	1.93	7.21	3.12	2.39	8.73	3.91
66	87	3.34	20.85	3.31	4.05	23.83	4.09
66	90	2.46	12.66	2.93	3.08	14.78	3.80
66	91	1.32	6.15	1.62	1.62	7.29	2.02
66	92	2.77	18.87	4.34	3.45	23.46	5.44
66	93	1.27	6.29	2.14	1.53	7.71	2.56
66	94	1.16	2.59	3.41	1.40	3.06	4.55
66	95	0.84	2.71	1.62	1.06	3.29	2.09
66	96	1.56	4.50	2.43	1.96	5.30	3.19
66	97	1.03	4.47	1.61	1.37	5.40	2.11
66	98	3.20	6.62	6.62	3.94	8.16	8.16
66	99	2.10	22.72	2.54	2.62	27.07	3.20
66	100	3.35	12.46	6.70	4.09	15.50	8.11
66	101	3.09	19.32	4.22	3.78	23.54	5.40
66	102	5.32	19.08	7.52	6.46	22.32	9.37
66	103	3.53	7.87	6.08	4.39	9.36	7.91
66	104	1.57	7.17	1.62	1.93	8.22	2.06
66	105	2.46	7.64	3.41	3.06	8.96	4.42
66	106	1.11	4.67	1.54	1.36	5.55	1.92
66	108	1.47	4.06	2.28	1.82	4.81	2.95
66	109	1.62	3.97	2.92	1.98	4.69	3.71
66	110	1.67	5.02	2.68	2.10	6.03	3.66
66	111	3.36	34.22	3.86	4.79	40.38	4.85
66	112	1.62	7.93	1.87	2.20	9.09	2.31
66	113	1.25	3.34	2.17	1.53	3.96	2.73
66	116	4.17	11.92	7.06	5.53	14.76	10.57
66	117	6.43	15.48	8.22	8.00	18.45	10.55

TABLE 5

Days deleted due to solar flares: All energy channels	Days deleted in low energy channel (20 - 40 MeV)
65/364	65/361
65/365	66/1
66/6	66/2
66/7	66/18
66/8	66/19
66/55	66/20
66/81	66/79
66/82	66/80
66/83	66/85
66/84	66/86
66/92	66/106

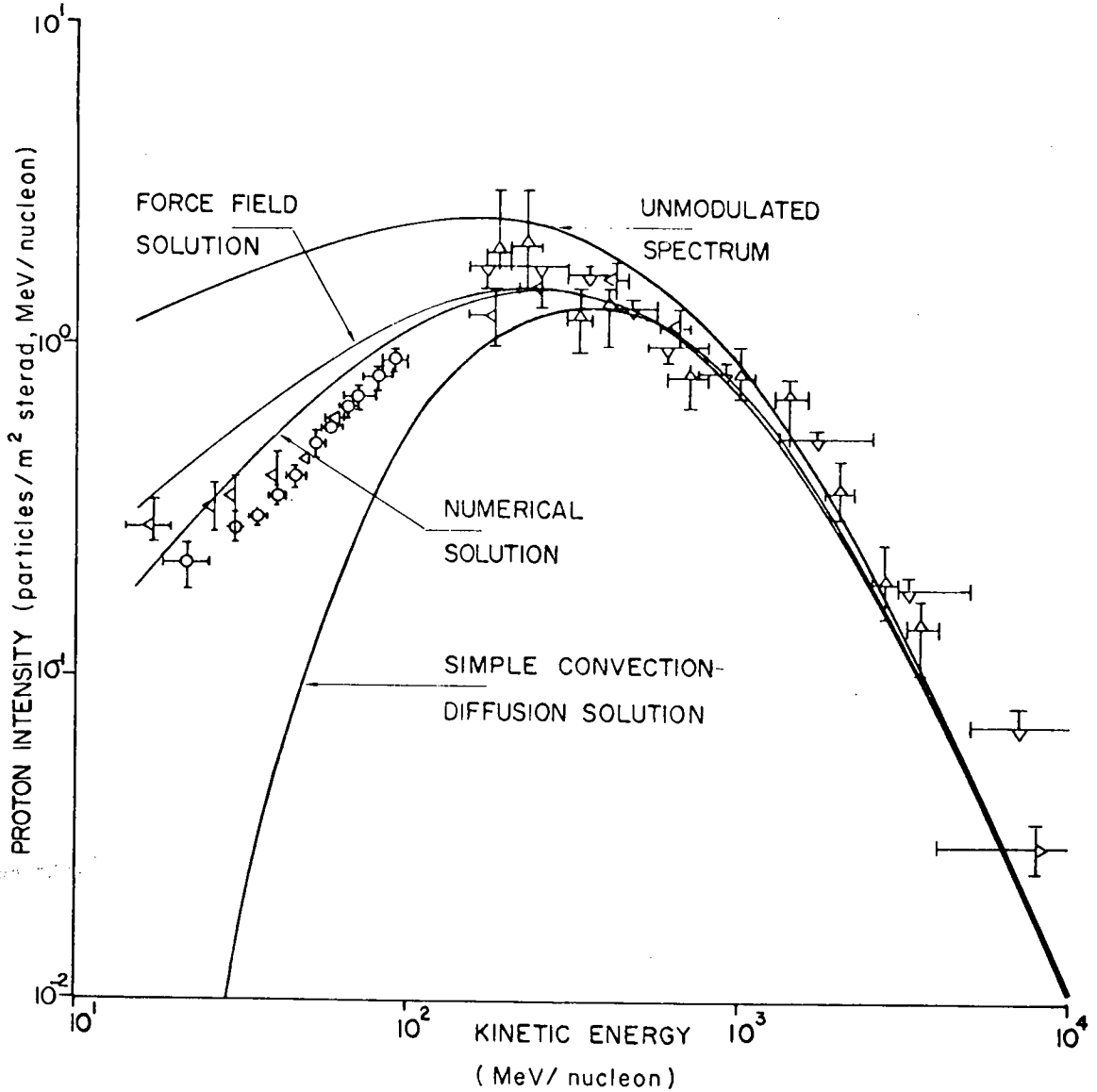
FORCE FIELD
SOLUTION
UNMODULATED
SPECTRUM
NUMERICAL
SOLUTION
SIMPLE CONVECTION-
DIFFUSION SOLUTION
PROTON INTENSITY (particles/m² sterad, MeV/nucleon)
KINETIC ENERGY
(MeV/nucleon)
10¹
10⁰
10⁻¹
10⁻²
10²
10³
10⁴

Figure 1

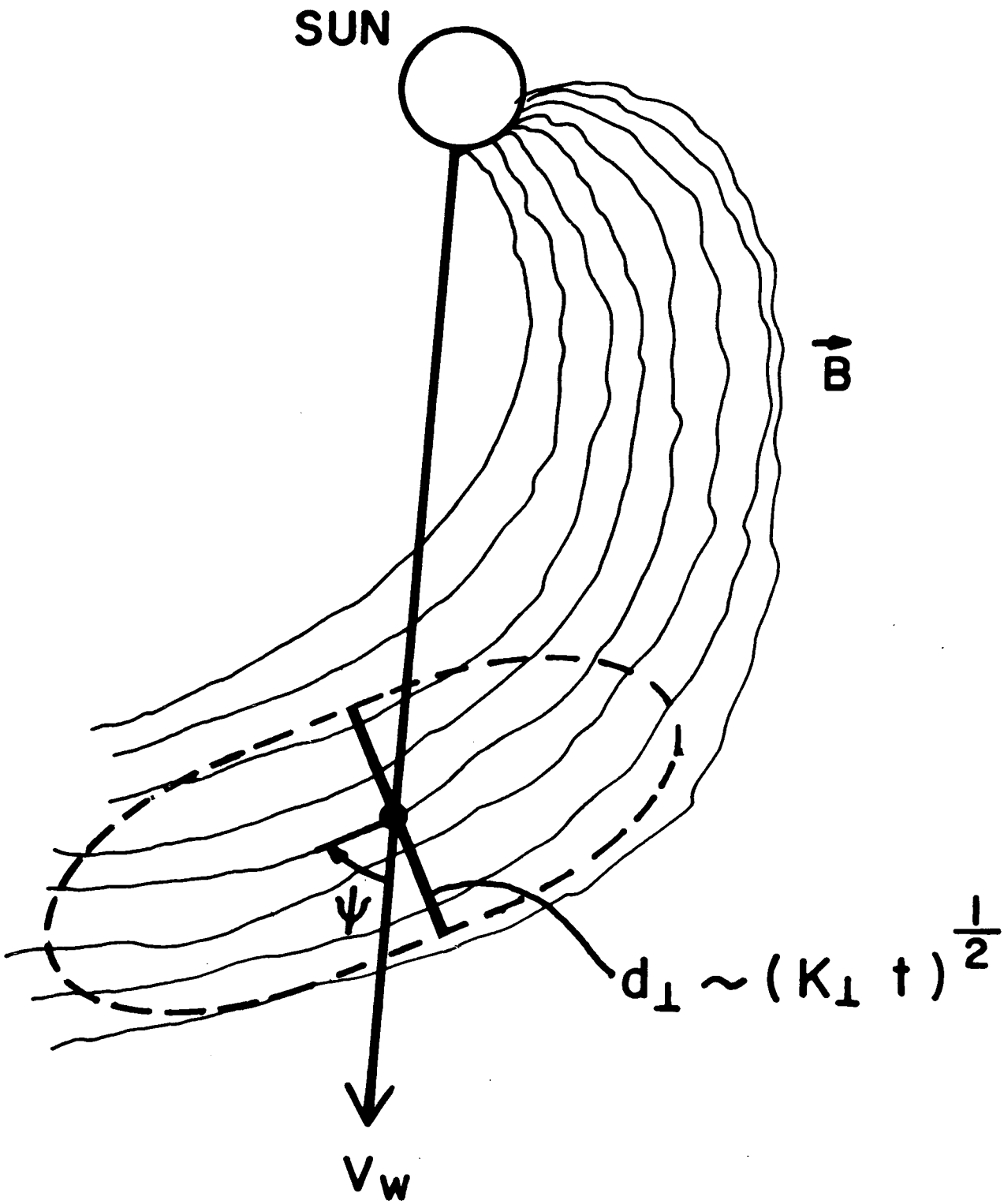

Figure 2

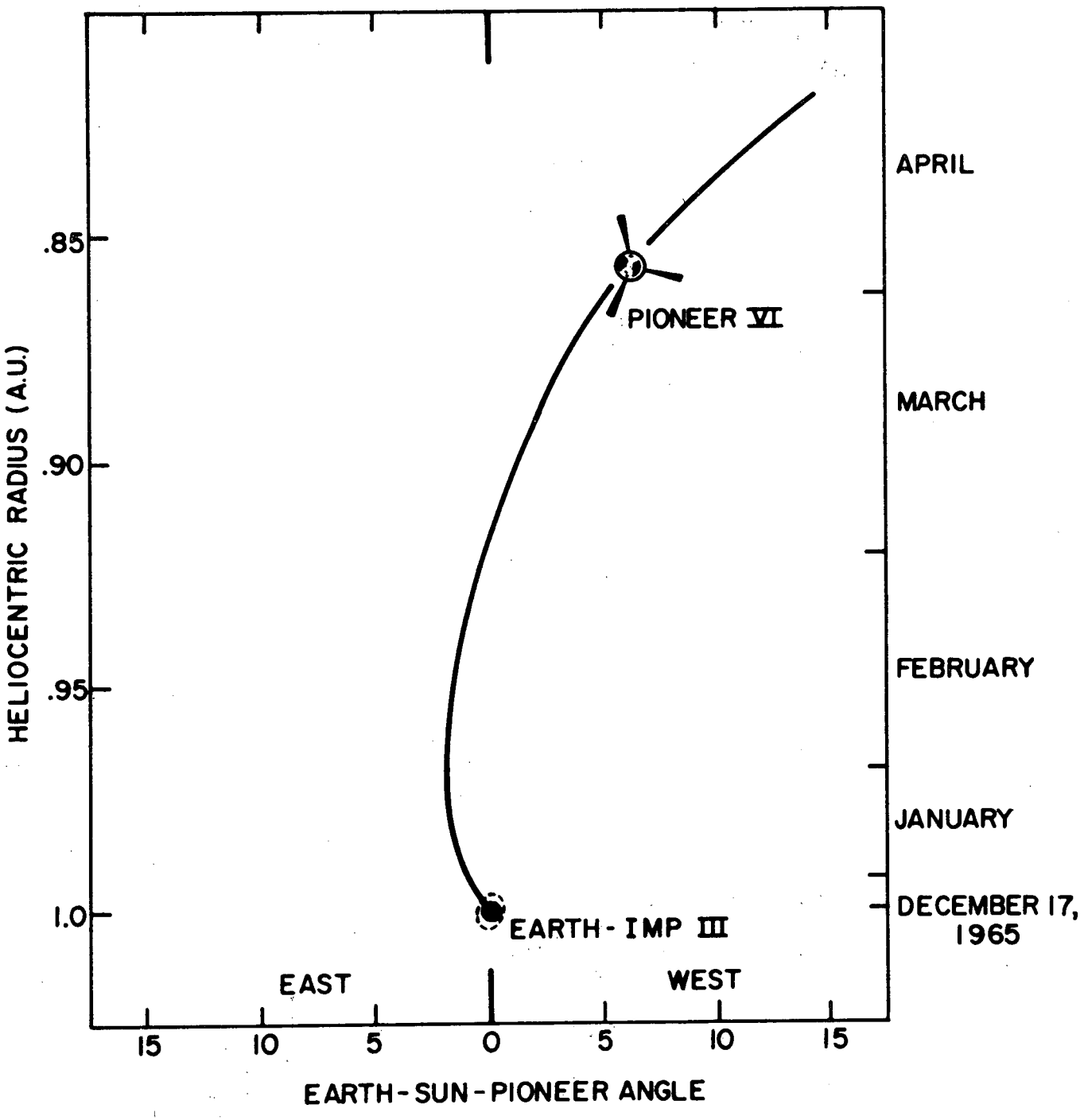
HELIOCENTRIC RADIUS (A.U.)
.85
.90
.95
1.0
APRIL
MARCH
FEBRUARY
JANUARY
DECEMBER 17, 1965
PIONEER VI
EARTH - IMP III
EAST
WEST
15
10
5
0
5
10
15
EARTH - SUN - PIONEER ANGLE

Figure 3

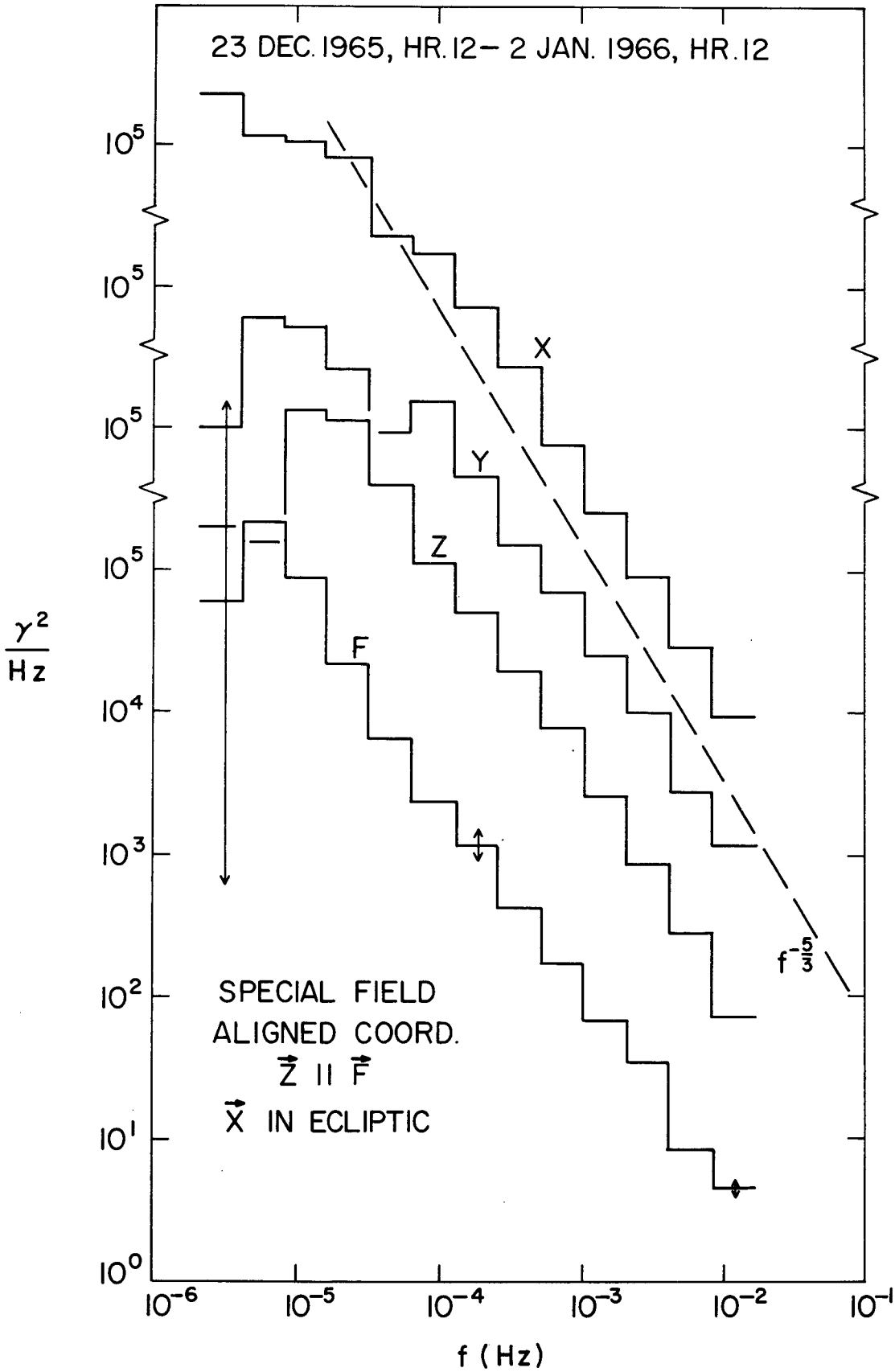
23 DEC. 1965, HR. 12 – 2 JAN. 1966, HR. 12
10^5
10^5
10^5
10^5
10^4
10^3
10^2
10^1
10^0
X
Y
Z
F
$f^{-\frac{5}{3}}$
SPECIAL FIELD
ALIGNED COORD.
$\vec{Z}$ II $\vec{F}$
$\vec{X}$ IN ECLIPTIC
$\frac{\gamma^2}{Hz}$
10^{-6}
10^{-5}
10^{-4}
10^{-3}
10^{-2}
10^{-1}
f (Hz)

Figure 4

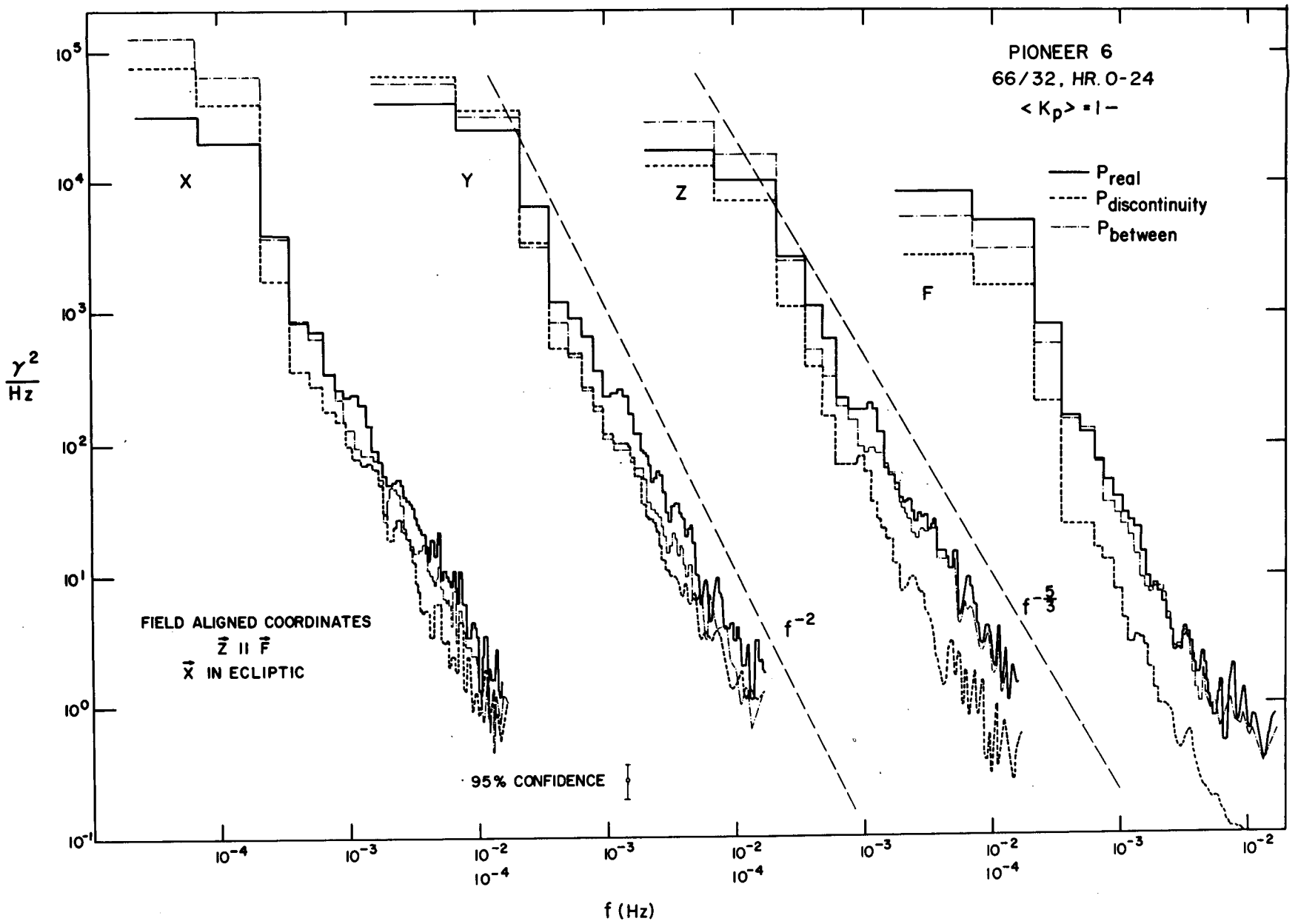
PIONEER 6
66/32, HR. 0-24
< Kp > = 1-
Preal
Pdiscontinuity
Pbetween
X
Y
Z
F
f^-2
f^-5/3
FIELD ALIGNED COORDINATES
Z II F
X IN ECLIPTIC
95% CONFIDENCE
γ^2/Hz
f (Hz)

Figure 5

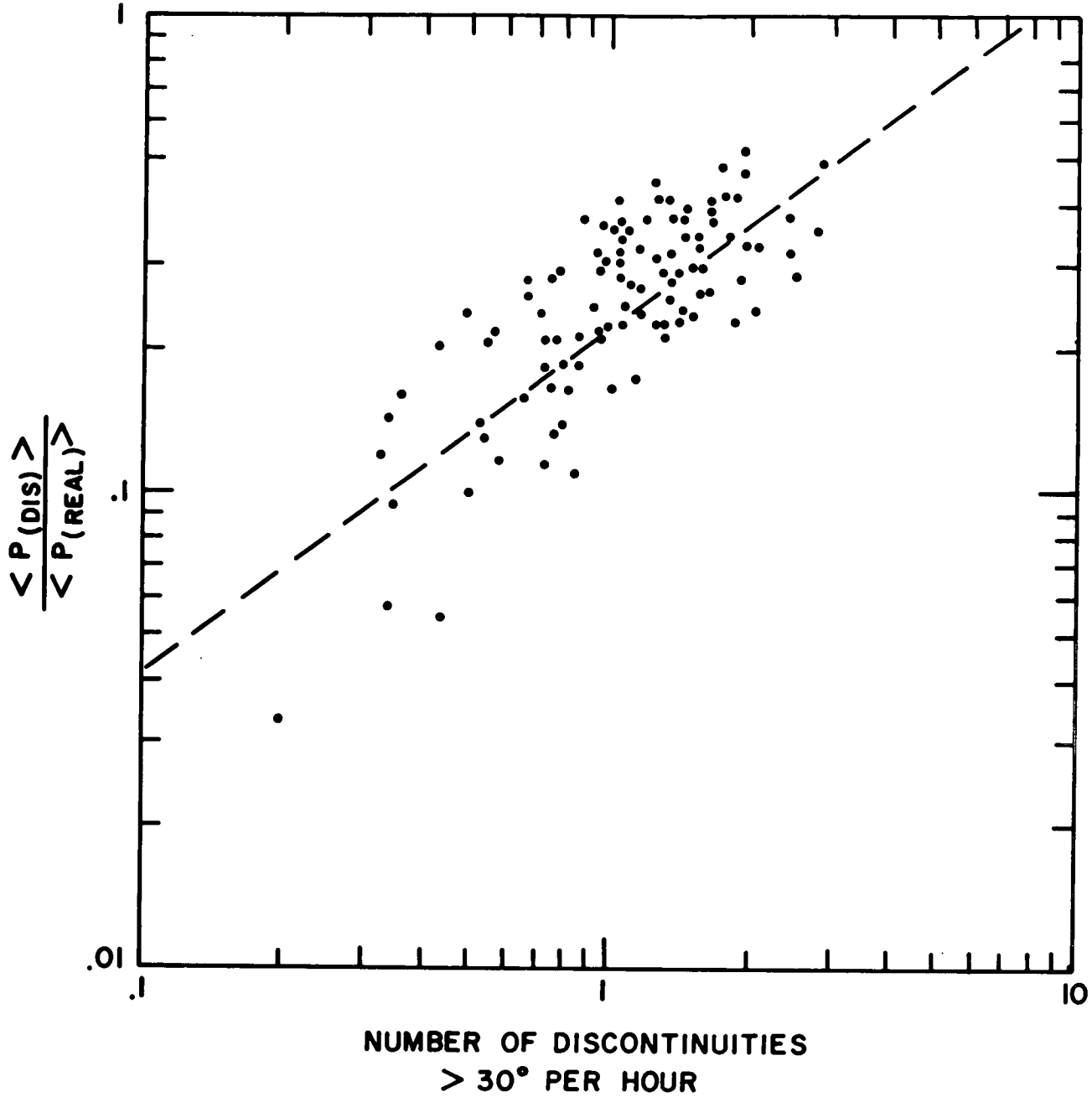
1
.1
.01
$\frac{<P_{(DIS)}>}{<P_{(REAL)}>}$
.1
1
10
NUMBER OF DISCONTINUITIES
> 30° PER HOUR

Figure 6

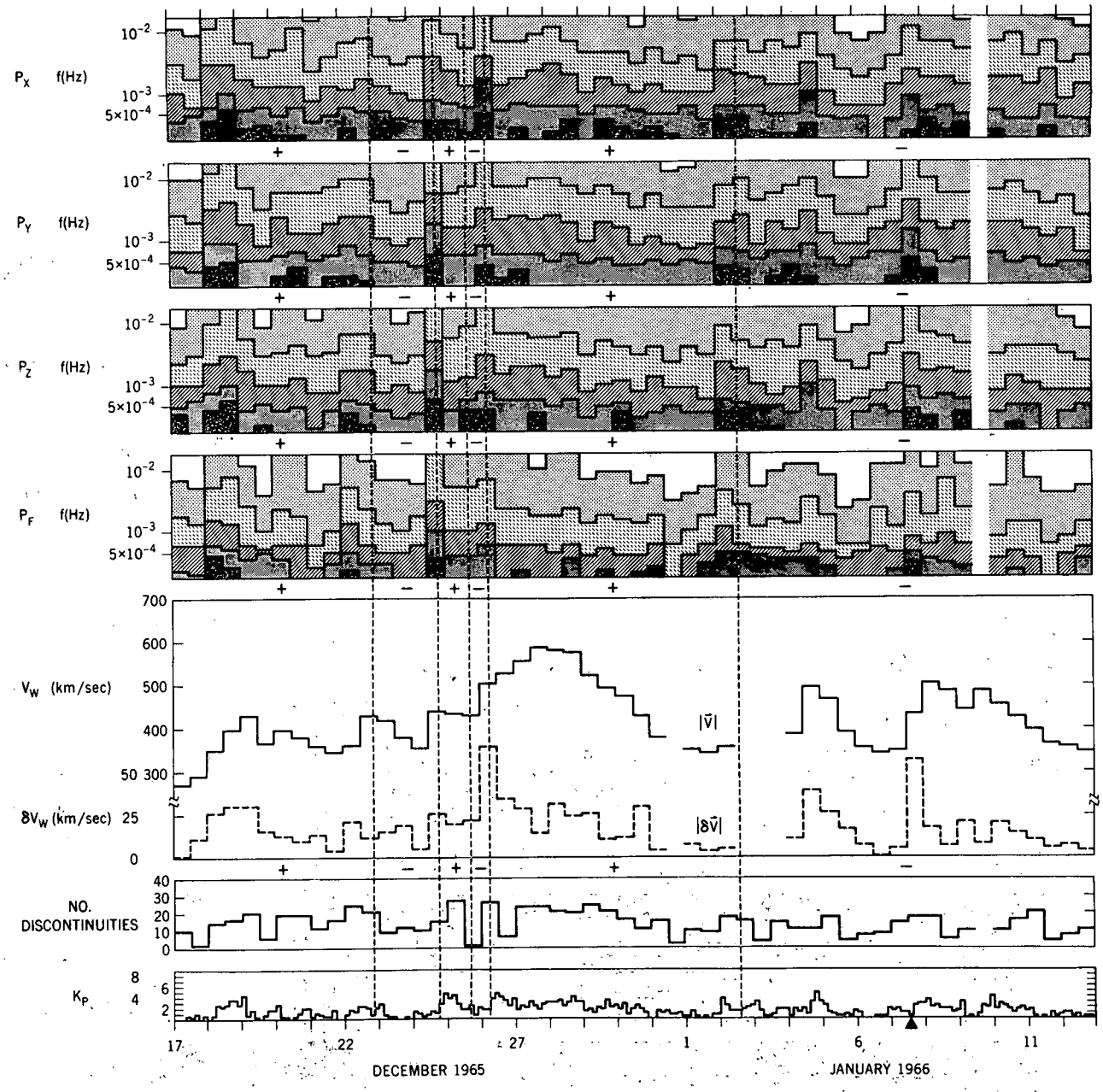
P_X f(Hz)
P_Y f(Hz)
P_Z f(Hz)
P_F f(Hz)
10^{-2}
10^{-3}
5×10^{-4}
+ − + − + −
V_W (km/sec)
700
600
500
400
300
$|\bar{V}|$
δV_W (km/sec)
50
25
0
$|\delta\bar{V}|$
NO. DISCONTINUITIES
40
30
20
10
0
K_P
8
6
4
2
17
22
27
1
6
11
DECEMBER 1965
JANUARY 1966

Figure 7

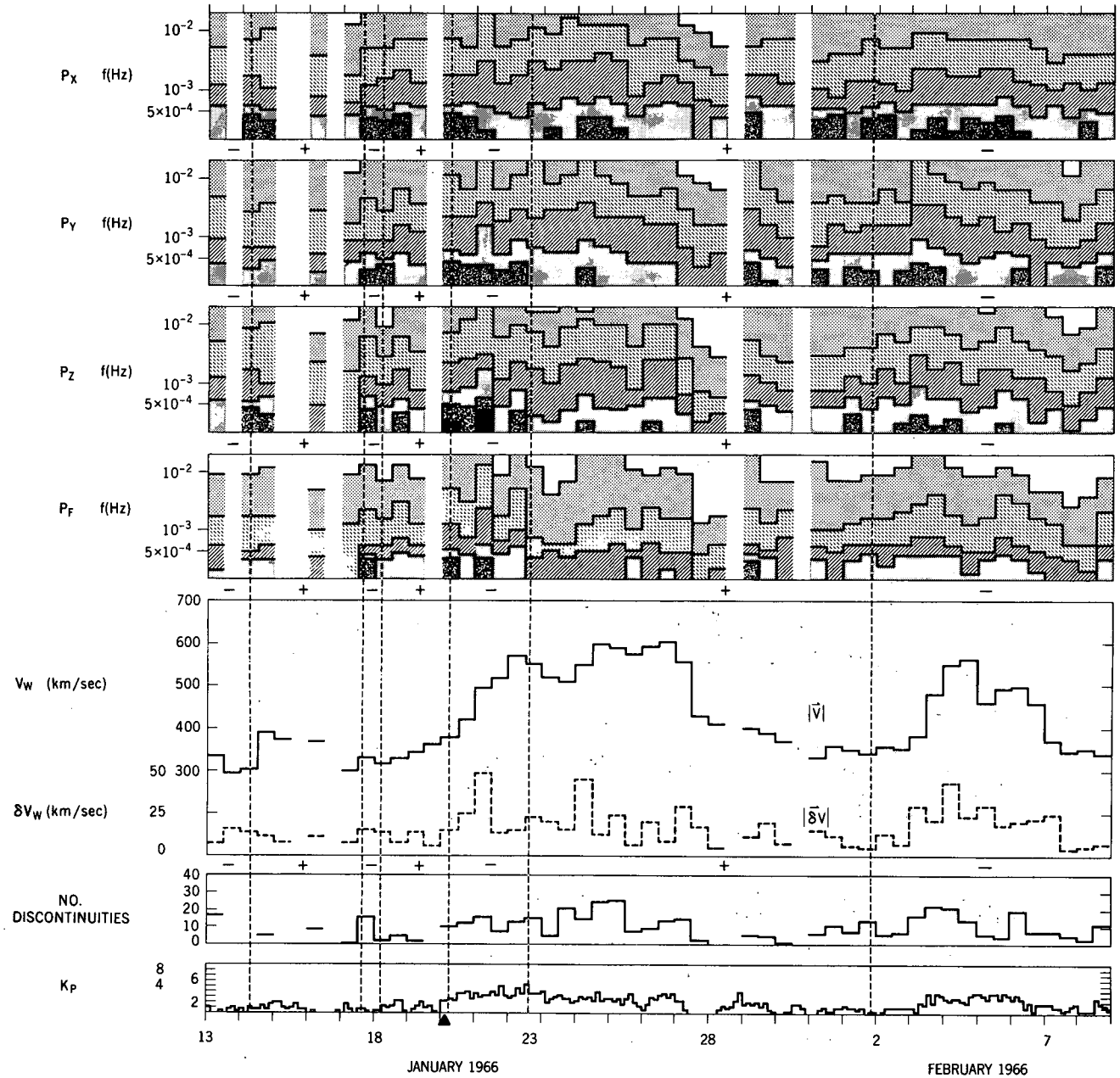
P_X f(Hz)
P_Y f(Hz)
P_Z f(Hz)
P_F f(Hz)
10^{-2}
10^{-3}
5×10^{-4}
V_W (km/sec)
700
600
500
400
300
$|\vec{V}|$
δV_W (km/sec)
50
25
0
$|\vec{\delta V}|$
NO. DISCONTINUITIES
40
30
20
10
0
K_P
8
6
4
2
13
18
23
28
2
7
JANUARY 1966
FEBRUARY 1966

Figure 8

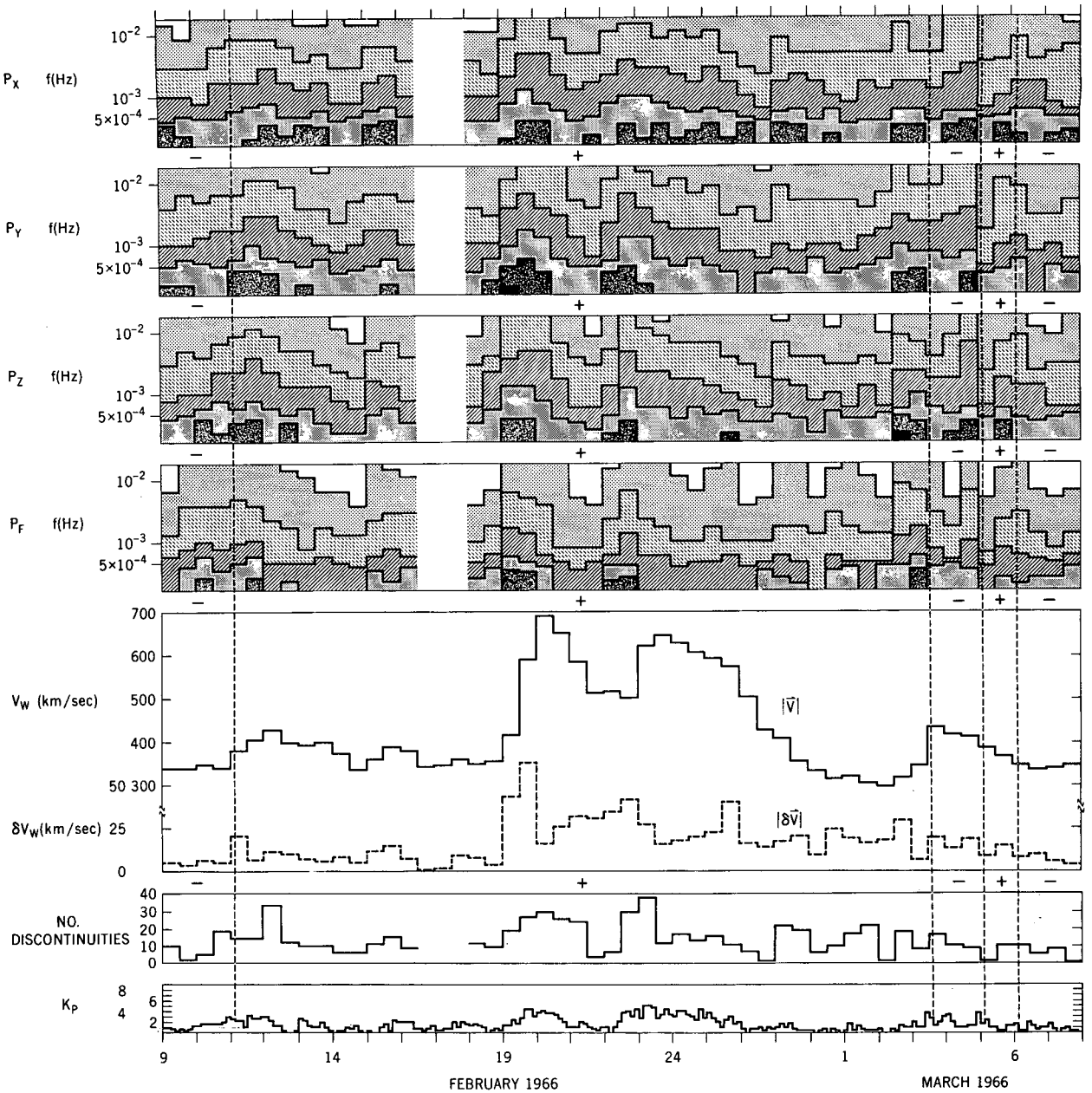
P_X f(Hz)
P_Y f(Hz)
P_Z f(Hz)
P_F f(Hz)
10^{-2}
10^{-3}
5×10^{-4}
V_W (km/sec)
700
600
500
400
300
$|\vec{V}|$
δV_W(km/sec)
50
25
0
$|\delta\vec{V}|$
NO. DISCONTINUITIES
40
30
20
10
0
K_P
8
6
4
2
9
14
19
24
1
6
FEBRUARY 1966
MARCH 1966

Figure 9

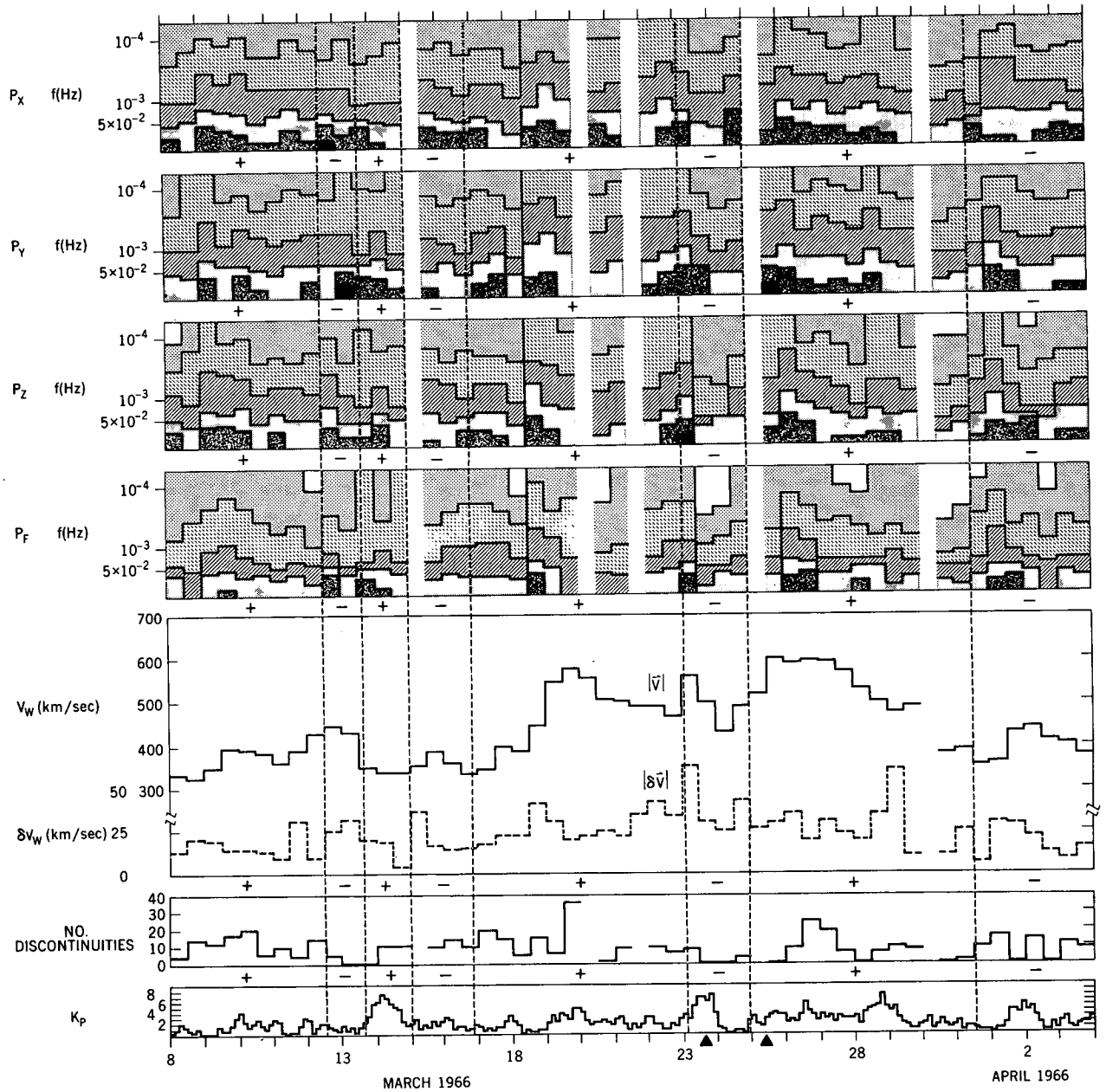
P_X f(Hz)
P_Y f(Hz)
P_Z f(Hz)
P_F f(Hz)
10^{-4}
10^{-3}
5×10^{-2}
V_W (km/sec)
δV_W (km/sec)
$|\vec{v}|$
$|\delta\vec{v}|$
NO. DISCONTINUITIES
K_P
8
13
18
23
28
2
MARCH 1966
APRIL 1966

Figure 10

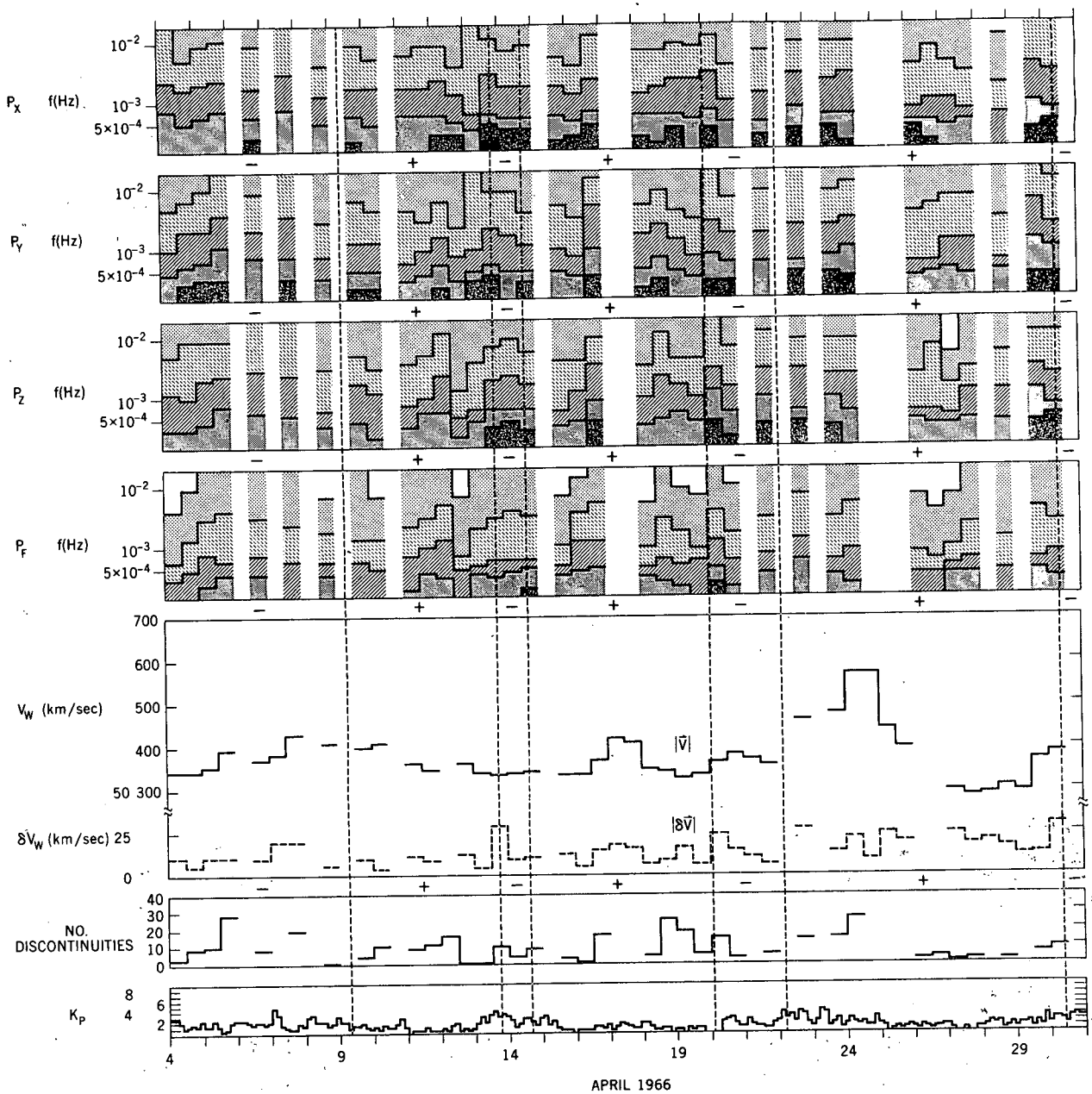
P_X f(Hz)
10^{-2}
10^{-3}
5×10^{-4}
P_Y f(Hz)
P_Z f(Hz)
P_F f(Hz)
V_W (km/sec)
700
600
500
400
300
$|\vec{V}|$
δV_W (km/sec)
50
25
0
$|\delta\vec{V}|$
NO. DISCONTINUITIES
40
30
20
10
0
K_P
8
6
4
2
4
9
14
19
24
29
APRIL 1966

Figure 11

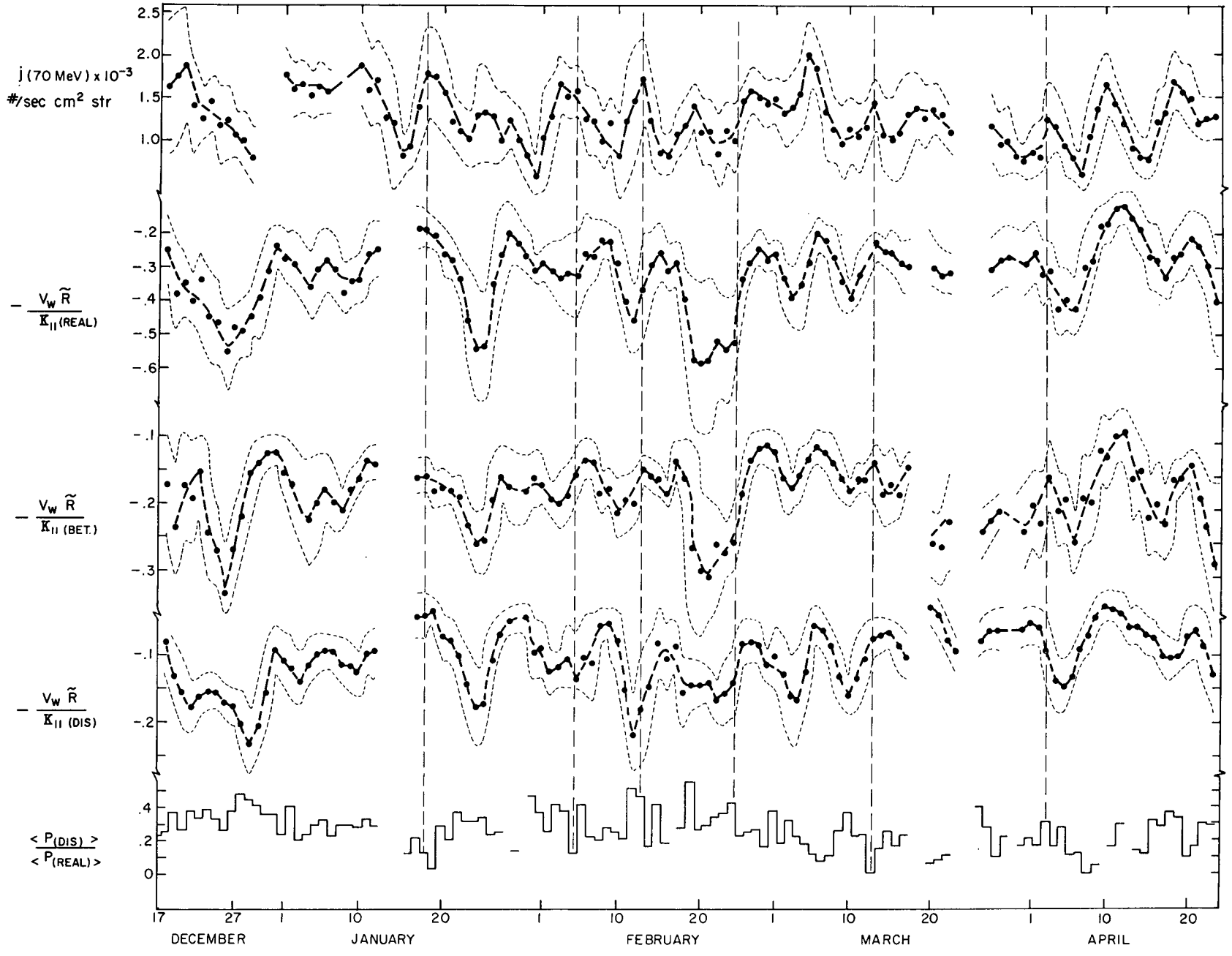
j (70 MeV) x 10⁻³
#/sec cm² str
2.5
2.0
1.5
1.0
$-\frac{V_w \tilde{R}}{K_{11}(REAL)}$
-.2
-.3
-.4
-.5
-.6
$-\frac{V_w \tilde{R}}{K_{11}(BET.)}$
-.1
-.2
-.3
$-\frac{V_w \tilde{R}}{K_{11}(DIS)}$
-.1
-.2
$\frac{<P_{(DIS)}>}{<P_{(REAL)}>}$
.4
.2
0
17
27
1
10
20
1
10
20
1
10
20
1
10
20
DECEMBER
JANUARY
FEBRUARY
MARCH
APRIL

Figure 12

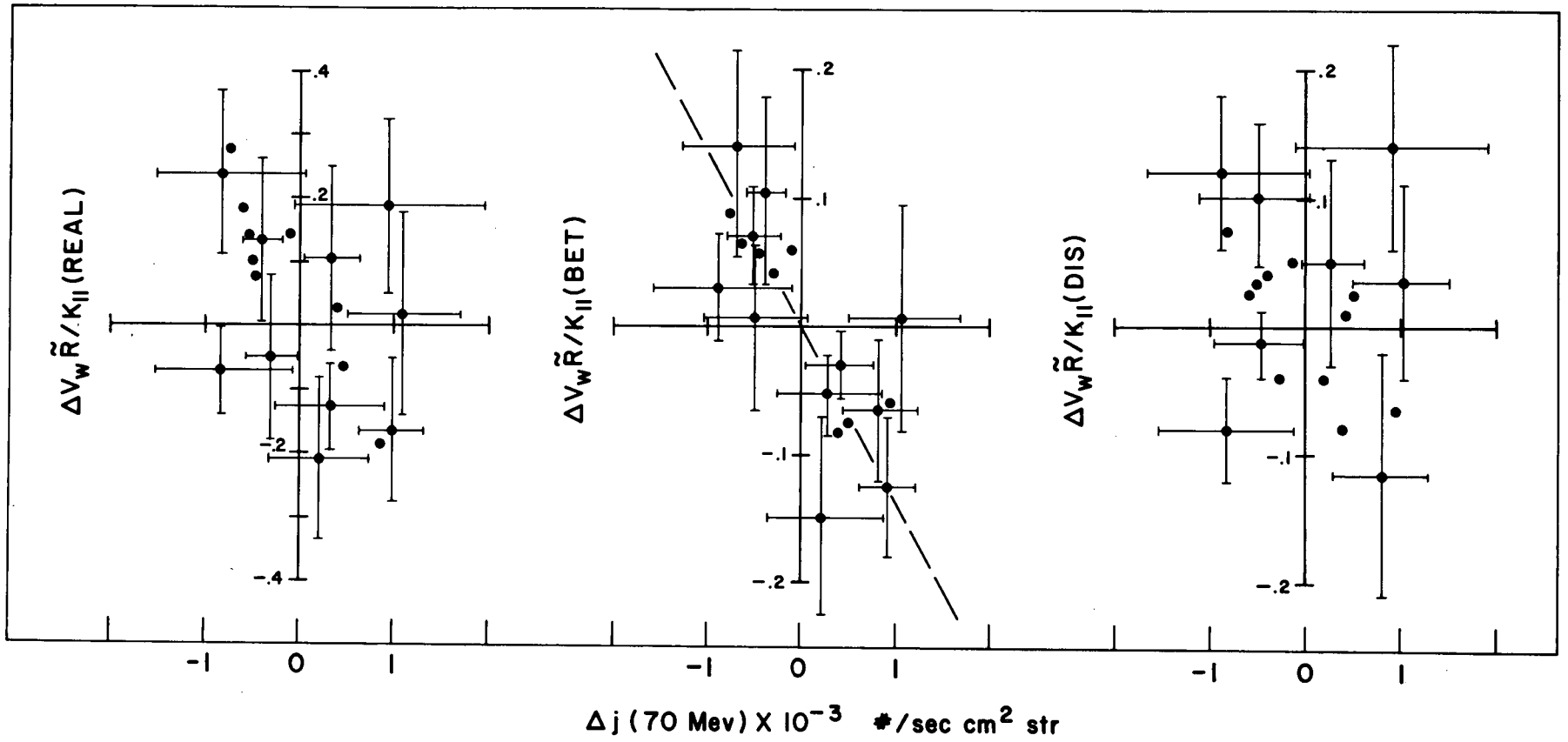
$\Delta V_w \tilde{R}/K_{II}$ (REAL)
$\Delta V_w \tilde{R}/K_{II}$ (BET)
$\Delta V_w \tilde{R}/K_{II}$ (DIS)
.4
.2
-.2
-.4
.2
.1
-.1
-.2
.2
.1
-.1
-.2
-1
0
1
Δj (70 Mev) X 10^{-3} #/sec cm^2 str

Figure 13

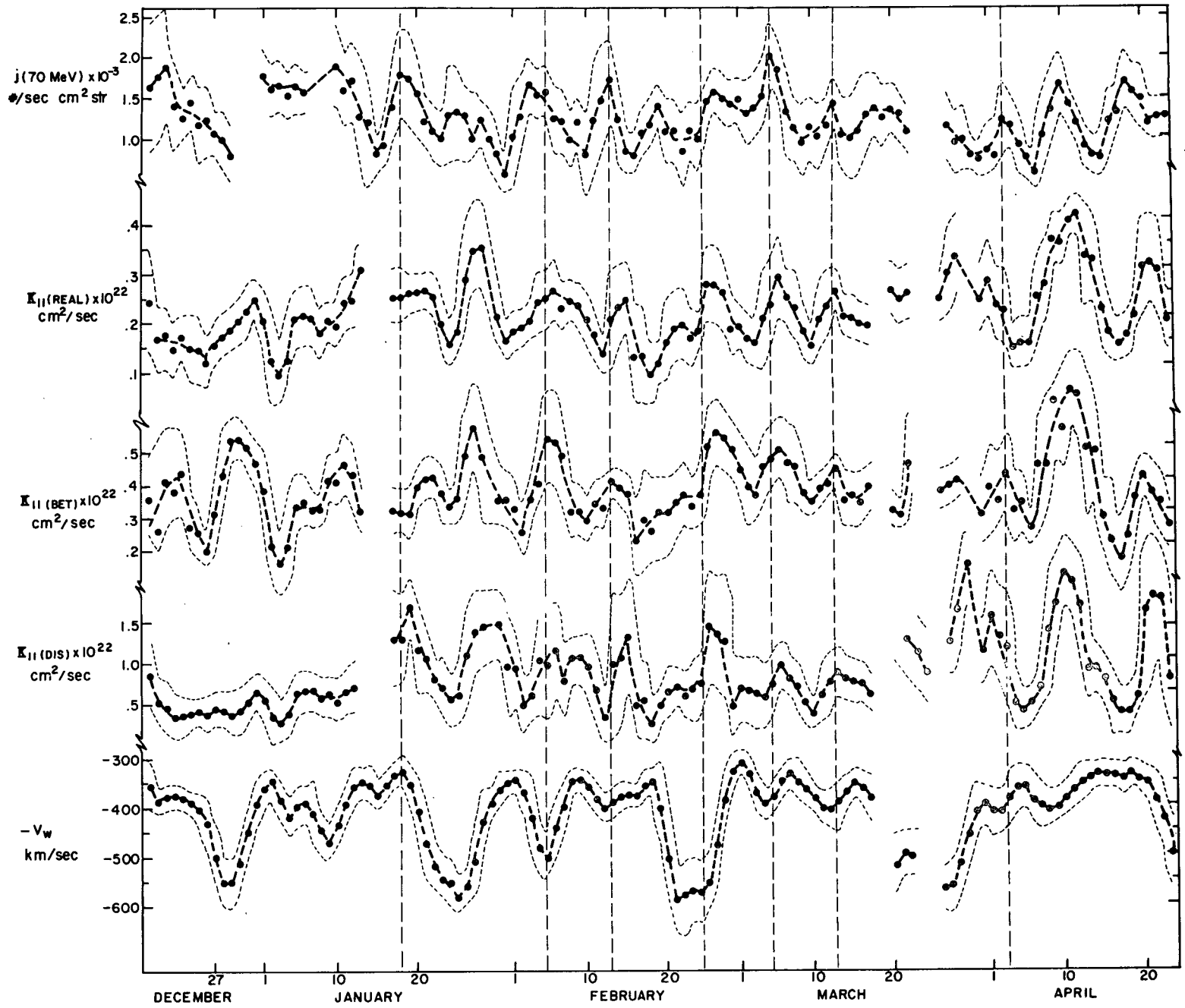
j(70 MeV) x10^-3
#/sec cm^2 str
2.5
2.0
1.5
1.0
K⊥(REAL) x10^22
cm^2/sec
.4
.3
.2
.1
K⊥(BET) x10^22
cm^2/sec
.5
.4
.3
.2
K⊥(DIS) x10^22
cm^2/sec
1.5
1.0
.5
-Vw
km/sec
-300
-400
-500
-600
27
DECEMBER
10
20
JANUARY
10
20
FEBRUARY
10
20
MARCH
10
20
APRIL

Figure 14

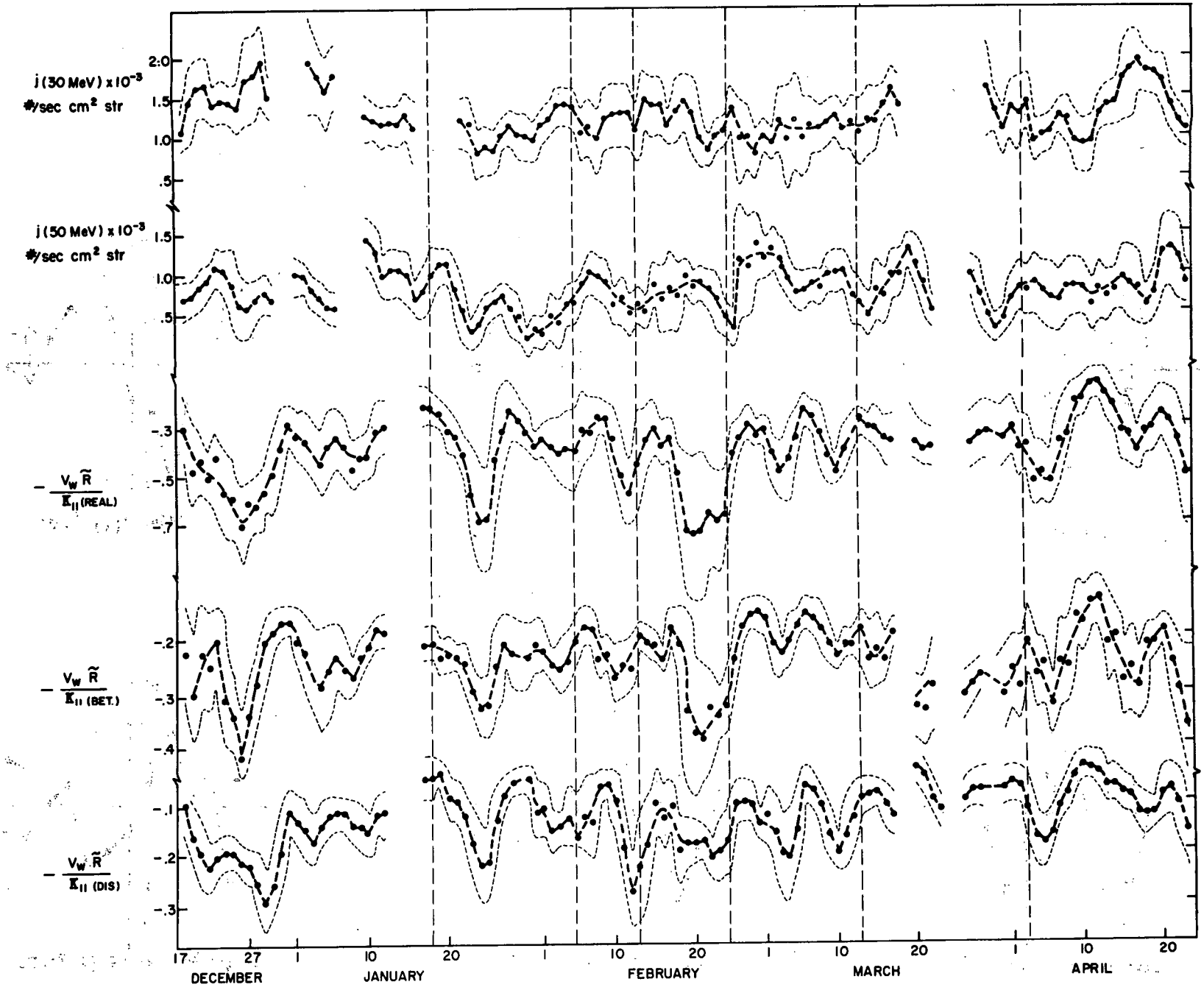
j(30 MeV) x 10⁻³
#/sec cm² str
2.0
1.5
1.0
.5
j(50 MeV) x 10⁻³
#/sec cm² str
1.5
1.0
.5
$-\frac{V_w \tilde{R}}{K_{\parallel (REAL)}}$
-.3
-.5
-.7
$-\frac{V_w \tilde{R}}{K_{\parallel (BET.)}}$
-.2
-.3
-.4
$-\frac{V_w \tilde{R}}{K_{\parallel (DIS)}}$
-.1
-.2
-.3
17
27
1
10
20
1
10
20
1
10
20
1
10
20
DECEMBER
JANUARY
FEBRUARY
MARCH
APRIL

Figure 15

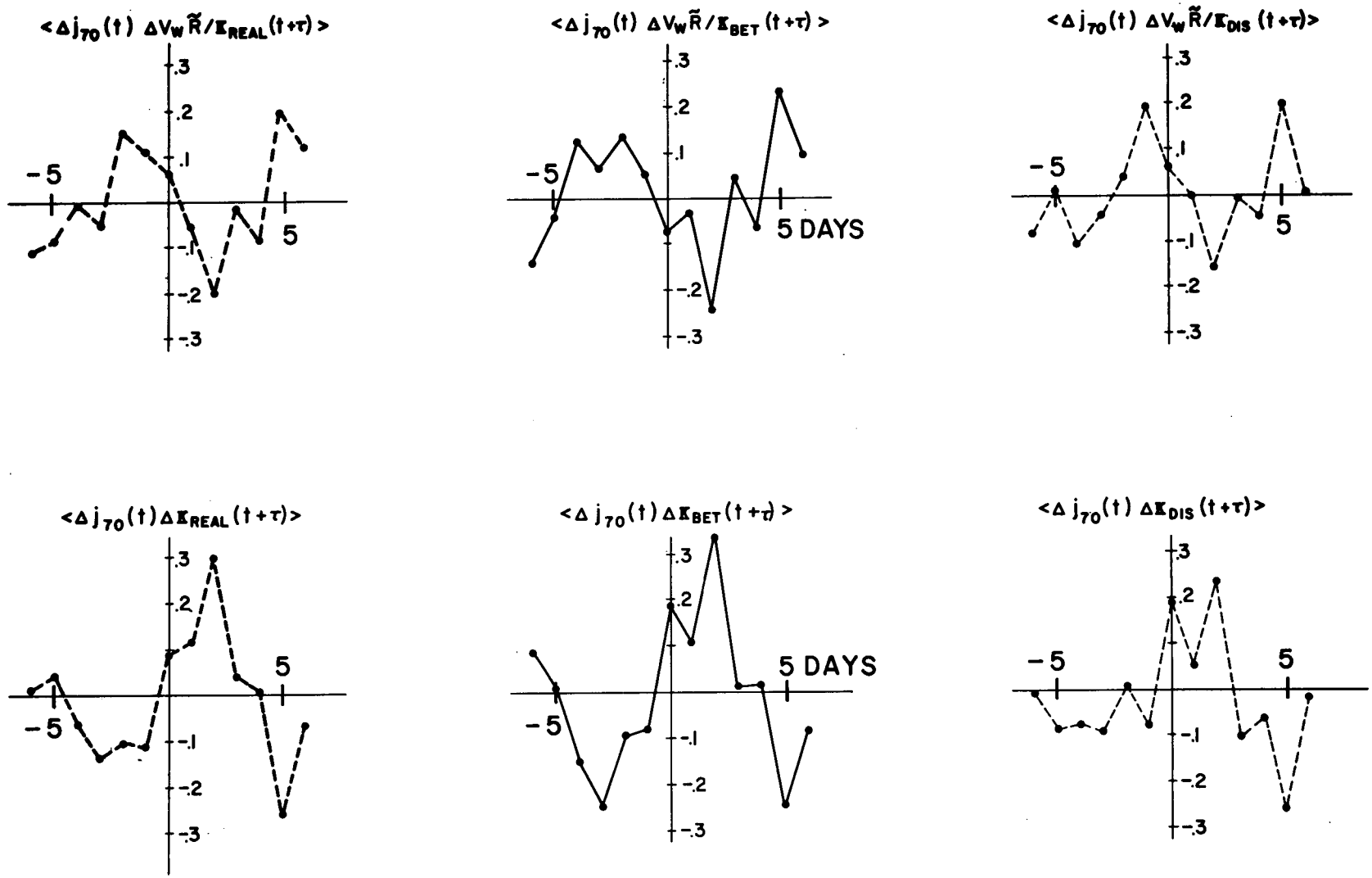
$\langle \Delta j_{70}(t)\ \Delta V_W \tilde{R}/E_{REAL}(t+\tau) \rangle$
$\langle \Delta j_{70}(t)\ \Delta V_W \tilde{R}/E_{BET}(t+\tau) \rangle$
$\langle \Delta j_{70}(t)\ \Delta V_W \tilde{R}/E_{DIS}(t+\tau) \rangle$
$\langle \Delta j_{70}(t)\ \Delta E_{REAL}(t+\tau) \rangle$
$\langle \Delta j_{70}(t)\ \Delta E_{BET}(t+\tau) \rangle$
$\langle \Delta j_{70}(t)\ \Delta E_{DIS}(t+\tau) \rangle$
.3
.2
.1
-.1
-.2
-.3
-5
5
5 DAYS

Figure 16

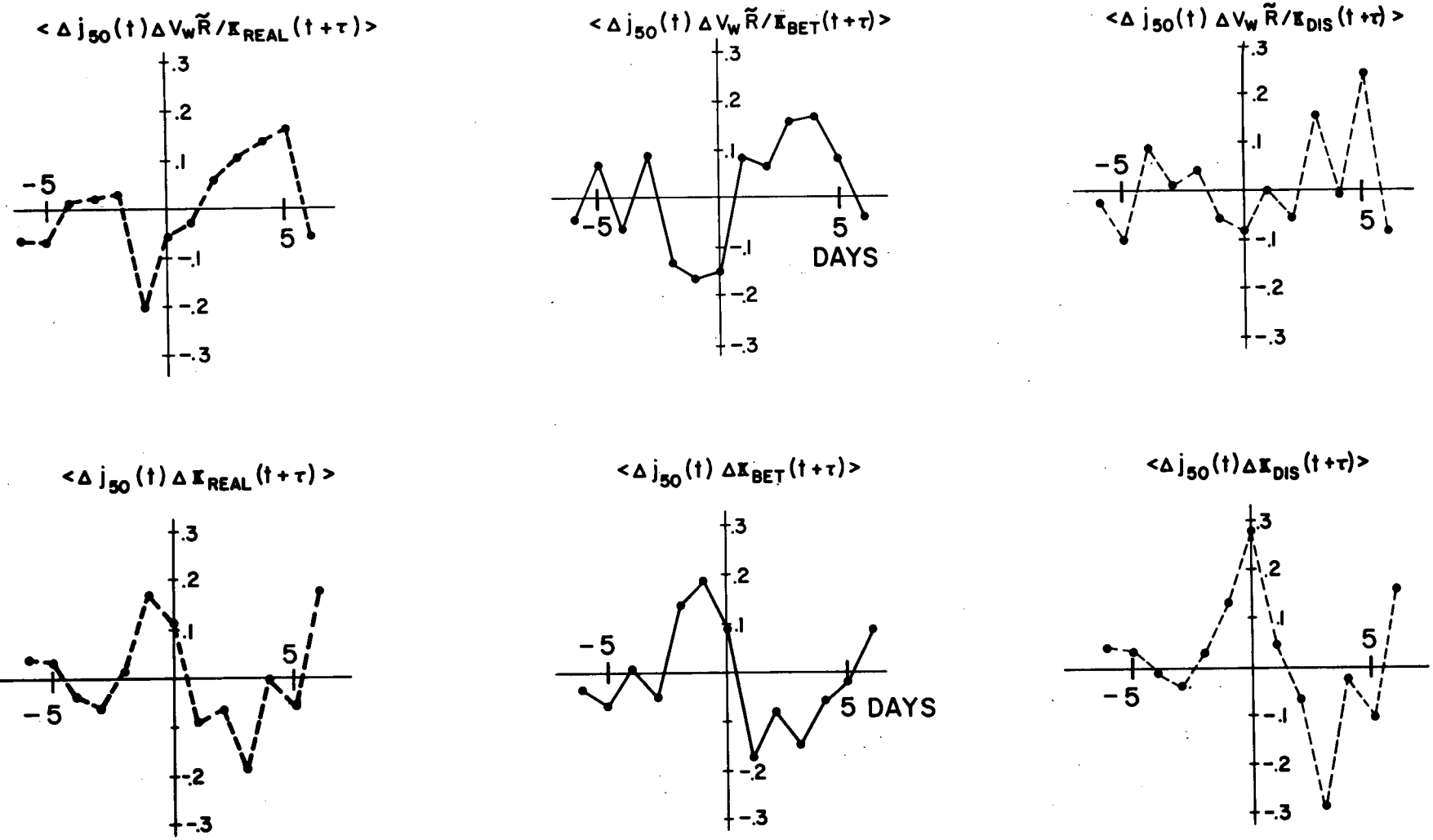
$<\Delta j_{50}(t)\Delta V_w \tilde{R}/\mathbb{K}_{REAL}(t+\tau)>$
$<\Delta j_{50}(t)\Delta V_w \tilde{R}/\mathbb{K}_{BET}(t+\tau)>$
$<\Delta j_{50}(t)\Delta V_w \tilde{R}/\mathbb{K}_{DIS}(t+\tau)>$
$<\Delta j_{50}(t)\Delta \mathbb{K}_{REAL}(t+\tau)>$
$<\Delta j_{50}(t)\Delta \mathbb{K}_{BET}(t+\tau)>$
$<\Delta j_{50}(t)\Delta \mathbb{K}_{DIS}(t+\tau)>$
.3
.2
.1
-.1
-.2
-.3
-5
5
DAYS

Figure 17

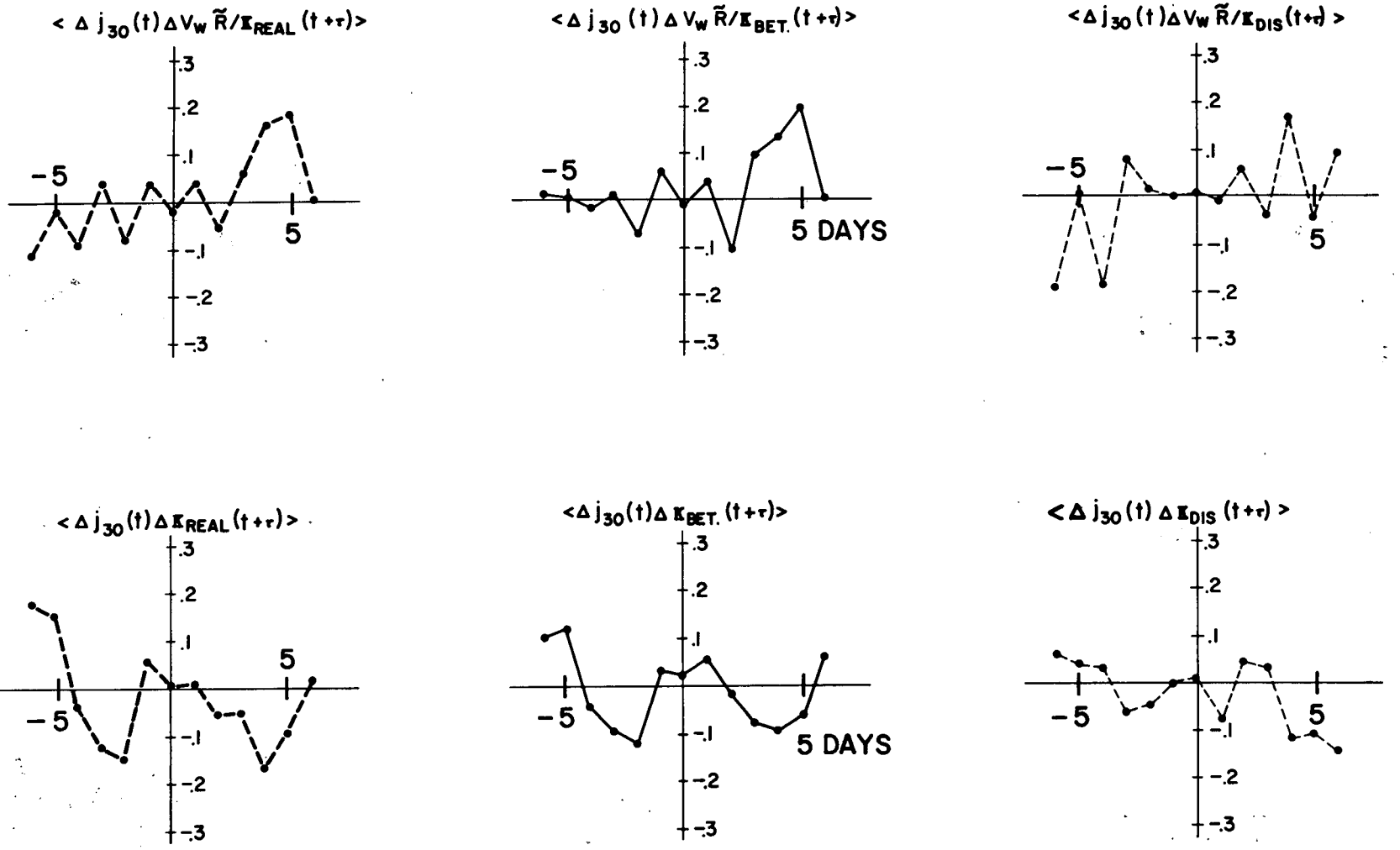
$< \Delta j_{30}(t) \Delta V_w \tilde{R}/\mathbb{K}_{REAL}(t+\tau) >$
$< \Delta j_{30}(t) \Delta V_w \tilde{R}/\mathbb{K}_{BET.}(t+\tau) >$
$< \Delta j_{30}(t) \Delta V_w \tilde{R}/\mathbb{K}_{DIS}(t+\tau) >$
$< \Delta j_{30}(t) \Delta \mathbb{K}_{REAL}(t+\tau) >$
$< \Delta j_{30}(t) \Delta \mathbb{K}_{BET.}(t+\tau) >$
$< \Delta j_{30}(t) \Delta \mathbb{K}_{DIS}(t+\tau) >$
.3
.2
.1
-.1
-.2
-.3
-5
5
5 DAYS

Figure 18

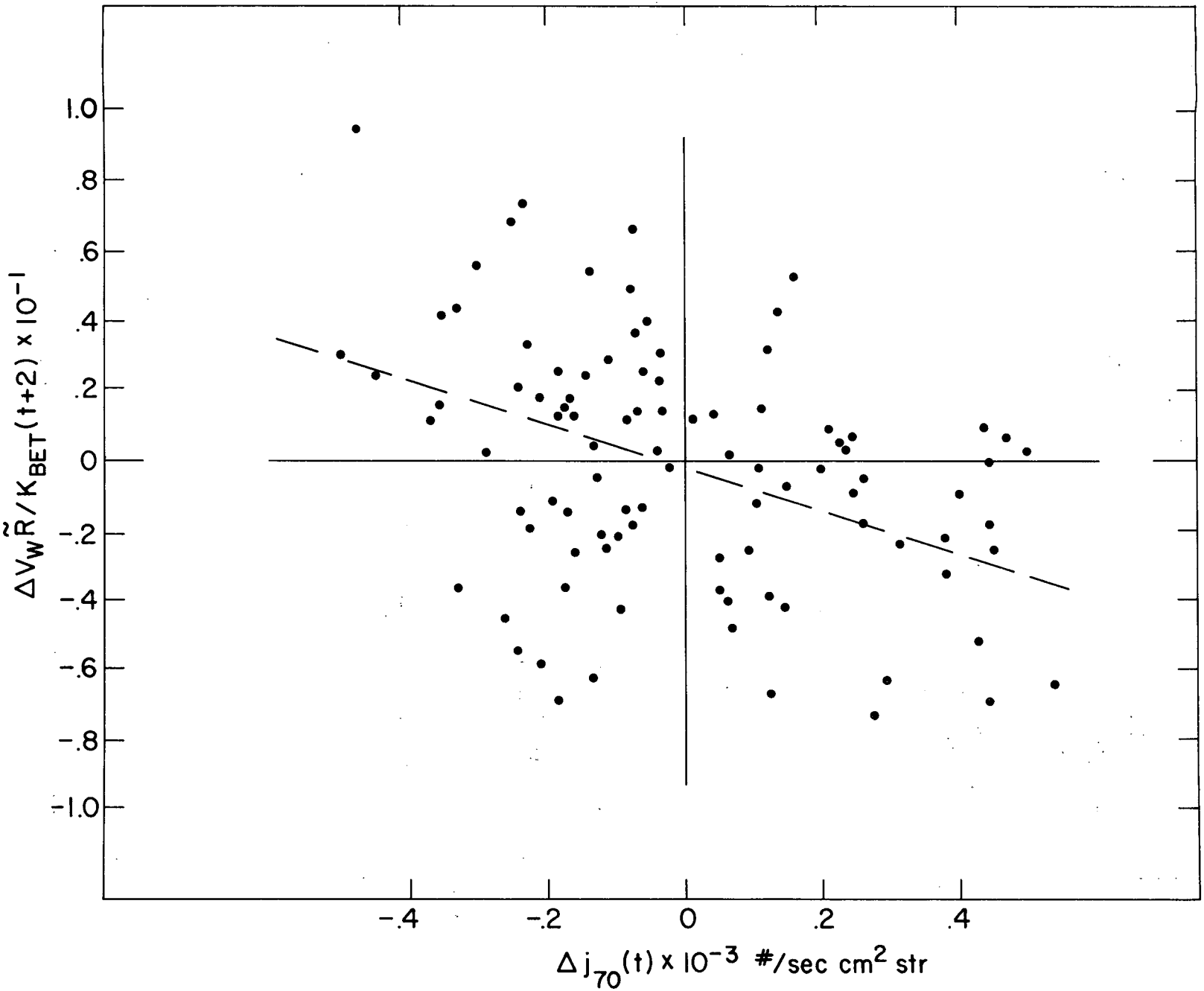
1.0
.8
.6
.4
.2
0
-.2
-.4
-.6
-.8
-1.0
$\Delta V_W \tilde{R} / K_{BET}(t+2) \times 10^{-1}$
-.4
-.2
0
.2
.4
$\Delta j_{70}(t) \times 10^{-3}$ #/sec cm^2 str

Figure 19

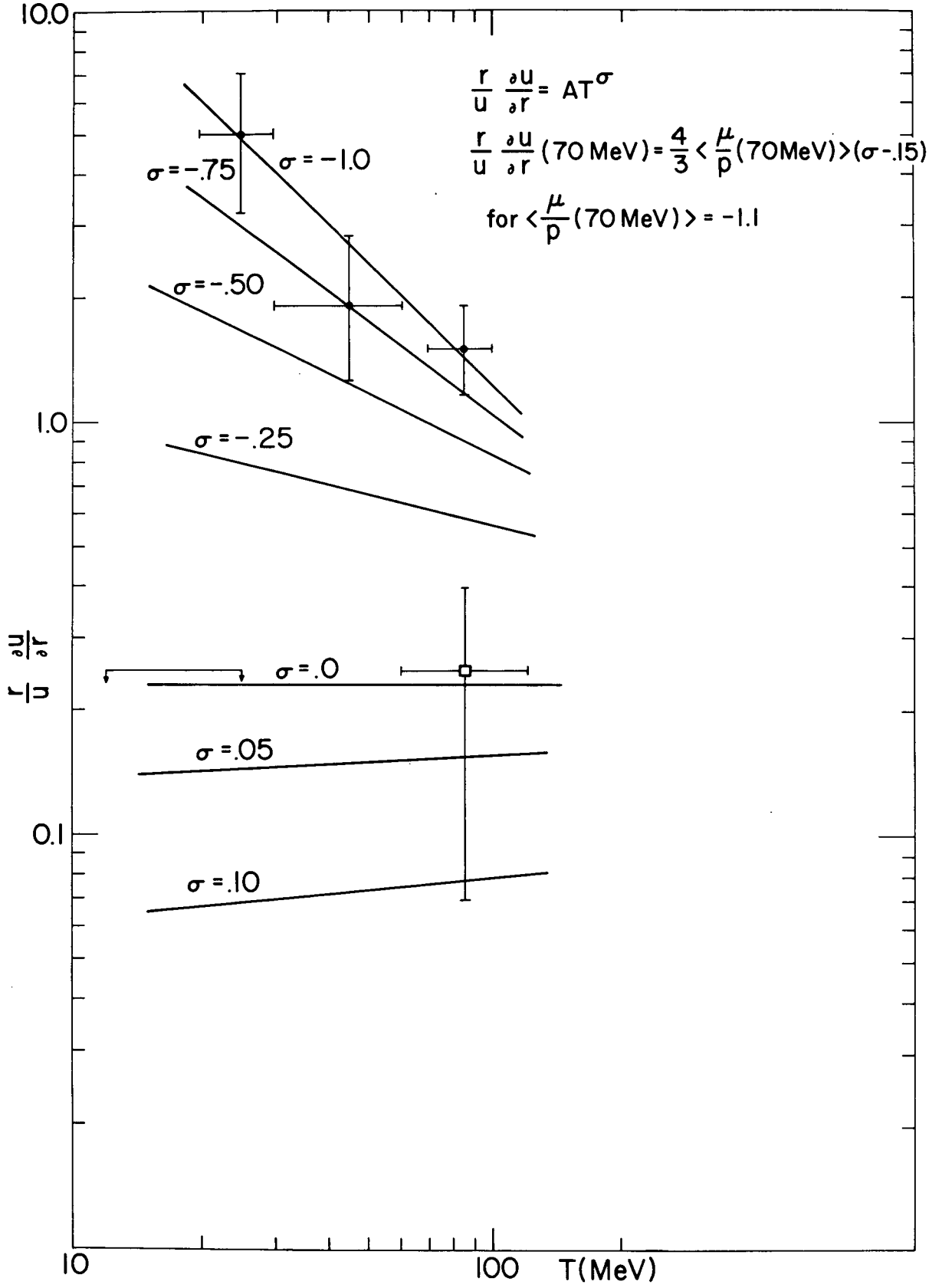
10.0
1.0
0.1
10
100
T(MeV)
$\frac{r}{u}\frac{\partial u}{\partial r}$
$\frac{r}{u}\frac{\partial u}{\partial r} = AT^{\sigma}$
$\frac{r}{u}\frac{\partial u}{\partial r}(70\,MeV) = \frac{4}{3}<\frac{\mu}{p}(70MeV)>(\sigma - .15)$
for $<\frac{\mu}{p}(70\,MeV)> = -1.1$
σ = −.75
σ = −1.0
σ = −.50
σ = −.25
σ = .0
σ = .05
σ = .10

Figure 20

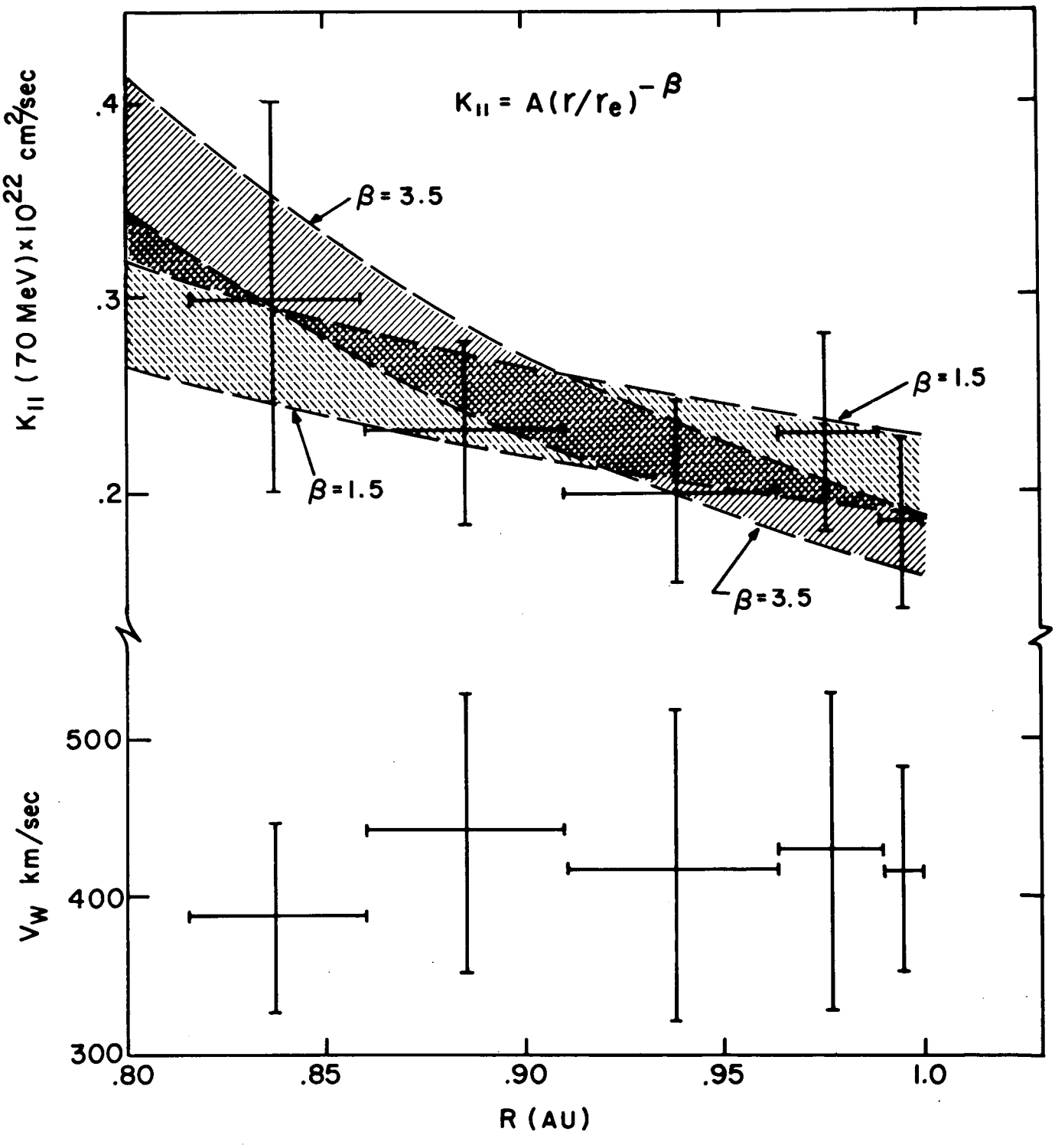
$K_{11} = A(r/r_e)^{-\beta}$
K_{11} (70 MeV) x 10^{22} cm^2/sec
.4
.3
.2
β = 3.5
β = 1.5
β = 1.5
β = 3.5
V_W km/sec
500
400
300
.80
.85
.90
.95
1.0
R (AU)

Figure 21

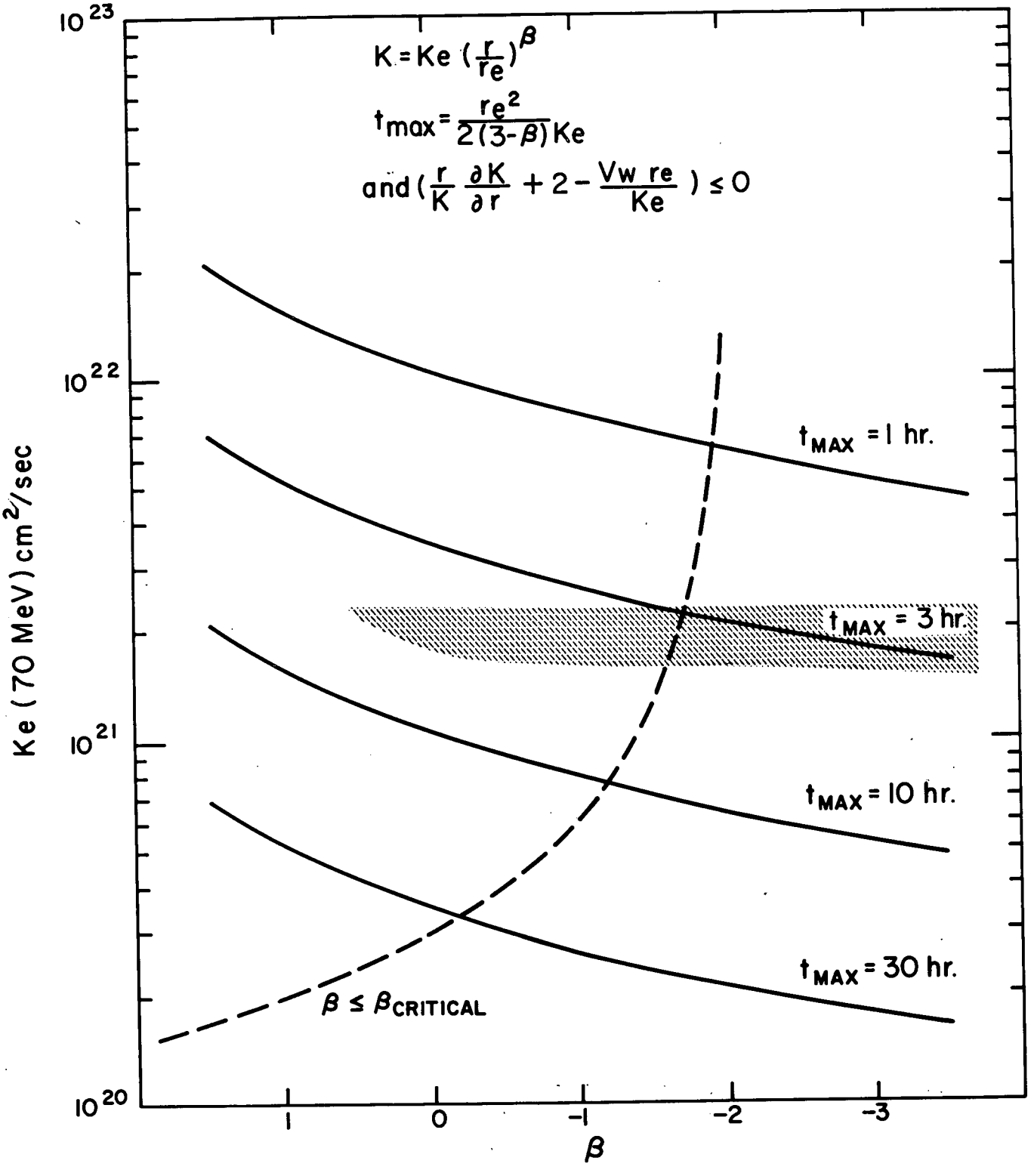
$K = Ke\,(\frac{r}{re})^{\beta}$
$t_{max} = \frac{re^2}{2(3-\beta)Ke}$
and $(\frac{r}{K}\frac{\partial K}{\partial r} + 2 - \frac{Vw\ re}{Ke}) \leq 0$
10^{23}
10^{22}
10^{21}
10^{20}
Ke (70 MeV) cm^2/sec
t_{MAX} = 1 hr.
t_{MAX} = 3 hr.
t_{MAX} = 10 hr.
t_{MAX} = 30 hr.
$\beta \leq \beta_{CRITICAL}$
1
0
-1
-2
-3
β

Figure 22

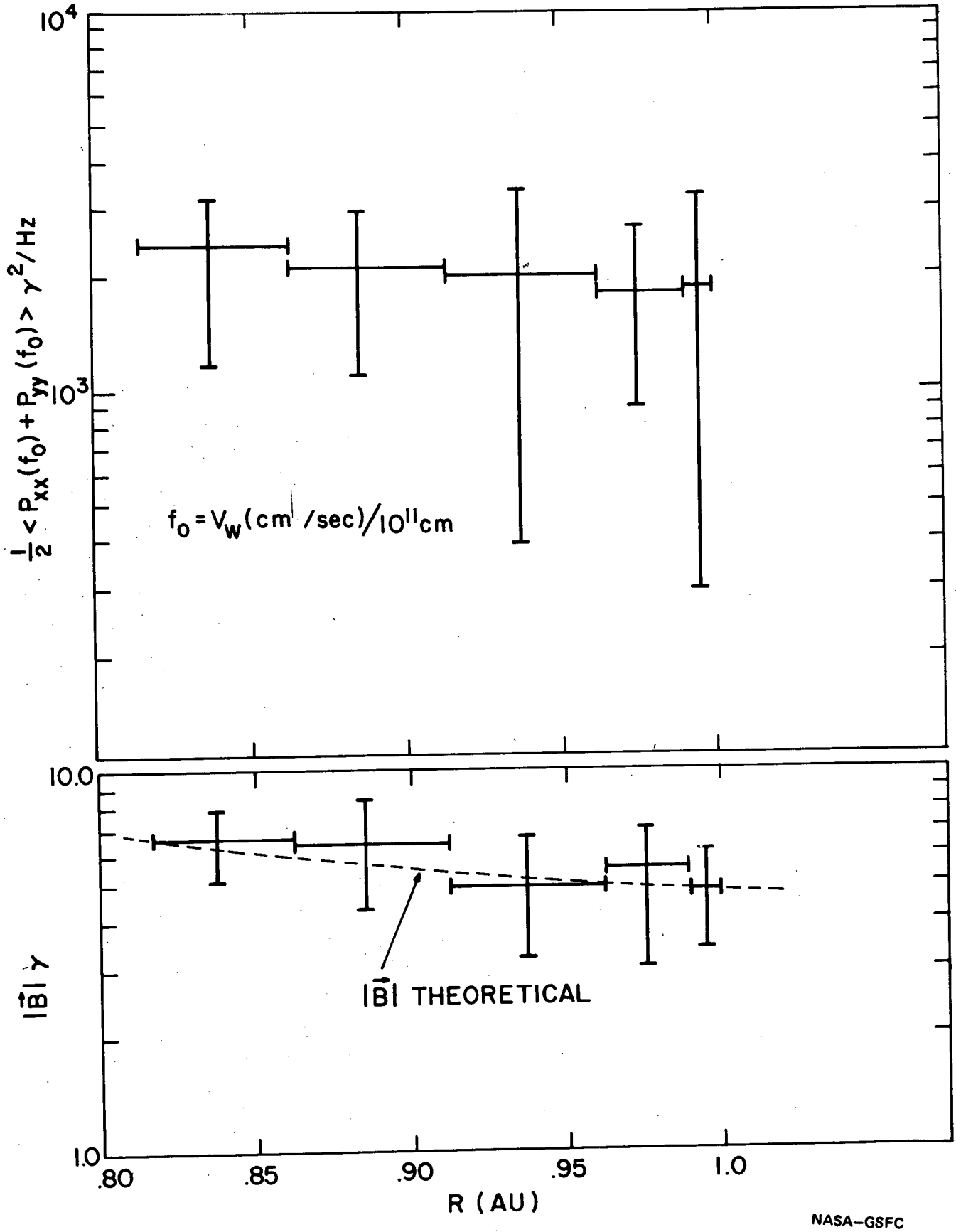
10^4
10^3
$\frac{1}{2} < P_{xx}(f_0) + P_{yy}(f_0) > \gamma^2/Hz$
$f_0 = V_w(cm/sec)/10^{11}cm$
10.0
1.0
$|\vec{B}|\ \gamma$
$|\vec{B}|$ THEORETICAL
.80
.85
.90
.95
1.0
R (AU)
NASA–GSFC

Figure 23